Atmospheric Sound Propagation: Fundamentals: **Part 1**

Keith Attenborough

Engineering and Innovation, STEM Faculty, The Open University,
Milton Keynes, MK7 6AA, UK
email: keith.attenborough@open.ac.uk

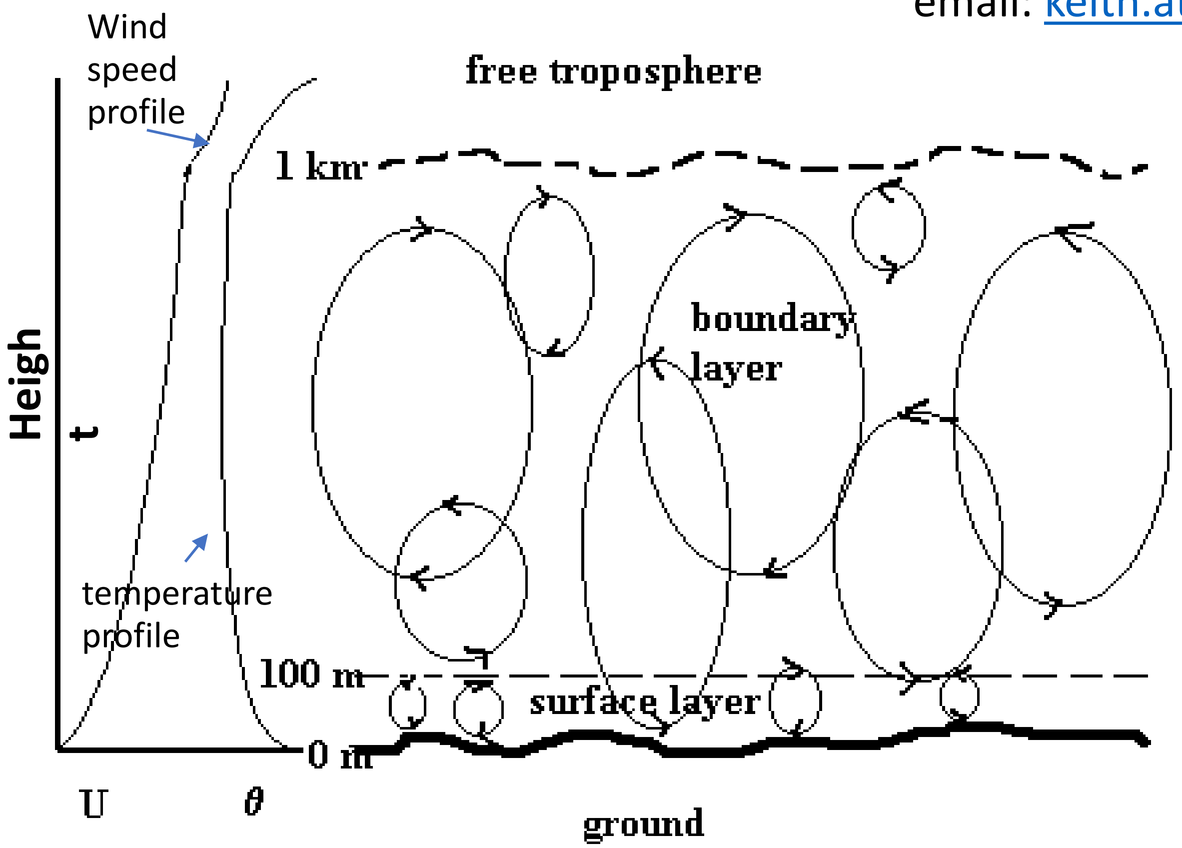

Consider propagation only in the lowest 10 - 100 m

- A brief history
- Data from fixed jet noise source at Hucknall
- Blast noise data over snow and ploughed ground
- Excess Attenuation and Level Difference
- Parkin and Scholes classical data
- Data on meteorological effects
- Pasquill classes and Monin-Obukhov
- Sound speed profiles
- Ground effect
    - ground impedance models
    - Physical admissibility
    - Seasonal variation
    - Smooth v rough
    - Artificial roughness effects

A brief history of outdoor sound studies

Scientist(s)	**Finding**	Date
Aristotle	Motion of air is involved *but speed depends on source (high notes faster than low)*	384-322 B.C.
Vitruvius	Corrected Aristotle's notion of source dependency	100 B.C.
Pierre Gassendi	Used flashes and reports from guns, speed = 1473 Paris ft/s (478.4 m/s*) and frequency independent*	1635
Marin Mersenne	Used flash and report from cannon, speed = 1380 Paris feet per second (450 m/s)	1640
Borelli and Viviani	Speed of sound 1057 Paris feet per second (350 m/s)	1656
Robert Boyle	Air is an elastic medium for sound transmission (bell in evacuated jar - misleading)	1660
Samuel Pepys and John Evelyn	Acoustic shadow zones reported during naval battles between British and Dutch	1666
William Derham	Wind and temperature affect sound speed and transmission loss over snow > than over hard frozen	1657 – 1735
French Academy of Sciences	Used cannon fire, speed = 332 m/s	1738
Laplace	Compressions and rarefactions associated with passage of sound are adiabatic	1816
1st world war	Acoustic shadow zones observed during the Battle of Antwerp	1914 – 1918
Parkin and Scholes	Observation and study of ground effect	1969
1st LRSP	Application of numerical codes devised for underwater acoustics to atmospheric acoustics	1981

Propagation from a fixed jet engine over grass

Unpublished OU report for ESDU

source nozzle centre height 2.16 m and 1.2 m high microphones over an airfield at Hucknall, Notts, UK, 1998, zero wind, low turbulence conditions

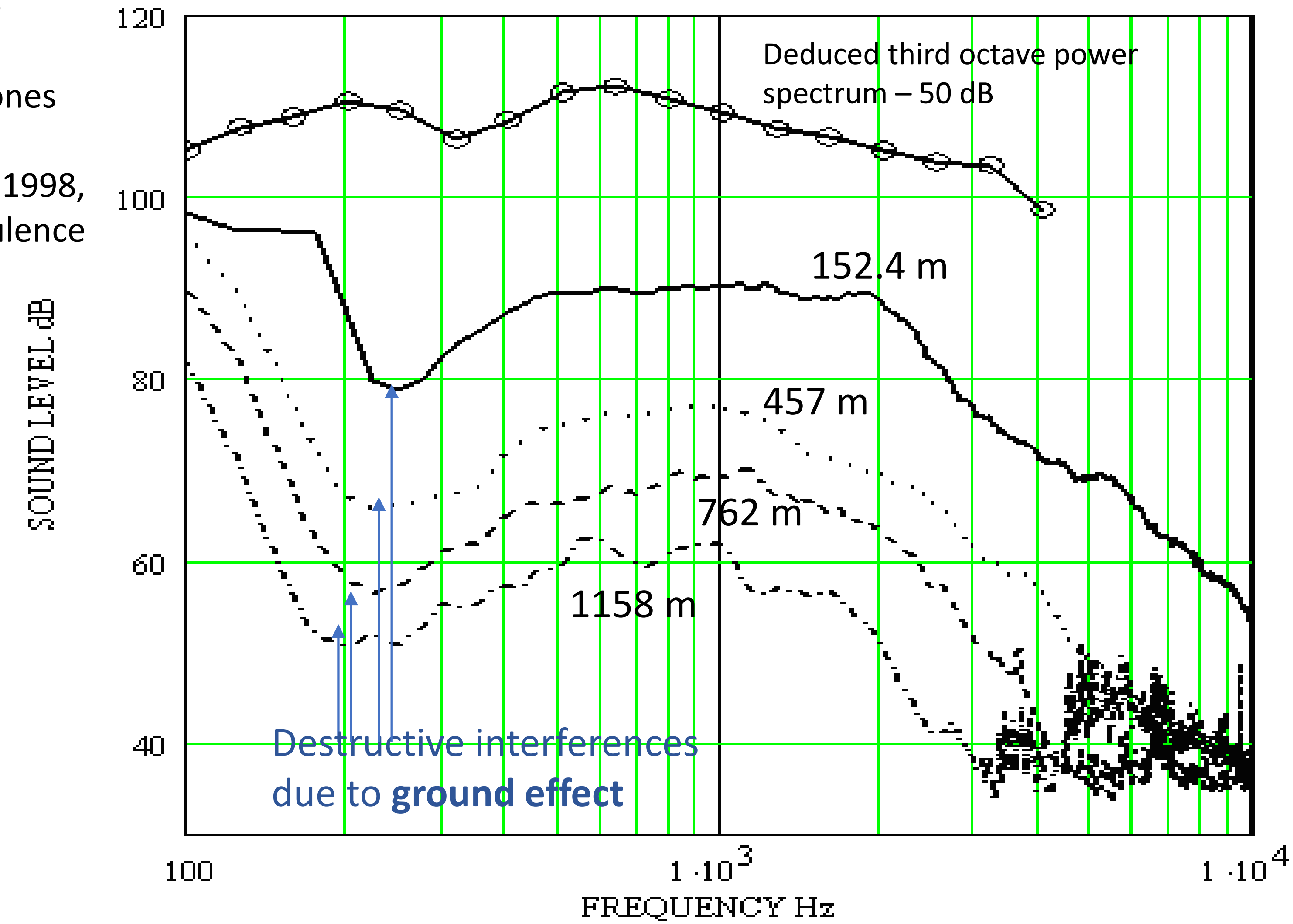

As a result of similar measurements made about 30 years earlier, Peter Parkin observed: " *These horizontal propagation trials showed up the* ***ground effect****, which at first we did not believe, thinking there was something wrong with the measurements. But by listening to the jet noise at a distance, one could clearly hear the gap in the spectrum.*"

P. Parkin, Acoustical reminiscences: the Rayleigh Lecture, Proc. Inst. Acoustics, 1, 7-31 (1978)

Noise from explosion of 1 stick (0.57 kg) C4

Measured at 15 m from the source

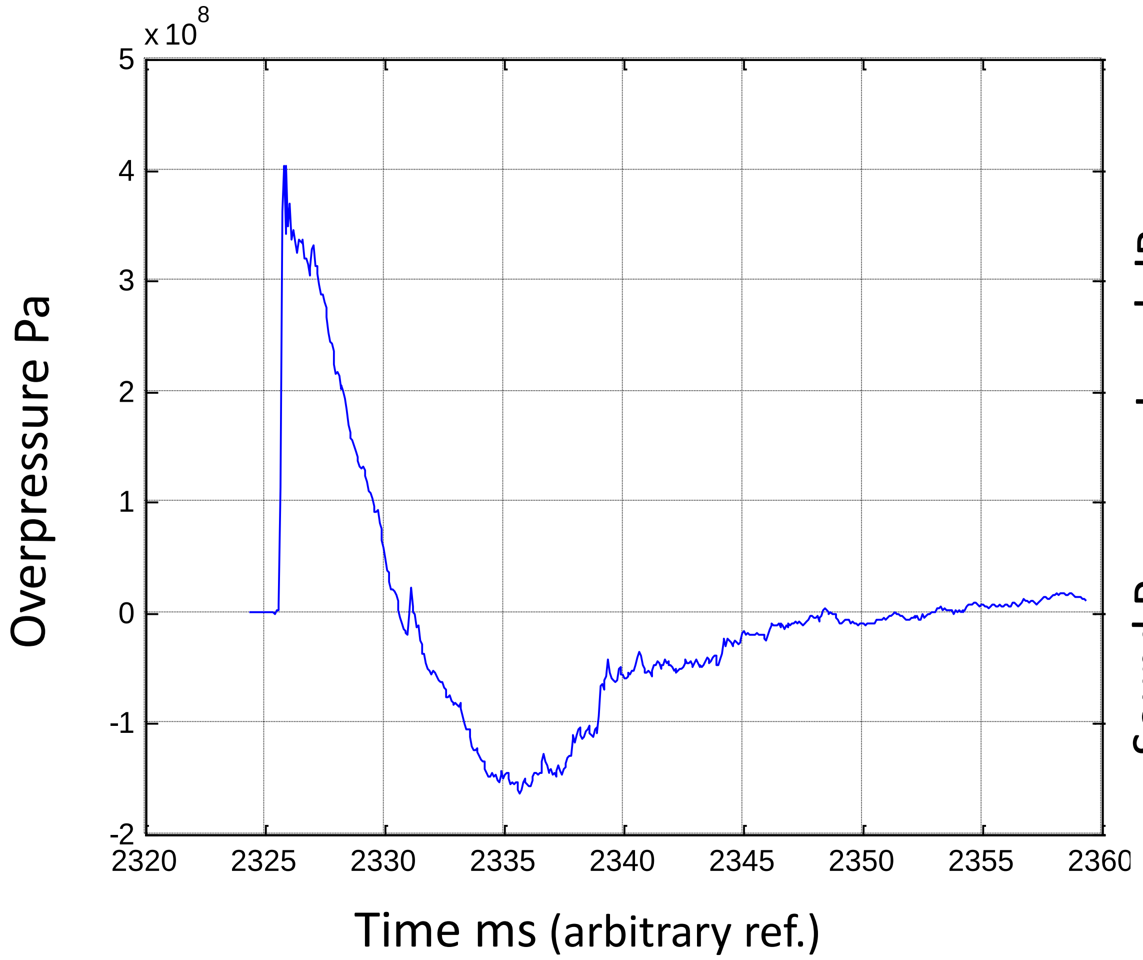

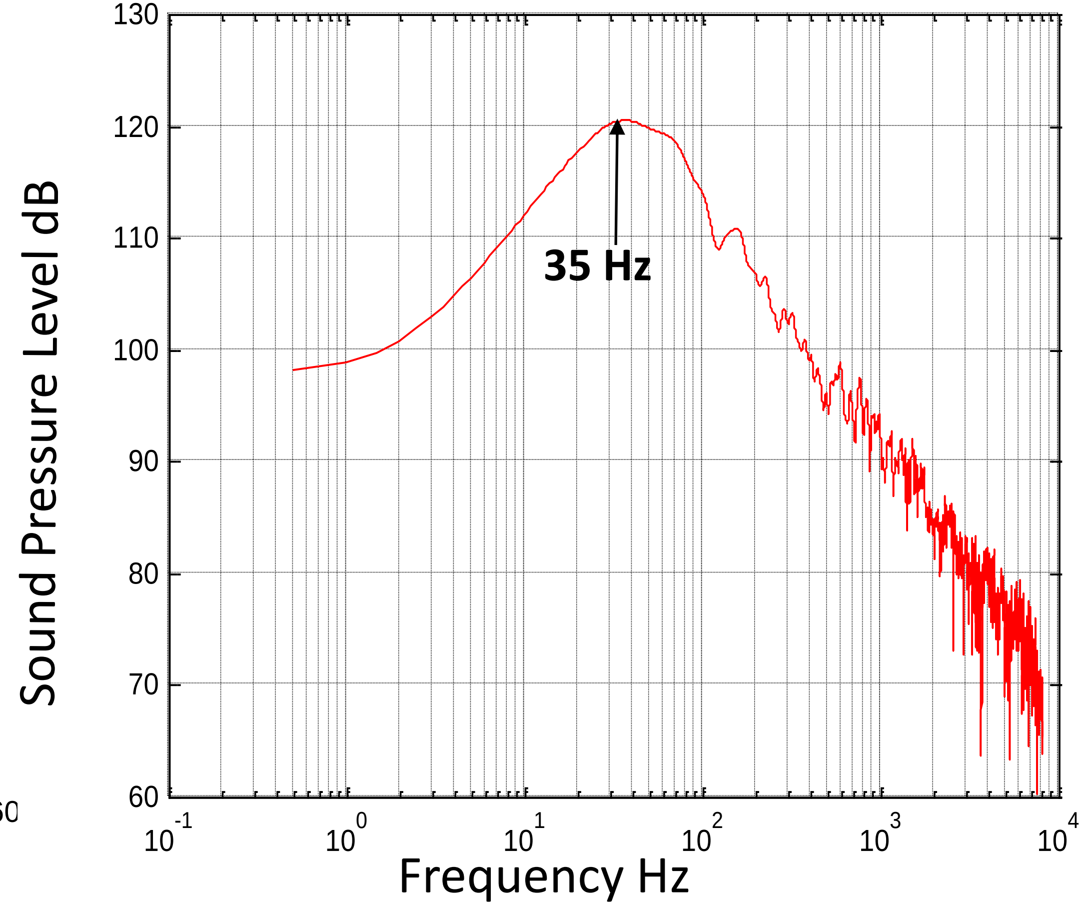

Blast Measurements Over Snow

D. Albert "*Blast noise mitigation by ground conditions*" NCEJ 2003

1.25 lbs. (0.57 kg) C4 at 30 m

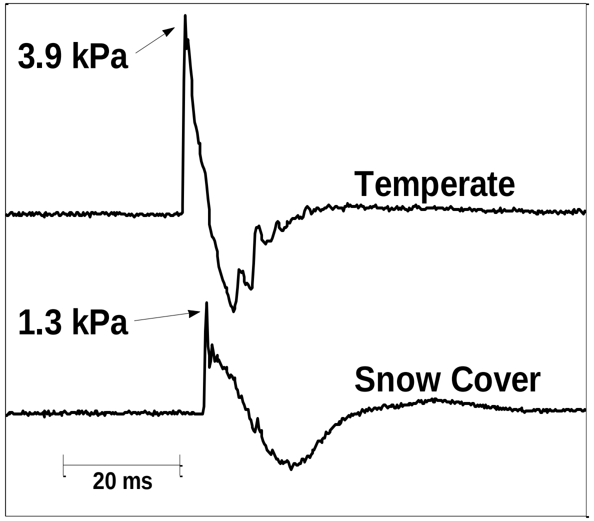

h_s =1.5m, h_r = 1.5 m

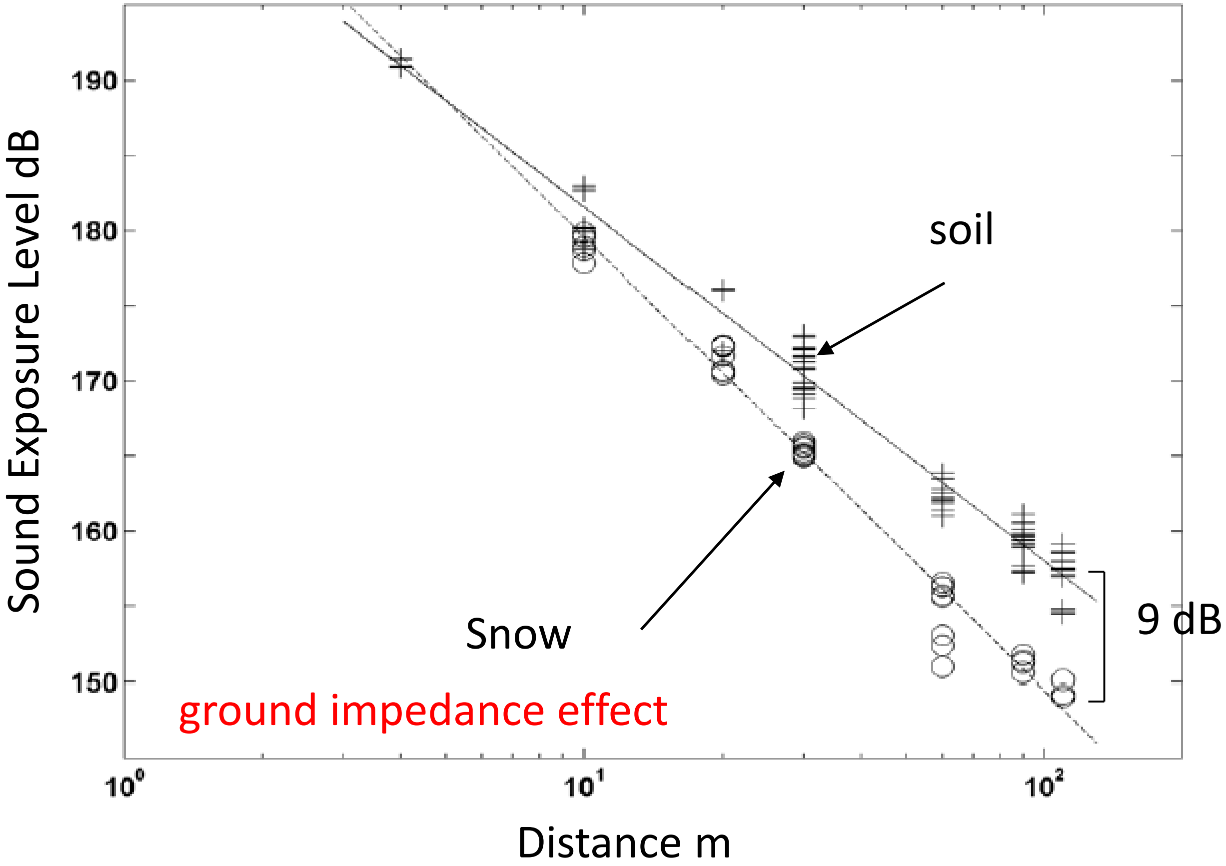

Effects on Blast Noise of ploughing

P. Schomer and K. Attenborough, *Basic results of tests at Fort Drum*, Noise Control Engineering Journal **53** 94 – 109 (2005)

1 stick of C4
at 2 m height

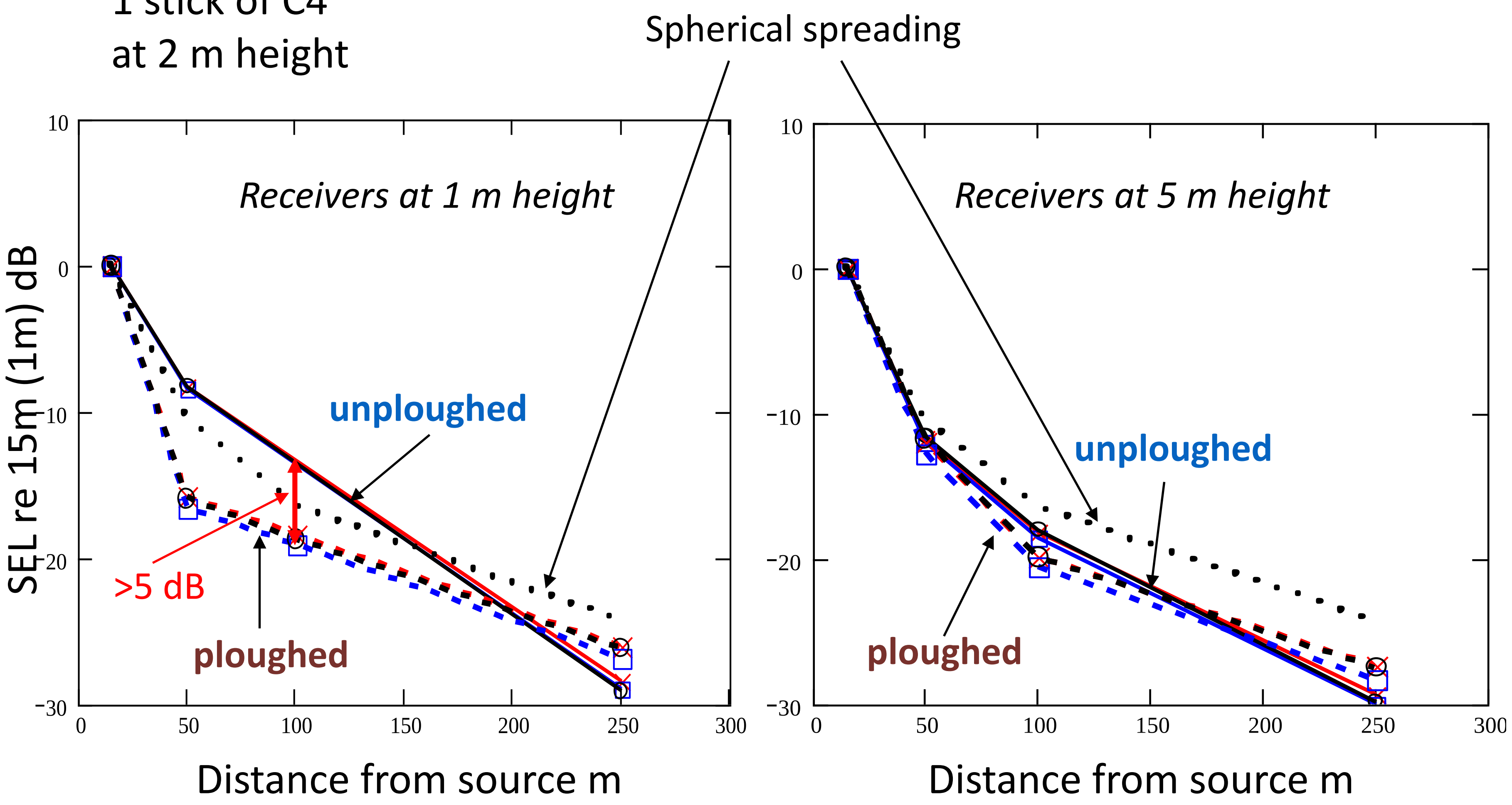

ground roughness effect

Geometrical spreading

spherical spreading

$$L_p = L_W - 20\log d - 11$$

cylindrical spreading

$$L_p = L_W - 10\log d - 8$$

Finite line (l) of incoherent point sources

$$L_p = L_W - 10\log d - 8 + 10\log\left[2\tan^{-1}\left(\frac{l}{2d}\right)\right] \text{ dB}$$

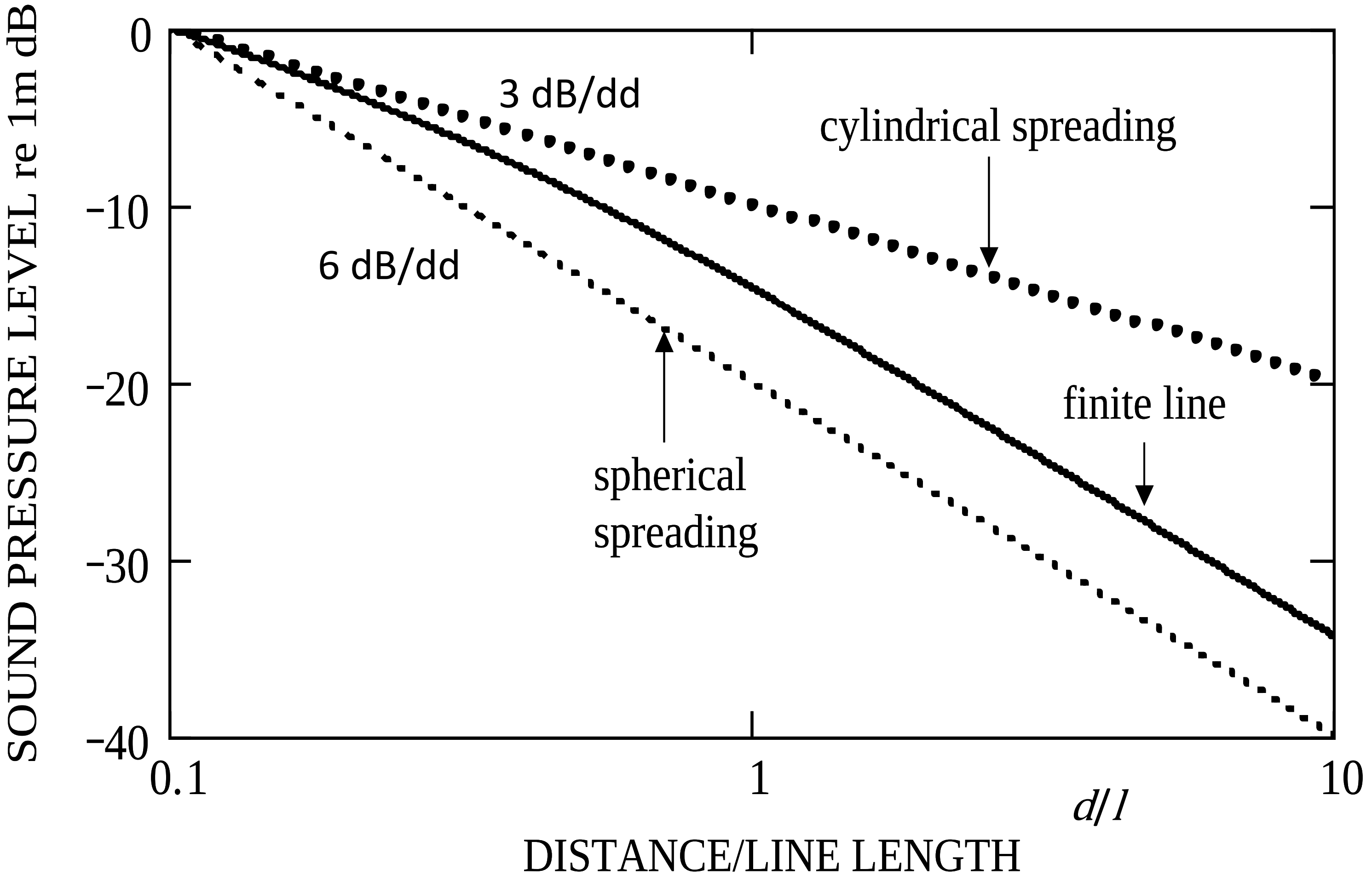

LABEX CELYA Université de Lyon

Air absorption

The Open University

Depends on temperature, pressure and relative humidity

$$p = p_0 e^{-\alpha x/2}$$

$$\alpha = f^2 \left[\left(\frac{1.84\times10^{-11}}{\left(\frac{T_0}{T}\right)^{\frac{1}{2}} \frac{p_s}{p_0}} \right) + \left(\frac{T_0}{T}\right)^{2.5} \left(\frac{0.10680 e^{-3352/T} f_{r,N}}{f^2 + f_{r,N}^2} + \frac{0.01278 e^{-2239.1/T} f_{r,O}}{f^2 + f_{r,O}^2} \right) \frac{nepers}{m \bullet atm} \right]$$

relaxation frequencies of vibration of nitrogen and oxygen molecules

$$f_{r,N} = \frac{p_s}{p_{s0}} \left(\frac{T_0}{T}\right)^{\frac{1}{2}} \left(9 + 280 H e^{-4.17\left[(T_0/T)^{1/3} - 1\right]}\right)$$

$$f_{r,O} = \frac{p_s}{p_{s0}} \left(24.0 + 4.04\times10^4 H \frac{0.02 + H}{0.391 + H}\right)$$

$$H = \rho_{sat} r_h p_0 / p_s \qquad \rho_{sat} = 10^{C_{sat}} \qquad C_{sat} = -6.8346 \left(T_0/T\right)^{1.261} + 4.6151$$

relative humidity (%)

H.E. Bass, L.C. Sutherland, A.J. Zuckewar: *Atmospheric absorption of sound: Further developments*, J. Acoust. Soc. Am. **97**, 680–683 (1995)

- varies through the day and the year
- diurnal variation greatest in summer
- (arithmetic) mean values of air absorption overestimate attenuation.
- in assessing worst case exposures better to use hourly means over a year

Indicative values

0.5 dB /km at 500 Hz

1.5 dB/km at 1 kHz

6 dB/km at 4 kHz

air acts as a low pass filter

Source-independent measurements

$$EA = 20\log\left(\frac{P_{total}}{P_{direct}}\right)$$

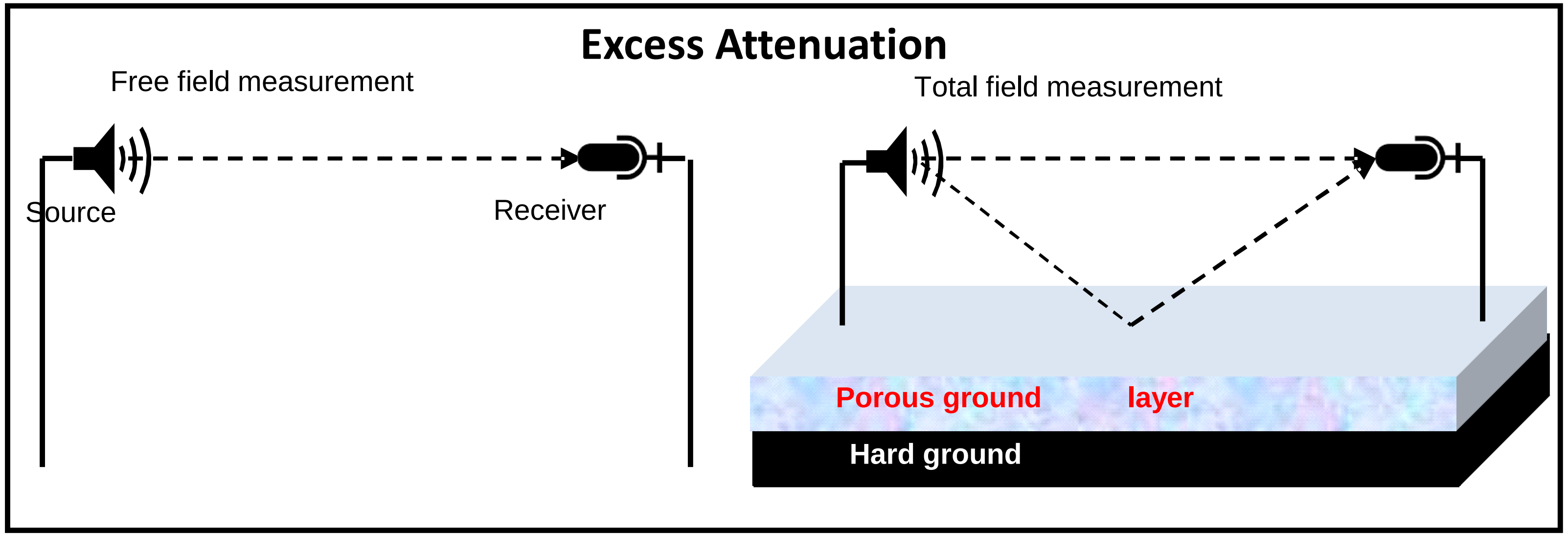

$$LD = 20\log\left(\frac{P_{UpperMic}}{P_{LowerMic}}\right)$$

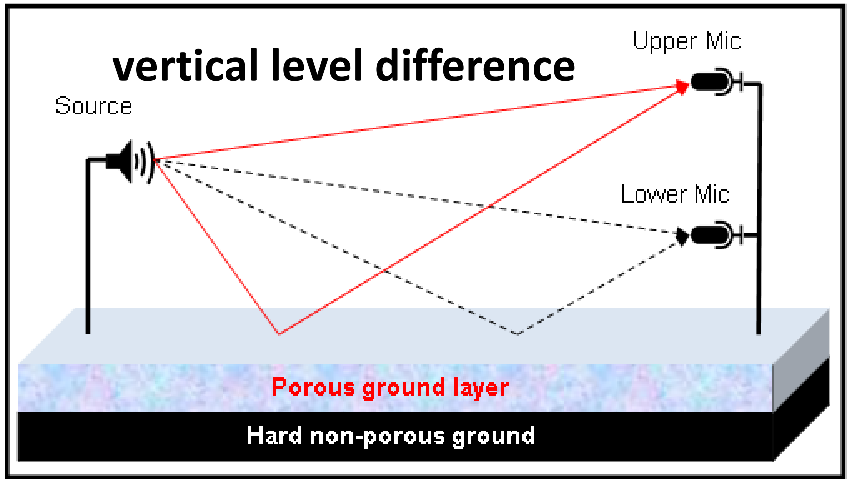

level difference between two locations

$$LD = 20\log\left[\frac{P_{mic1}}{P_{mic2}}\right]$$

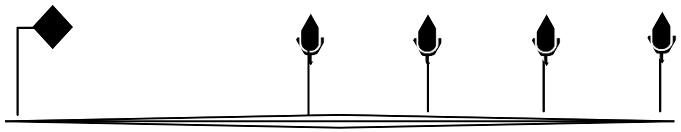

Parkin and Scholes ‘classical’ data

‘Horizontal’ level difference (third octaves) between 19 m and 347 m from a fixed Avon jet engine (source height ~2 m) above two airfields corrected for wavefront spreading and air absorption

"…. measurements [were] made at Site 2 [Radlett] with 6 to 9 in. of snow on the ground. The snow had fallen within the previous 24 hours and had not been disturbed. The attenuations with snow on the ground were very different from those measured under comparable wind and temperature conditions without snow….The maximum of the ground attenuation appears to have moved down the frequency scale by approximately 2 octaves…"

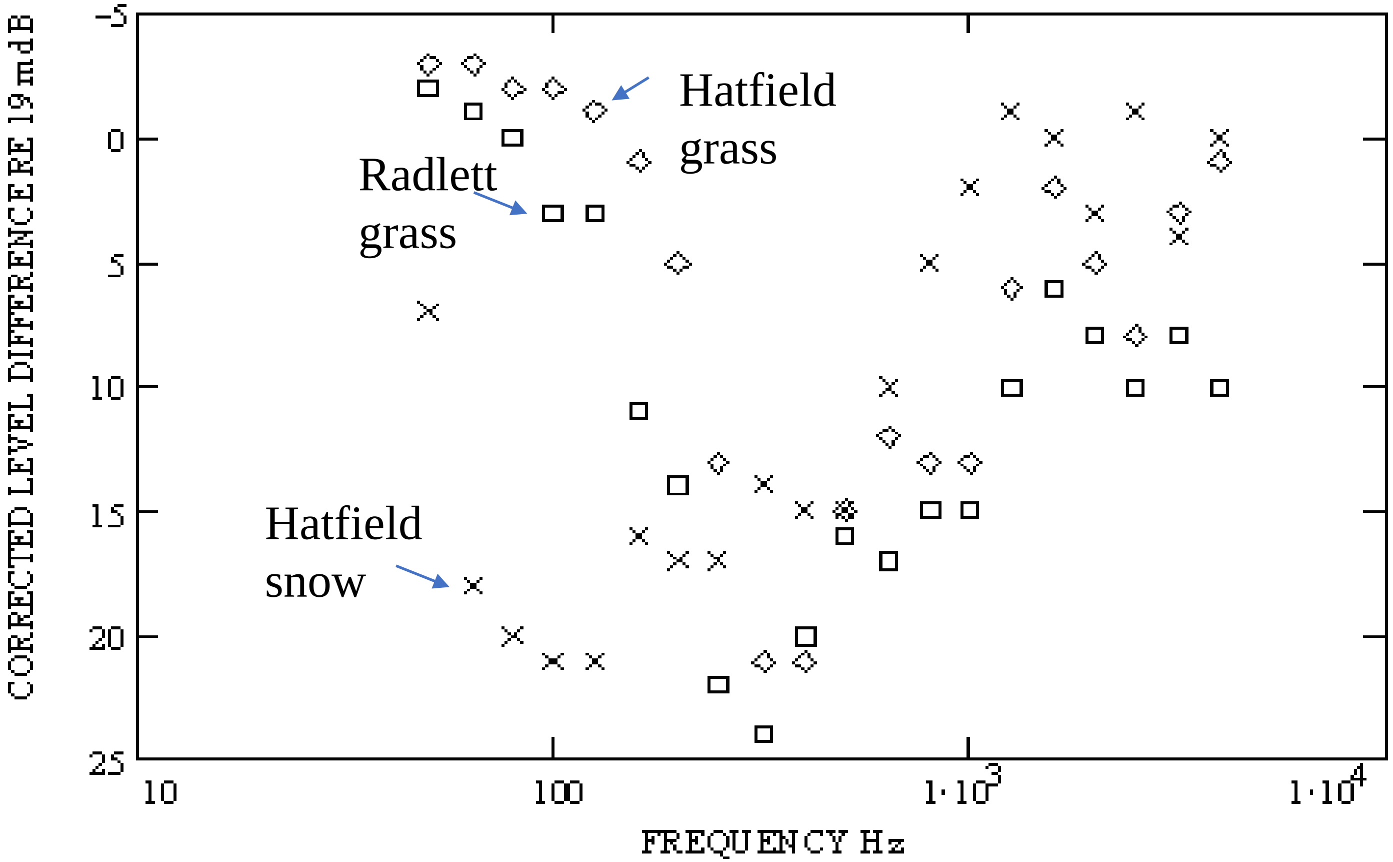

P. H. Parkin and W. E. Scholes, *The horizontal propagation of sound from a jet engine close to the ground at Radlett*, J. Sound Vib., **1** 1 –13 (1965)
P. H. Parkin and W. E. Scholes, *The horizontal propagation of sound from a jet engine close to the ground at Hatfield*, J. Sound Vib., **2** 353 –374 (1965)

A-weighted levels deduced from simultaneously-measured narrow band spectra (25 Hz intervals between 50 Hz and 10 kHz averaged over 26s intervals) at low (1.2 m) and high (6.4 m) microphones due to a fixed Avon jet engine source during low wind, low turbulence conditions at Hucknall

Run 454 Block No.	wind speed at ground (0.025 m) m s[-1]	wind speed at 6.4m height m s[-1]	Direction relative to line of mics. degrees	Temp. at ground °C	Temp. at 6.4m °C	Turbulence variable
2	1.57	1.86	23.3	10.4	9.9	0.0486
3	1.34	1.61	26.9	10.4	9.9	0.0962
4	1.27	1.96	349.0	10.5	9.8	0.0672
5	0.00	1.57	343.2	10.5	9.8	0.0873
6	0.00	1.46	346.0	10.5	9.8	0.1251
7	0.00	1.81	342.8	10.7	9.9	0.2371
19	0.00	0.00	301.6	10.2	9.8	0.0000
20	0.00	0.00	236.9	10.2	9.8	0.0000

$$c = \sqrt{\frac{\gamma P}{\rho}} = c_0\sqrt{\frac{T + 273.15}{273}}$$

$$c_{tot}(z) = c(T, z) + \boldsymbol{u}(\boldsymbol{z})$$

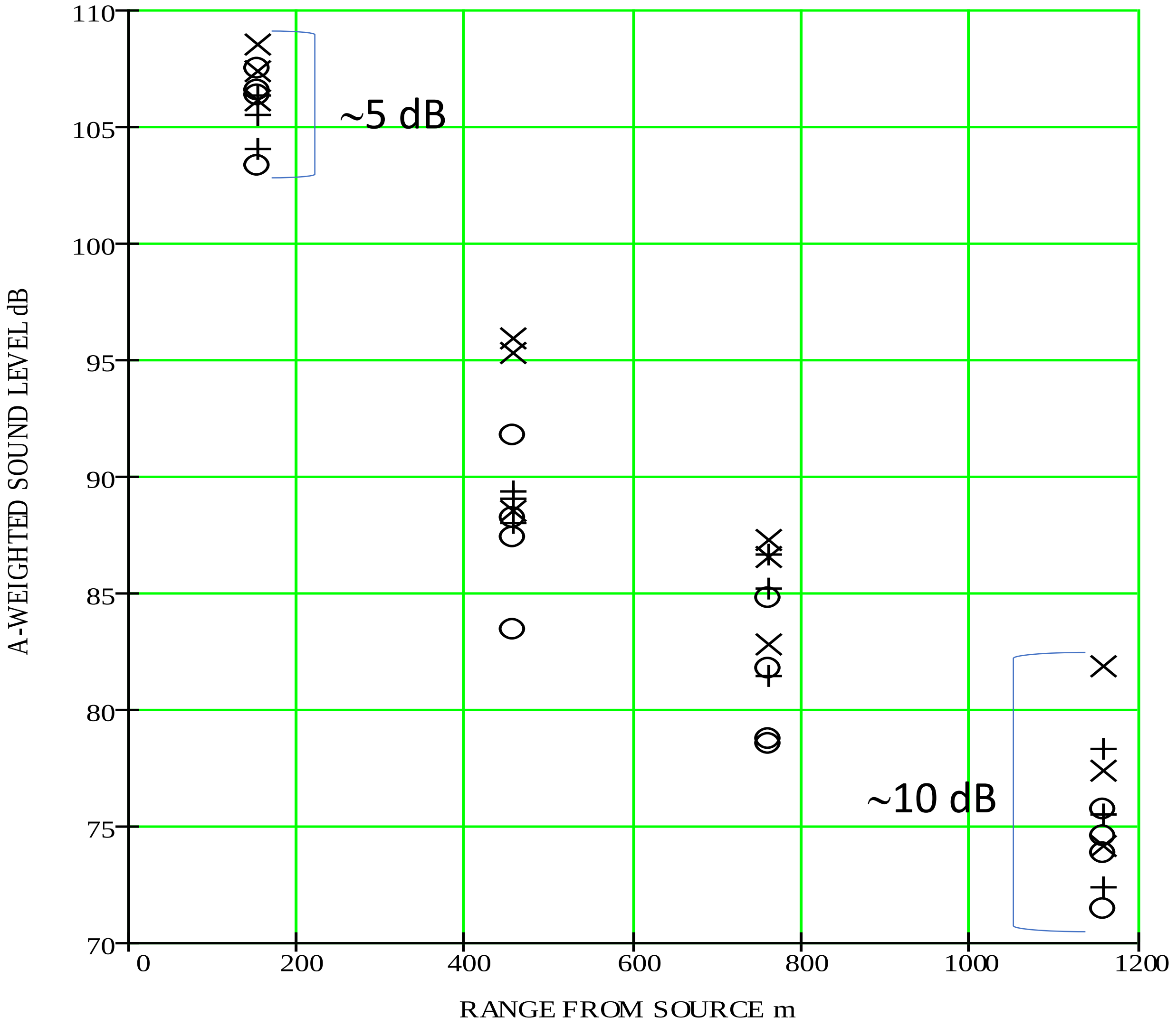

Even low wind and temperature gradients and low turbulence have significant effects on sound levels

Unpublished OU report for ESDU

Maximum, mean and minimum total attenuation for 10-minute L_{Aeq}.

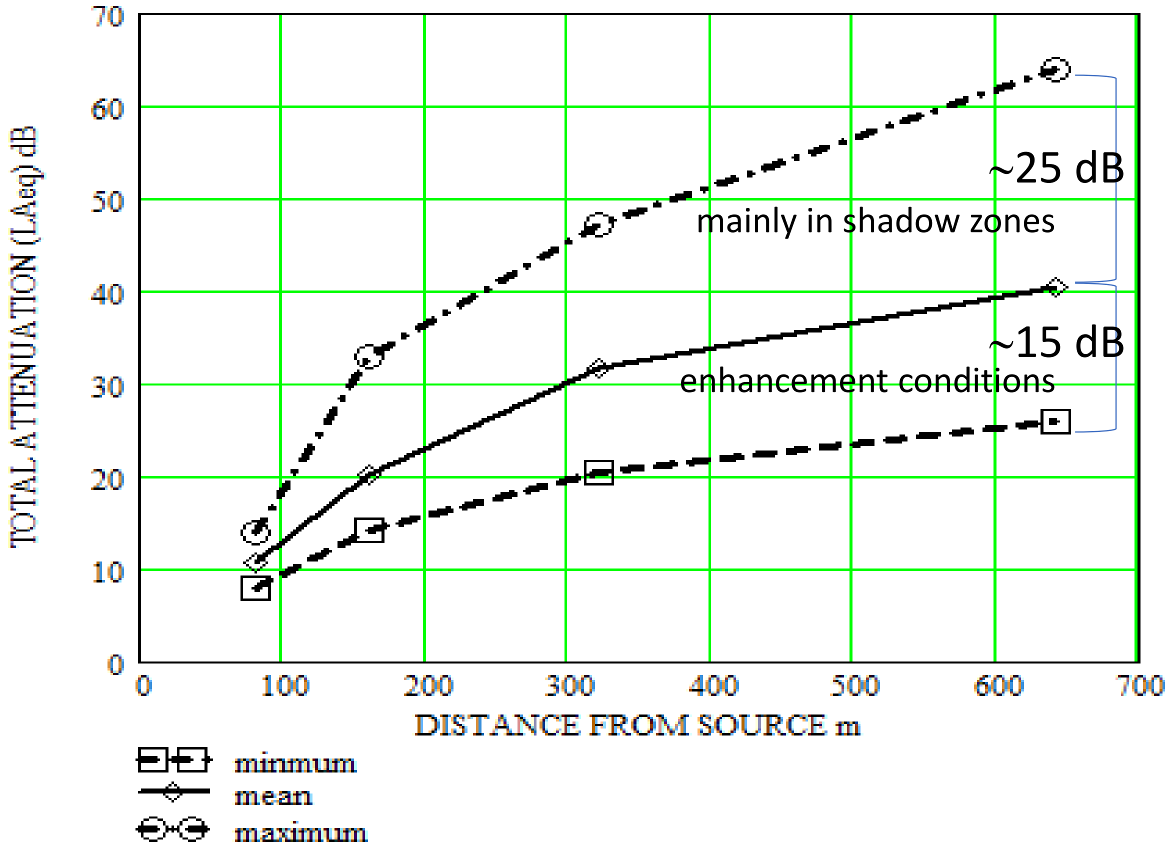

Temperature Gradient	Zero wind	Strong wind	Very strong wind
Very large neg. temp. grad.	Frequent	Occasional	Rare or Never
Large neg. temp. grad.	Frequent	Occasional	Occasional
Zero temp. grad.	Occasional	Frequent	Frequent
Large pos. temp. grad	Frequent	Occasional	Occasional
Very large pos. temp. grad.	Frequent	Occasional	Rare or Never

V. Zouboff, Y. Brunet, M. Berengier and E. Sechet, Proc. 6th International Symposium on Long range Sound propagation, ed. D.I.Havelock and M.Stinson, NRCC, Ottawa, 251-269, 1994

LABEX CELYA Université de Lyon

Pasquill Stability Classes

used for predicting air pollution dispersion

A: Extremely unstable conditions
B: Moderately unstable conditions
C: Slightly unstable conditions
D: Neutral conditions
E: Slightly stable conditions
F: Moderately stable conditions
G: Extremely Stable

The Open University

Meteorological conditions defining Pasquill stability classes

	Daytime insolation			Night-time conditions	
Surface wind speed (m/s)	**Strong**	**Moderate**	**Slight**	**Thin overcast or > 4/8 cloud**	**<= 4/8 cloud cover**
< 2	A	A - B	B	E	F
2 - 3	A - B	B	C	E	F
3 - 5	B	B - C	C	D	E
5 - 6	C	C - D	D	D	D
> 6	C	D	D	D	D

NOTES:

1. Strong insolation corresponds to sunny midday in midsummer (in England); slight insolation to similar conditions in midwinter.
2. Night refers to the period from 1 hour before sunset to 1 hour after sunrise.
3. The neutral category D should also be used, regardless of wind speed, for overcast conditions during day or night and for any sky conditions during the hour preceding or following night as defined above.

Pasquill 'neutral' classes are not acoustically-neutral

LABEX CELYA
Université de Lyon

The Open University

Meteorological classes for noise prediction

K.J. Marsh: *The CONCAWE Model for Calculating the Propagation of Noise from Open-Air Industrial Plants*, Appl. Acoust. **15**, 411–428 (1982)

W1	Strong wind (> 3 – 5 m/s) from receiver to source
W2	Moderate wind (≈ 1 – 3 m/s) from receiver to source, or strong wind at 45°
W3	No wind, or any cross wind
W4	Moderate wind (≈ 1 – 3 m/s) from source to receiver, or strong wind at 45°
W5	Strong wind (> 3 – 5 m/s) from source to receiver
TG1	Strong negative: Daytime with strong radiation (high sun, little cloud cover), dry surface and little wind
TG2	Moderate negative: as T1 but one condition missing
TG3	Near isothermal: early morning or late afternoon (e.g. one hour after sunrise or before sunset)
TG5	Moderate positive: night-time with overcast sky or substantial wind
TG6	Strong positive: night-time with clear sky and little or no wind

inversions

TG4 = acoustically-neutral

	W1	W2	W3	W4	W5
TG1	--------------	large attenuation	Small attenuation	Small attenuation	--------------
TG2	large attenuation	Small attenuation	Small attenuation	**Zero meteorological influence**	Small enhancement
TG3	Small attenuation	Small attenuation	**Zero meteorological influence**	Small enhancement	Small enhancement
TG4	Small attenuation	**Zero meteorological influence**	Small enhancement	Small enhancement	Large enhancement
TG5	---------------	Small enhancement	Small enhancement	Large enhancement	---------------

LABEX CELYA Université de Lyon

Monin-Obukhov Similarity Theory

The Open University

R.B. Stull: *An Introduction to Boundary Layer Meteorology* (Kluwer, Dordrecht 1991)

E. M. Salomons, *Computational Atmospheric Acoustics*, (Kluwer, Dordrecht, 2001)

Source to receiver wind speed profile

$$u(z)=\frac{u_*}{k}\left[\ln\left\{\frac{z+z_M}{z_M}\right\}+\psi_M\left(\frac{z}{L}\right)\right]$$

Temperature profile

$$T(z)=T_0+\frac{T_*}{k}\left[\ln\left\{\frac{z+z_H}{z_H}\right\}+\psi_H\left(\frac{z}{L}\right)\right]+\Gamma z$$

u_*	Friction velocity (m/s)	(depends on surface roughness)
z_M	Momentum roughness length	(depends on surface roughness)
z_H	Heat roughness length	(depends on surface roughness)
$T*$	Scaling temperature °K	A convenient value is 283 °K.
k	Von Karman constant	(= 0.41)
T_0	Temperature °C at zero height	Again, it is convenient to use 283 °K
Γ	Adiabatic correction factor	= –0.01 °C/m for dry air Small moisture influence.
L	Obukhov length (m) $> 0 \rightarrow$ stable, $< 0 \rightarrow$ unstable	$=\pm\frac{u_*^{\,2}}{kgT_*}(T_{av}+273.15)$, boundary layer thickness = 2L m.
T_{av}	Average temperature °C	
ψ_M	Diabatic momentum profile correction (mixing) function	$=-2\ln\left(\frac{(1+\chi_M)}{2}\right)-\ln\left(\frac{(1+\chi_M{}^2)}{2}\right)+2\arctan(\chi_M)-\pi/2$ if L<0 $= 5(z/L)$ if L > 0
ψ_H	Diabatic heat profile correction (mixing) function [2]	$=-2\ln\left(\frac{(1+\chi_H)}{2}\right)$ if L < 0 $= 5(z/L)$ if L > 0 or for z ≤ 0.5L
χ_M	Inverse diabatic influence or function for momentum	$=\left[1-\frac{16z}{L}\right]^{0.25}$
χ_H	Inverse diabatic influence function for momentum	$=\left[1-\frac{16z}{L}\right]^{0.5}$

Downward refracting sound speed profiles

E.M. Salomons: *Downwind propagation of sound in an atmosphere with a realistic sound speed profile: A semi-analytical ray model*, J. Acoust. Soc. Am. **95**, 2425–2436 (1994)

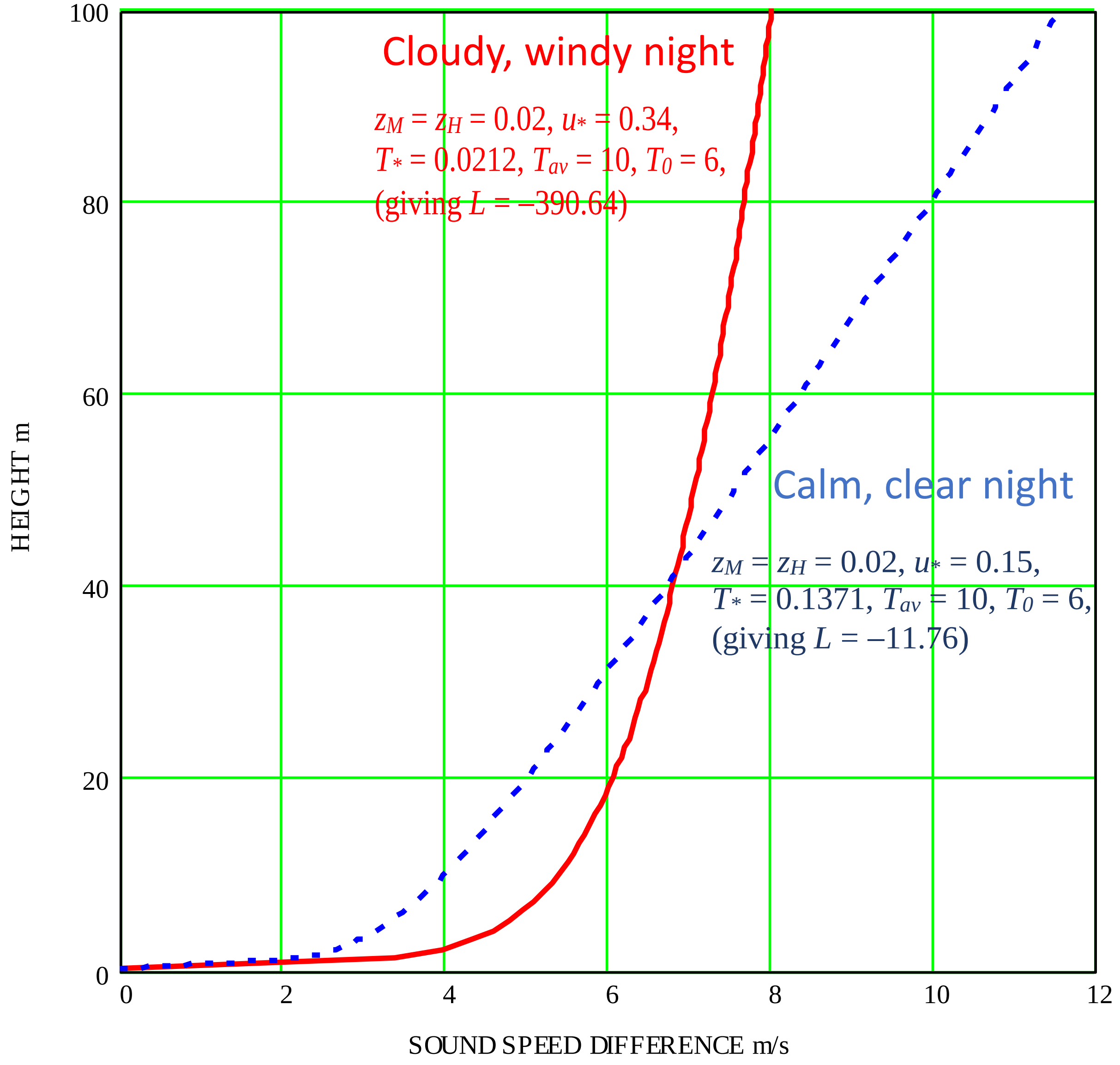

Daytime sound speed profiles

approximately logarithmic

$$c(z) = c(0) + b\ln\left[\frac{z}{z_0} + 1\right]$$

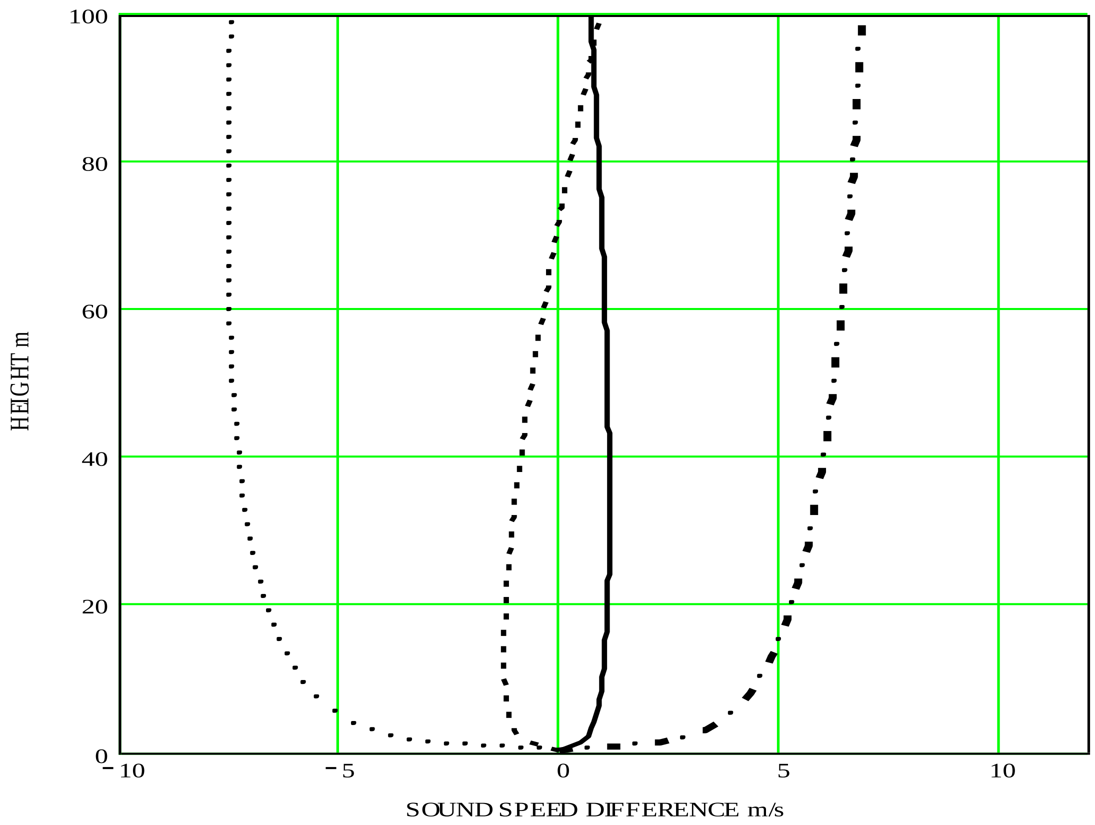

Meteorological effects are discussed again later.
Concentrate now on **ground effect**.

Line type	Wind speed at 10 m in m/s	Cloud Cover in octels	Pasquill Class	Direction
solid	1	0	A	downwind
dashed	1	0	A	upwind
dash-dot	5	4	C	downwind
dotted	5	4	C	upwind

Excess attenuation due to smooth hard ground

“Lloyd’s mirror” effect

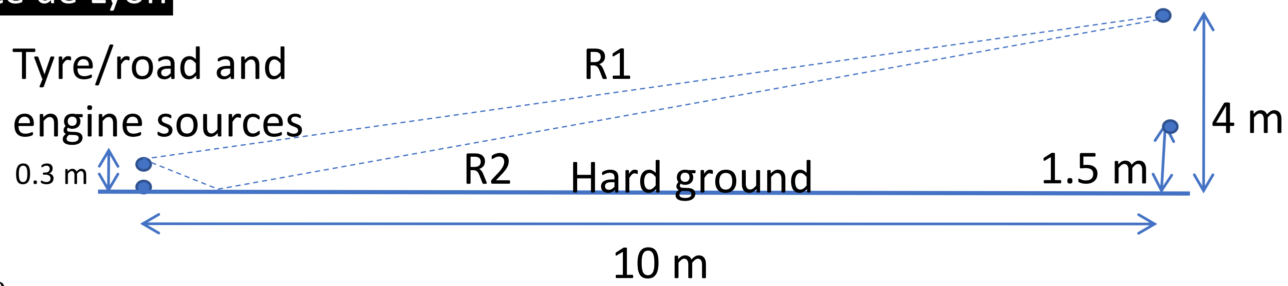

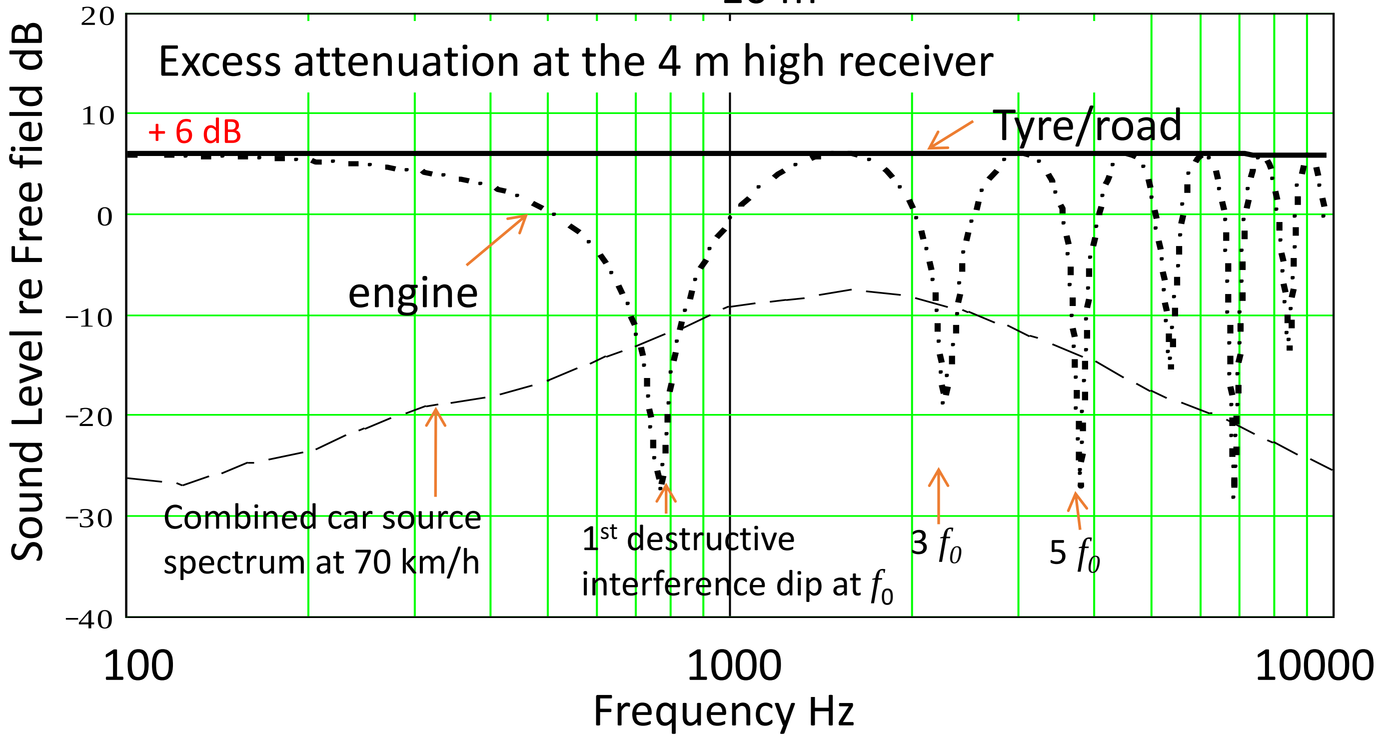

$(2\pi f_n/c)(R2 - R1) = (2n + 1)\pi/2$

$f_n = (2n + 1)c/2(R2 - R1)$

$n = 0,1,2,3\ldots$

First destructive interference is above 10 kHz for tyre/road source

For the 4 m high receiver and 0.3 m high (engine) source:

R2 – R1 = 0.223 m

$f_0 = 340/(2(R2 - R1))$
$= 763$ Hz

- ❑ At a 1.5 m high receiver, smooth hard ground increases car noise levels by 6 dB
- ❑ At a 4 m high receiver, hard ground increases car noise levels by 3 dB

Point source over impedance plane

K Attenborough, K M Li, K Horoshenkov, *Predicting Outdoor Sound*, Taylor and Francis 2007

Weyl - van der Pol formula

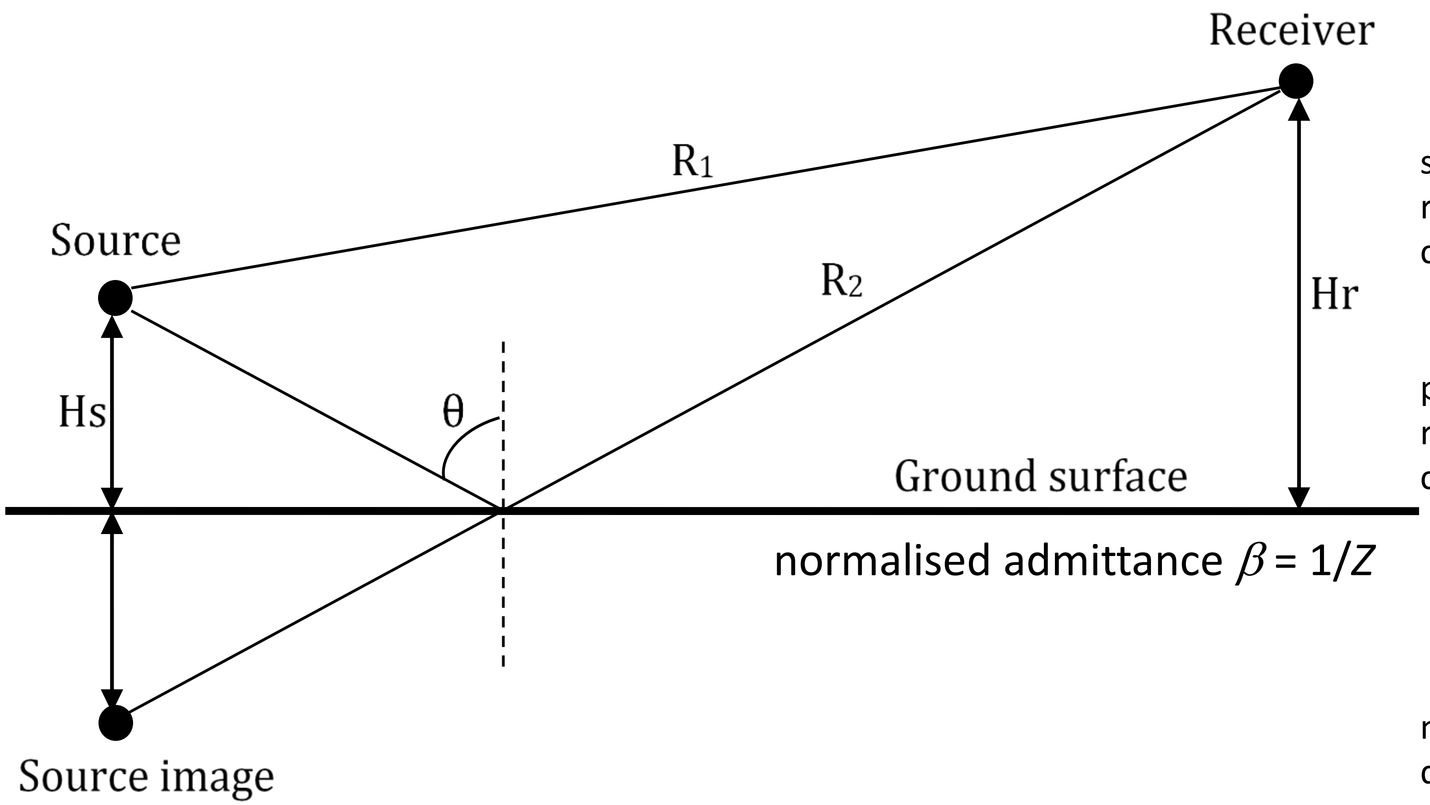

normalised admittance $\beta = 1/Z$

$$P_{total} = \frac{Pe^{ikR_1}}{R_1} + \frac{QPe^{ikR_2}}{R_2}$$

spherical wave reflection coefficient

$$Q = R_p + (1 - R_p)F(w)$$

Correction for wavefront curvature

plane wave reflection coefficient

$$R_p = \frac{\cos\theta - \beta}{\cos\theta + \beta}$$

$$F(w) = 1 + i\sqrt{\pi}we^{-w^2}\,\mathrm{erfc}(-iw)$$

numerical distance

$$w = \sqrt{\frac{ikR_2}{2}}(\cos\theta + \beta)$$

most outdoor surfaces are locally-reacting so acoustical properties represented completely by normal surface impedance (1/normalised admittance)

Ground Impedance Models - a short list

K. Attenborough, I. Bashir, S. Taherzadeh, *Outdoor ground impedance models*, J. Acoust. Soc. Am., **129** 2806-2819, (2011)

Model	No. of parameters*	Parameters
Delany and Bazley (1970), Miki (1990), modified Miki (2014)	1	Flow resistivity
Variable porosity (1977, 1992)	2	Flow resistivity, rate of porosity variation with depth or effective depth
Three-parameter Miki (1990)	3	Porosity, flow resistivity, structure factor
Zwikker and Kosten (1949)/ phenomenological (1951)	3	Porosity, flow resistivity, structure factor
Hamet (1993,1997)	3	Porosity, flow resistivity, structure factor
identical tortuous pores (1949, 1956, 1992)	3	Porosity, flow resistivity, tortuosity
Wilson Relaxation (1993)	4 or 2	Viscous and thermal relaxation times for low and high frequencies

* The impedance of many surfaces is best described as that of a hard-backed *layer so an* additional parameter of *thickness* is necessary

One-parameter polynomial impedance models

$$R = \rho_0 c_0 \left\{1 + a\left(\frac{f}{\sigma}\right)^b\right\} \qquad X = -\rho_0 c_0 \left\{c\left(\frac{f}{\sigma}\right)^d\right\}$$

$$\alpha = \frac{\omega}{c_0} p\left(\frac{f}{\sigma}\right)^q \qquad \beta = \frac{\omega}{c_0}\left\{1 + r\left(\frac{f}{\sigma}\right)^s\right\}$$

σ = effective flow resistivity

Model/ coefficient	a	b	c	d	p	q	r	s
Delany and Bazley [1]	0.0497	–0.754	0.0758	–0.732	0.169	–0.595	0.0858	–0.700
Miki [2]	0.070	–0.632	0.107	–0.632	0.160	–0.618	0.0109	–0.618
Modified Miki [3]	0.251	–0.632	0.384	–0.632	0.351	–0.632	0.539	–0.632

$$Z(L) = Z\coth(ikL) \qquad Z = R + iX \qquad k = \beta + \mathrm{i}\alpha$$

[1] M. E. Delany and E. N. Bazley, *Acoustical properties of fibrous materials*, Applied Acoustics **3** 105-116 (1970)

[2] Y. Miki, *Acoustical properties of porous materials - modifications of Delany-Bazley models*, J. Acoust. Soc. Japan (E) **11** 19 - 24 (1990)

[3] D. Dragna and P. Blanc-Benon, *Physically Admissible Impedance Models for Time-Domain Computations of Outdoor Sound Propagation*, Acta Acustica united with Acustica **100** 401 – 410 (2014)

One parameter models are not physically admissible

(Dragna and Blanc-Benon, Acta Acustica combined with *Acustica* **100** 401 – 410 *(2014))*

Passivity test

Condition	Test
Reality	Conj[$Z_S(\omega)$] = $Z_S(-\omega)$: $Z_s = Z_c$ or $Z(d)$
Passivity	Re[$Z_S(\omega)$] ≥ 0 for $\omega > 0$
Causality	No impulse response for $t < 0$

Hard-backed layer: σ = 100 kPa s m^{-2}, d = 0.01 m

$$Z(d) = Z_c \coth(-ikd)$$

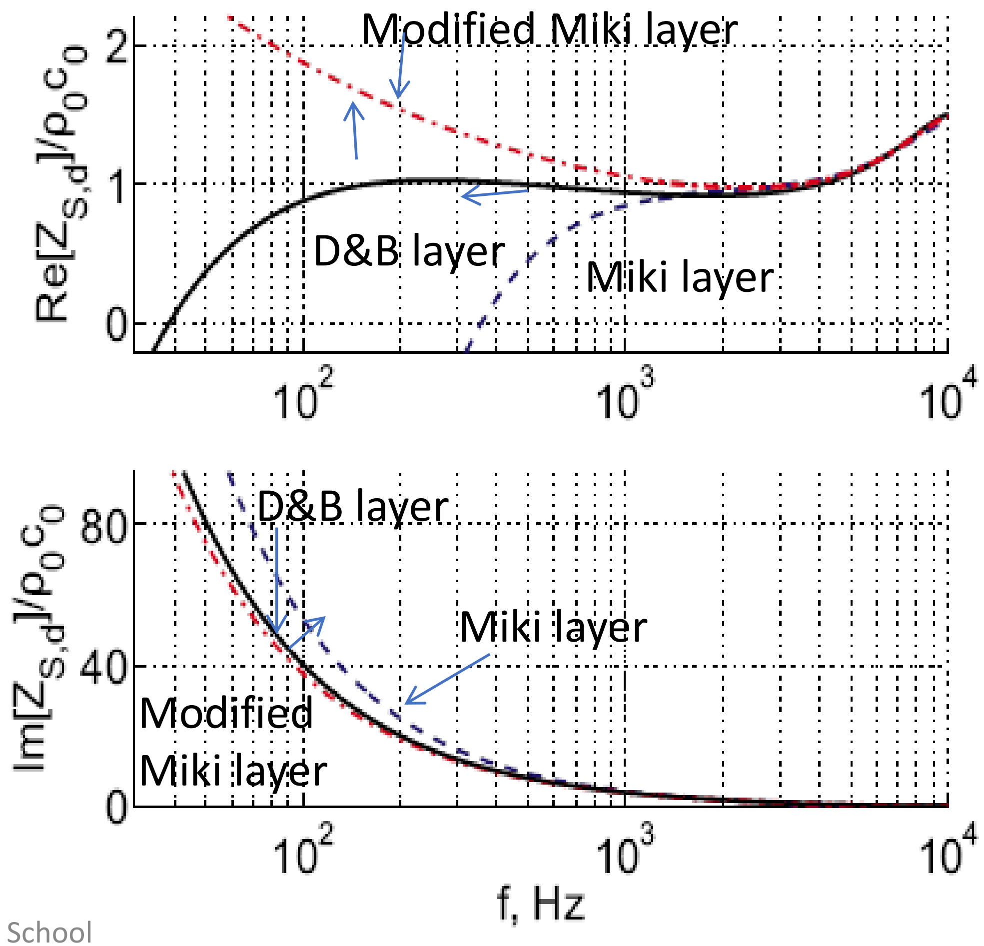

(Alternatively - Kramers-Krönig $\Rightarrow$ real and imaginary parts are related by Hilbert Transforms)

R. Kirby [Applied Acoustics **86** 47 - 49 (2014)]

Test Re(complex density) ≥ 0

Tests with 'soil-like' layer parameter values:
σ = 200 kPa s m^{-2}, Ω = 0.4, L = 0.03 m

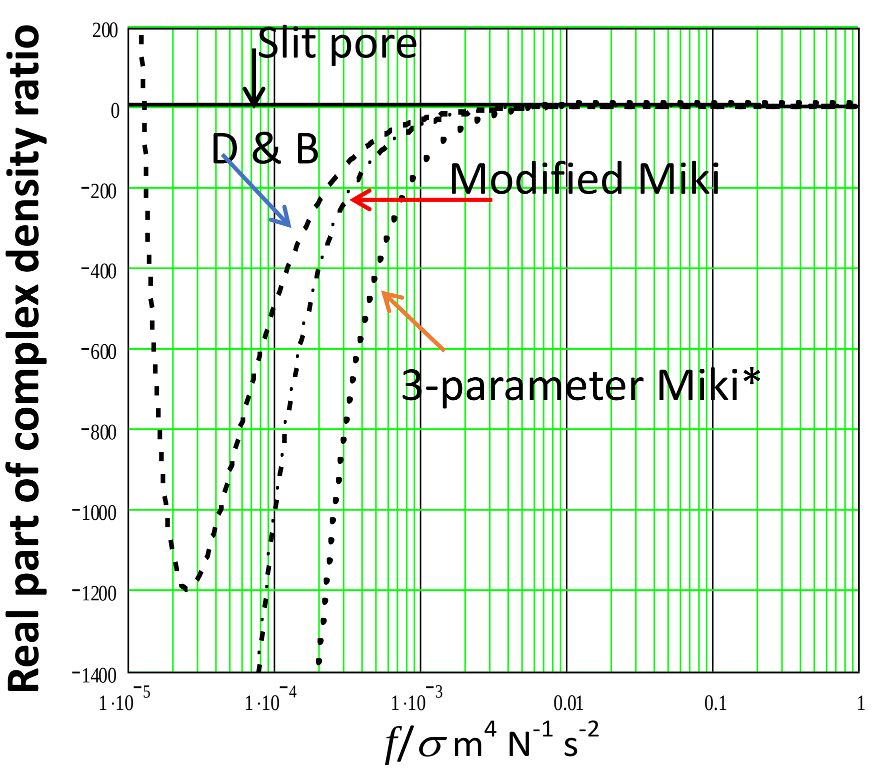

Real part of density ratio becomes negative below 2 kHz for D&B layer and Miki layer models. Slit pore layer model is OK.

Tests with 'snow-like' layer parameter values:
σ = 10 kPa s m^{-2}, Ω = 0.7, L = 0.1 m

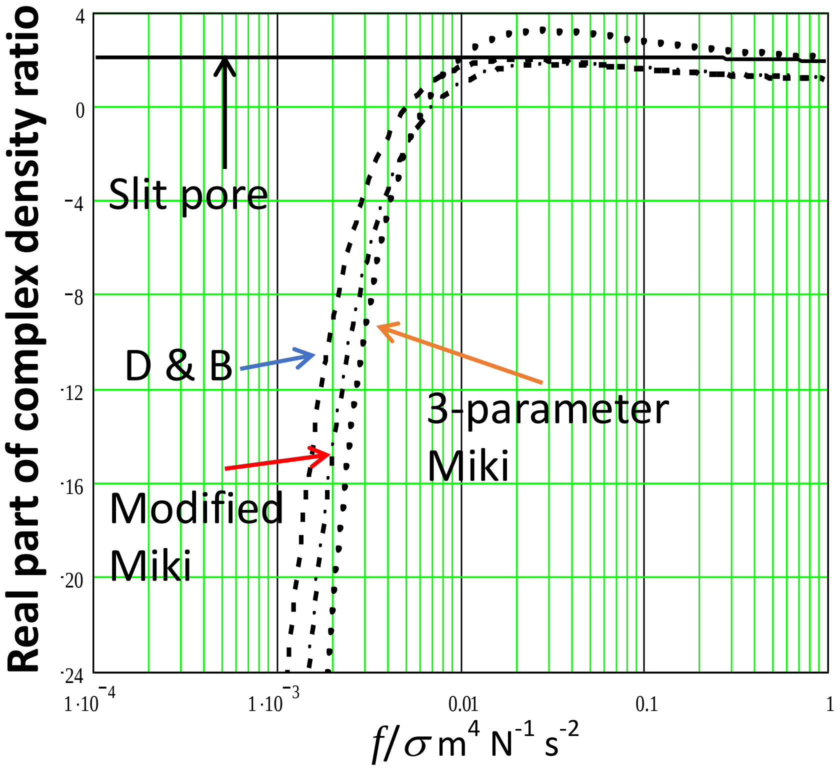

Real part of density ratio becomes negative below 100 Hz for D&B and both Miki models. Slit pore model is OK.

*Y. Miki, *Acoustical properties of porous materials generalizations of empirical models*, J. Acoust. Soc. Japan (E) **11** 25 - 28 (1990)

more passivity tests

‘soil-like’ layer

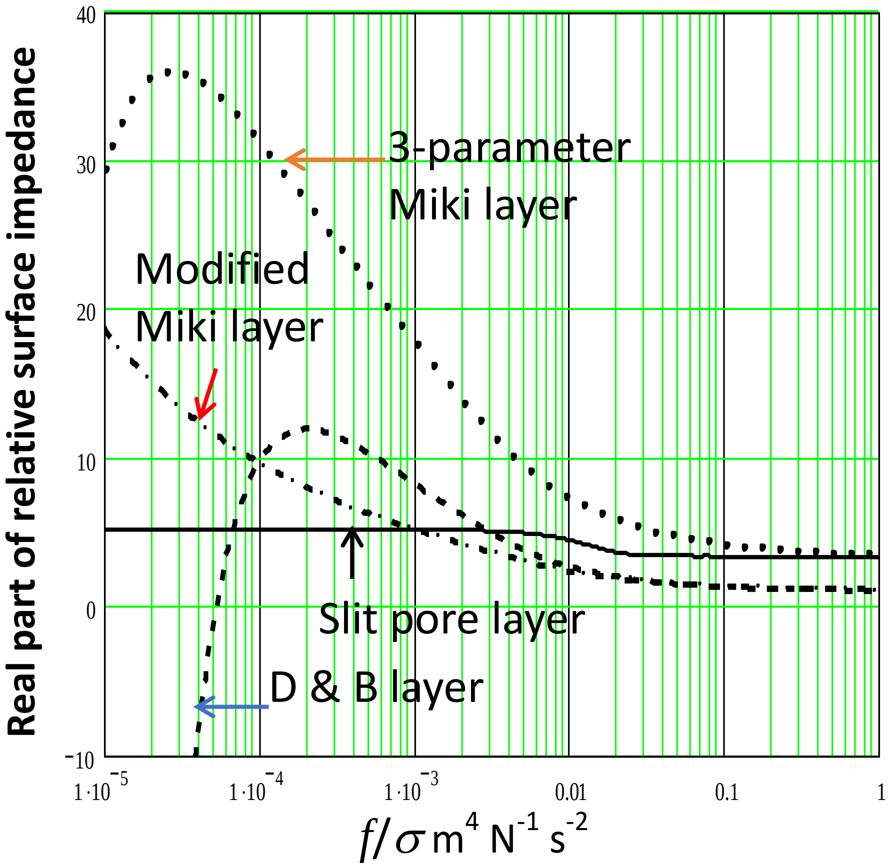

‘snow-like’ layer

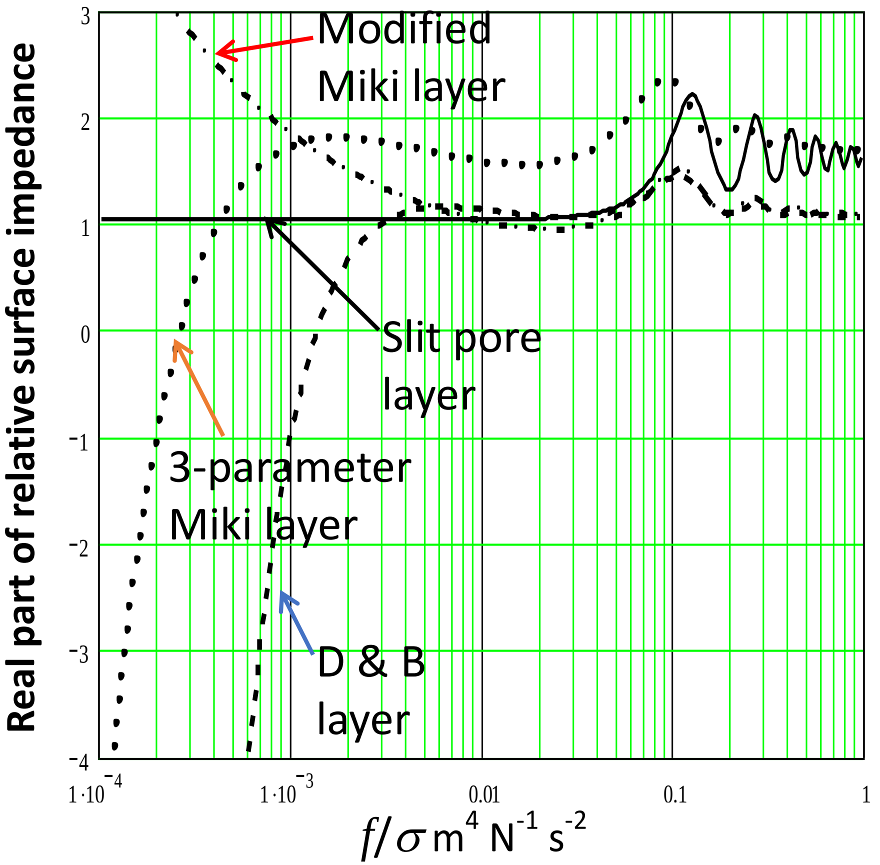

Real part of relative surface impedance becomes negative below 10 Hz for D&B layer.
Slit pore layer and modified Miki layer models are OK but Miki model predictions implausible.

Real part of relative surface impedance negative below 40 Hz for D&B and below 5 Hz for 3-parameter Miki layer models.
Slit pore layer and modified Miki layer models are OK.

Physically-admissible ground impedance models

Variable Porosity (2 parameters: R_e, α_e)

effective flow resistivity

effective rate of change of porosity with depth = 4/effective depth

$$Z = \frac{1+i}{\sqrt{\pi\gamma\rho_0}}\sqrt{\frac{R_e}{f} + \frac{ic_0\alpha_e}{8\pi\gamma f}}$$

Hamet (3 parameters: R_s, Ω, T)

$$Z_C = \left(\frac{1}{\Omega}\right)\left(\frac{T}{\gamma}\right)^{\frac{1}{2}}\left\{1 + \frac{\gamma-1}{\gamma}\left(\frac{1}{F_0}\right)^{\frac{1}{2}}\right\}F_\mu^{\frac{1}{2}},\ k = \gamma\Omega k_0 Z_c$$

$$F_\mu = 1 + i\,\omega_\mu/\omega,\ F_0 = 1 + i\,\omega_0/\omega,\ \omega_\mu = (R_s/\rho_0)(\Omega/T),\ \omega_0 = \omega_\mu(T/N_{PR})$$

Identical slit pores (3 parameters: R_s, Ω, T)

$$\rho(\omega) = \rho_0[1 - \tanh(\lambda\sqrt{-i})/(\lambda\sqrt{-i})]^{-1}$$

$$C(\omega) = (\gamma P_0)^{-1}[\gamma - (\gamma-1)H(\lambda\sqrt{(N_{PR})})]$$

$$H(\lambda) = 1 - \tanh(\lambda\sqrt{-i})/(\lambda\sqrt{-i})]$$

$$\lambda = \left(\frac{3\rho_0\omega T}{\Omega R_s}\right)^{1/2}$$

tortuosity

porosity

flow resistivity

$$k(\omega) = \omega[T\rho(\omega)C(\omega)]^{0.5}$$

$$Z_C(\omega) = (\rho_0 c_0)^{-1}[(T/\Omega^2)\rho(\omega)/C(\omega)]^{0.5}$$

Wilson Relaxation (3 parameters: R_s, Ω, T (or 2 or 4))

$$k = \frac{\omega\sqrt{T}}{c_0}\left[\left(1+\frac{\gamma-1}{\sqrt{1-i\omega\tau_e}}\right)\Big/\left(1-\frac{1}{\sqrt{1-i\omega\tau_v}}\right)\right]^{1/2}\quad Z = \frac{\sqrt{T}}{\Omega}\left[\left(1+\frac{\gamma-1}{\sqrt{1-i\omega\tau_e}}\right)\left(1-\frac{1}{\sqrt{1-i\omega\tau_v}}\right)\right]^{-1/2}$$

$$\tau_v = 2\rho_0 T/\Omega R_s \qquad \tau_e \cong 3.1\rho_0/R_s$$

Hard-backed layer $\quad Z(d) = Z_c \coth(-ikd)$

Notes on physically-admissible models

- The commonly-used Phenomenological Model is inconsistent between LF and HF

Morse and Ingard
also called Zwikker and Kosten

$$Z_c = \frac{1}{\Omega}\sqrt{K + \frac{iR_s\Omega}{\omega\rho_0}} \qquad k = \Omega k_0 Z_c$$

K is structure factor,
R_s is flow resistivity

LF approximation of identical tortuous pore models

$$Z_c = \frac{1}{\Omega\sqrt{\gamma}}\sqrt{T + \frac{iR_s\Omega}{\omega\rho_0}} \qquad k = \sqrt{\gamma}\,\Omega k_0 Z_c$$

LF conditions in pores are isothermal rather than adiabatic

- Structure factor $K \equiv$ Tortuosity T

- Slit pore, Wilson and Hamet models give similar predictions

- Use $T = \Omega^{-n}$ to reduce 3 parameters to 2 in Phenomenological, Hamet, 3-para Miki and identical pore models

  Ω = porosity,
  n = grain shape factor = 0.5 or 1

Comparisons with short range data for grasslands

LABEX CELYA
Université de Lyon

The Open University

NORDTEST ACOU 104 geometry
source height 0.5 m,
receiver heights at 0.5 and 0.2 m,
separation 1.75 m

$$E = \sum_{f} |LD_M(f) - LD_C(f)|$$

$$LD_C = EA(1) - EA(2)$$

$$EA(1) = 20\lg\left[\left|1 + \frac{QR_2}{R_1} e^{k(R_2 - R_1)}\right|\right]$$

$$EA(2) = 20\lg\left[\left|1 + \frac{QR_4}{R_3} e^{k(R_4 - R_3)}\right|\right]$$

Mean fitting errors over 29 grassland sites

Model	Fitting error dB
Delany and Bazley	9.3
Phenomenological	8.7
Variable porosity	6.7

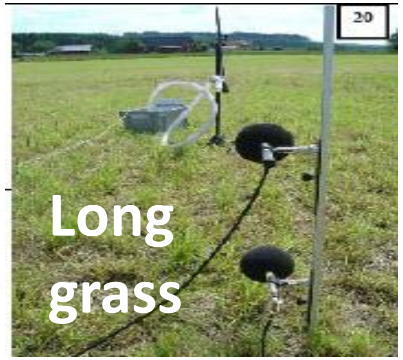

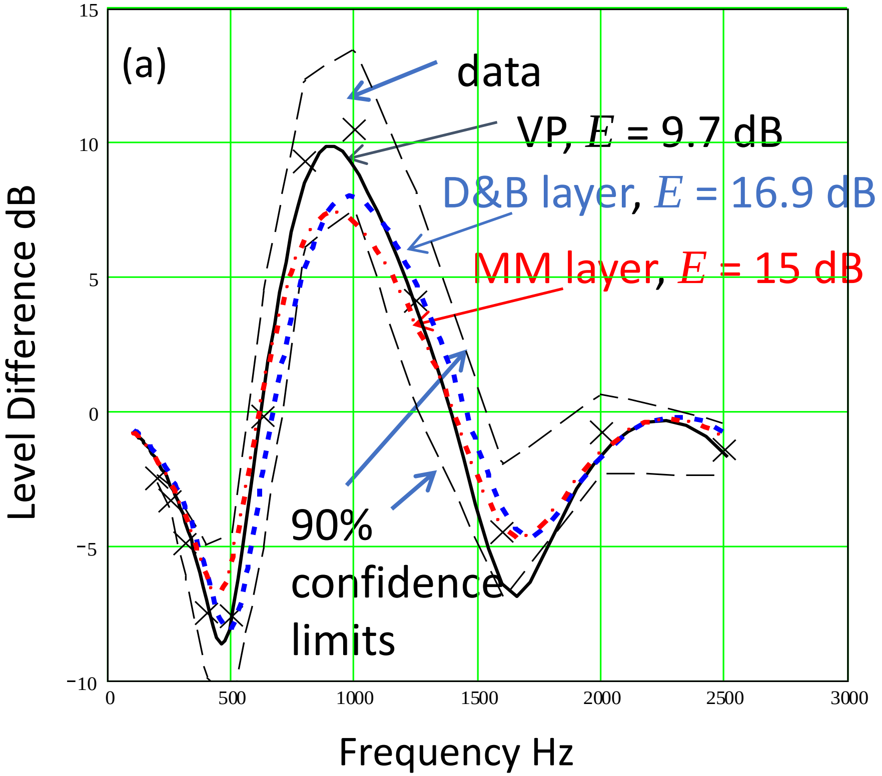

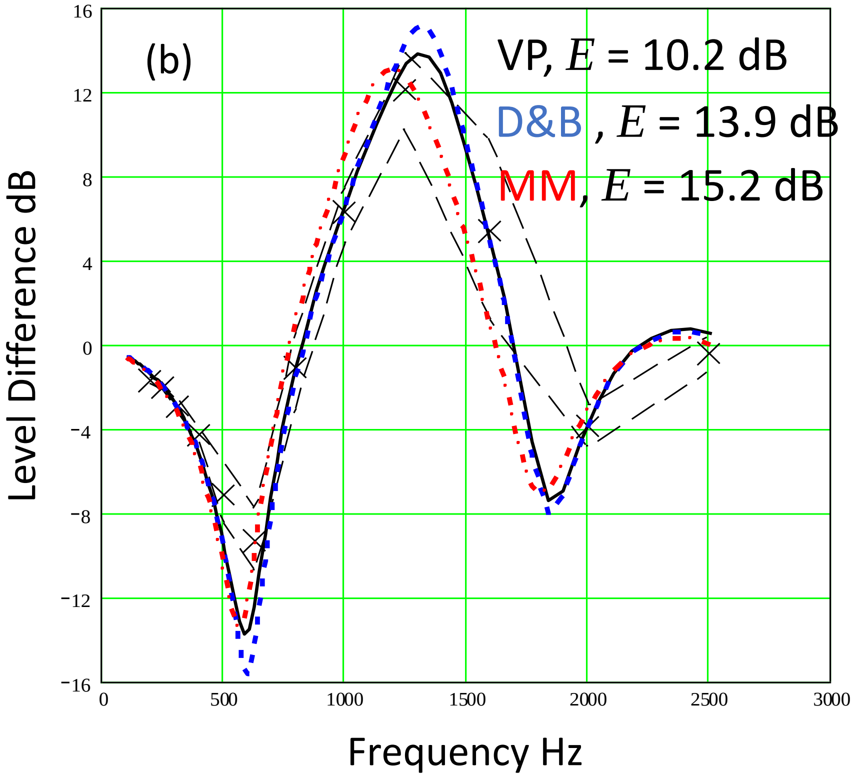

Comparisons with short range data for gravel

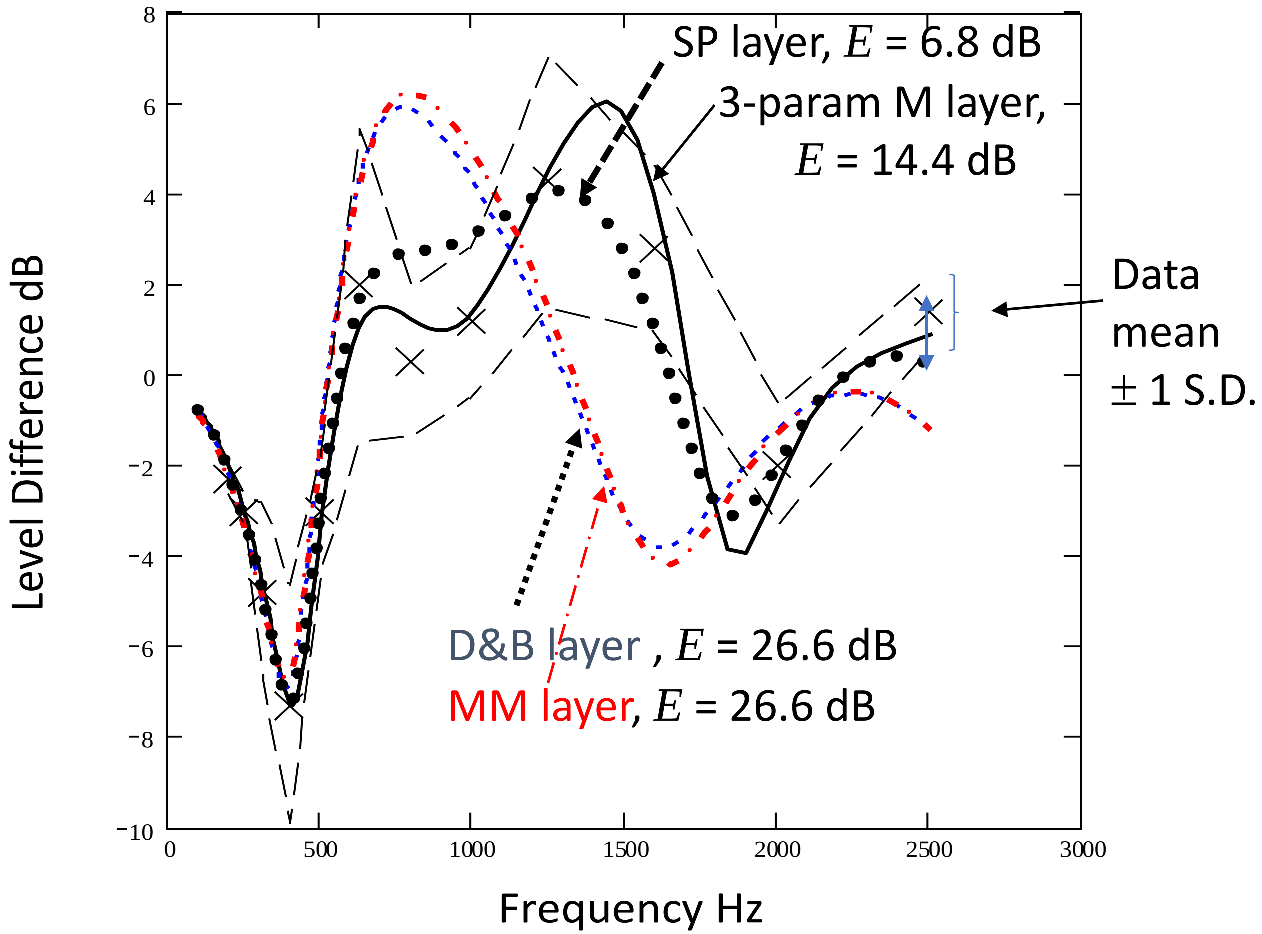

Although requiring more than one parameter, slit pore, Wilson and Hamet models are physically admissible, give more or less identical predictions and enable better agreement with short range data over low flow resistivity surfaces than physically inadmissible single parameter models.

Ground Parameter Values

Grassland (variable porosity)

Grassland description	Flow resistivity kPa s m^{-2}	Effective depth m
Pasture NORDTEST site #26	824.6	0.07
Pasture NORDTEST site #19	383.4	0.09
long grass NORDTEST #20	167.2	0.08
Lawn NORDTEST site #1	75.3	0.09
Heath NORDTEST #44	51.9	0.12

Various (2-parameter slit pore)

Ground description	Effective flow resistivity kPa s m^{-2}	Effective porosity
Beech wood floor	14	0.51
Pine forest floor	27	0.44
gravel	34	0.33
Pine forest floor	62	0.38
Institutional grass	159	0.45

CNOSSOS-EU (based on Delany and Bazley one-parameter model)

Description	Type	Flow resistivity kPa s m^{-2}	G value
Very soft (snow or moss like)	A	12.5	1
Soft forest floor (short, dense heather-like or thick moss)	B	31.5	1
Uncompacted, loose ground (turf, grass, loose soil)	C	80	1
Normal uncompacted ground (forest floor, pasture field)	D	200	1
Compacted field and gravel (compacted lawns, park area)	E	500	0.7
Compacted dense ground (gravel road, parking lot)	F	2000	0.3
Hard surfaces (most normal asphalt, concrete)	G	20000	0
Very hard and dense surfaces (dense asphalt, concrete, water)	H	200000	0

Annex to Commission Directive 2015/996 in Official Journal of the European Union L168 (2015)

Grassland variation v Seasonal variation

G Guillaume, O Faure, B Gaivreau, F. Junker and M Berengier, '*Estimation of impedance model input parameter from in situ measurements: Principles and applications*' Applied Acoustics **95** 27 - 36 (2015)

Fits to short range data for Lawn

	Summer		Winter	
	flow resistivity kPa s m^{-2}	**layer thickness m**	**flow resistivity kPa s m^{-2}**	**layer thickness m**
mean	80	0.035	200	0.011
maximum	105	0.023	285	0.008
minimum	60	0.035	115	0.018

Predicted ground-type variation (based on fits to NORDTEST grassland data and CNOSSOS-EU)

source height 0.05 m, receiver height 4 m and horizontal separation 100 m, moderate turbulence

Predictions include moderate turbulence

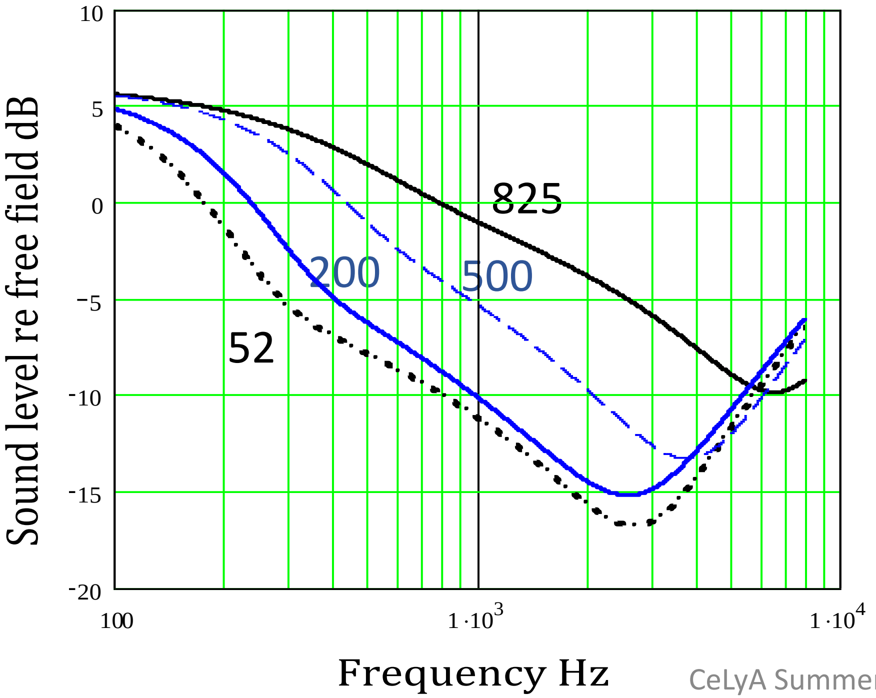

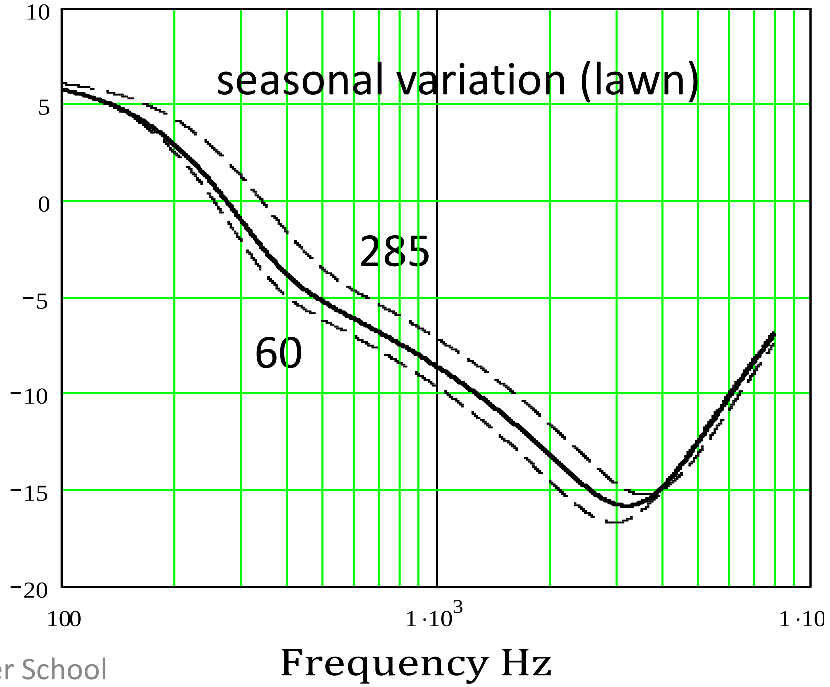

Measurements and predictions over smooth and rough soil

J. P. Chambers, J. M. Sabatier, *Recent advances in utilizing acoustics to study surface roughness in agricultural surfaces*, Applied Acoustics **63** 795–812 (2002)

$$\beta_{rough} = \beta_{smooth} + ik\,\langle H \rangle/2$$

$\langle H \rangle$ = mean roughness height

Surface condition	Effective flow resistivity kPa s m^{-2}	porosity	tortuosity
undisturbed	159	0.46	1.6
ploughed	10	0.60	3.3

Hs = 7.5 cm, Hr = 0.3 cm, r = 10.0 m.

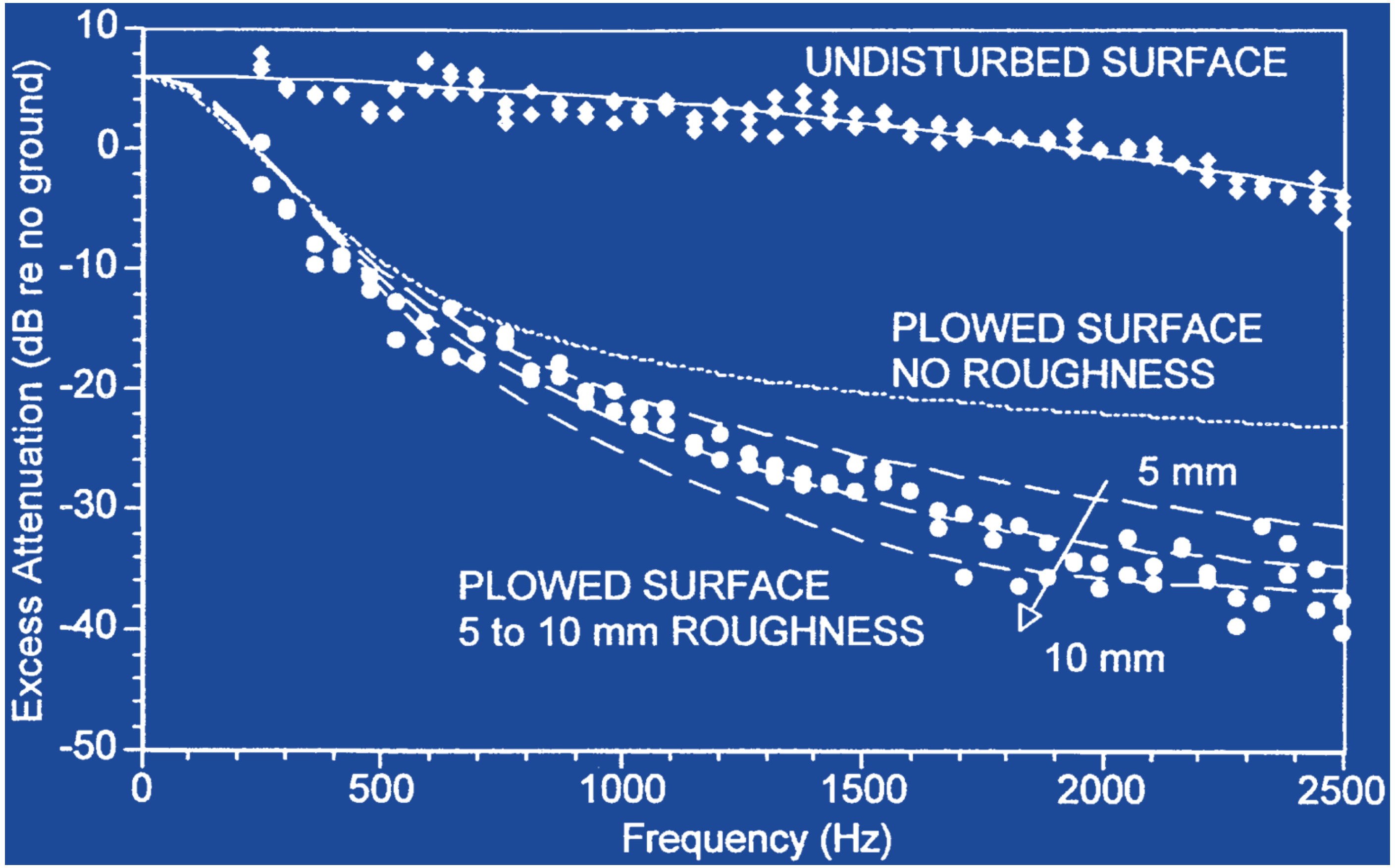

Effects of ploughing and crops to 50 m

loudspeaker source at 1.6 m height , receiver at 1.2 m height

Slightly downwind conditions

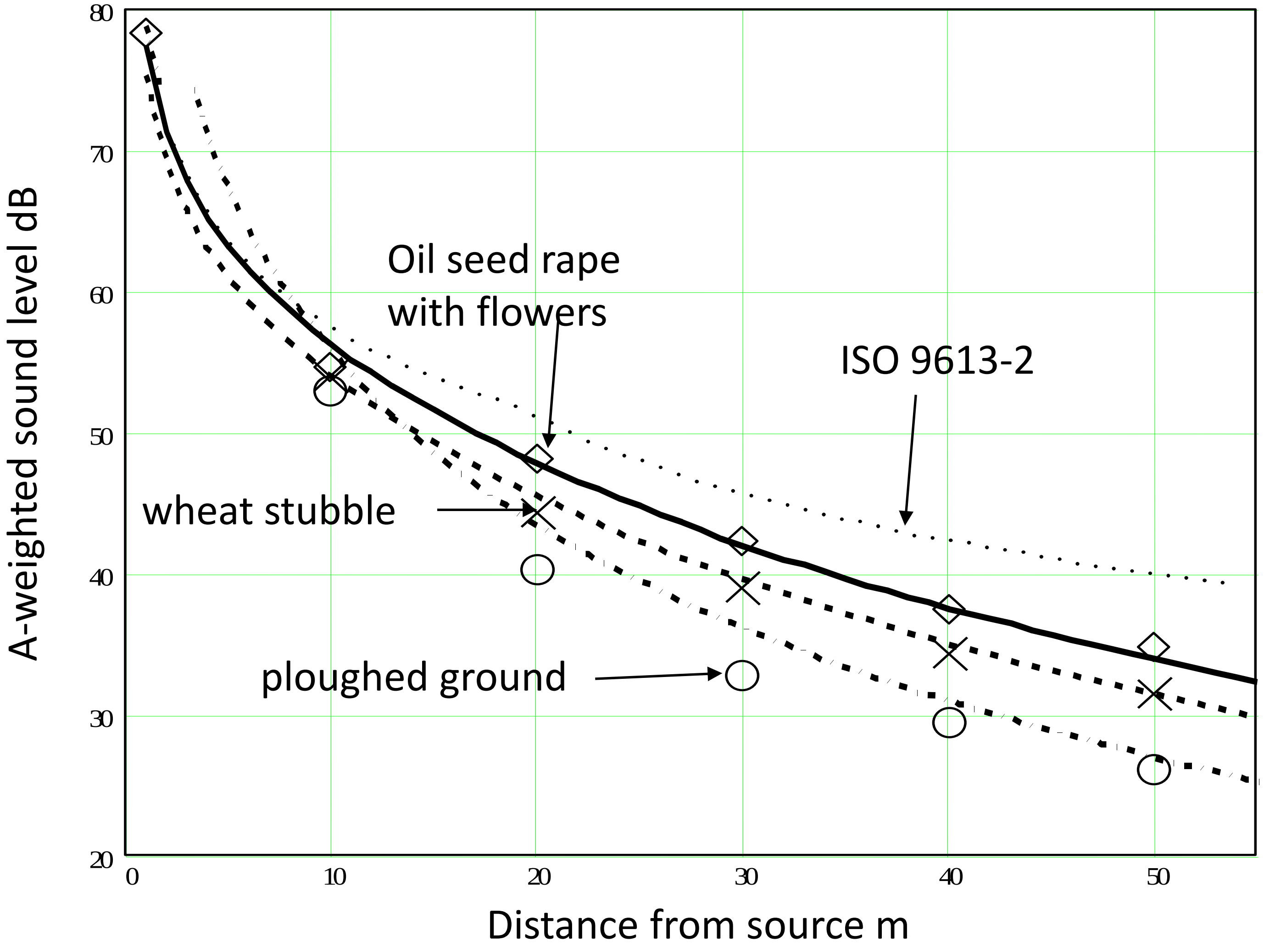

Measured vertical LD over artificial roughness

0.2 m high rectangular brick lattice on a car park:
source height 0.1 m, upper microphone height 0.15 m, lower microphone height 0.05 m
horizontal separation 2.0 m.

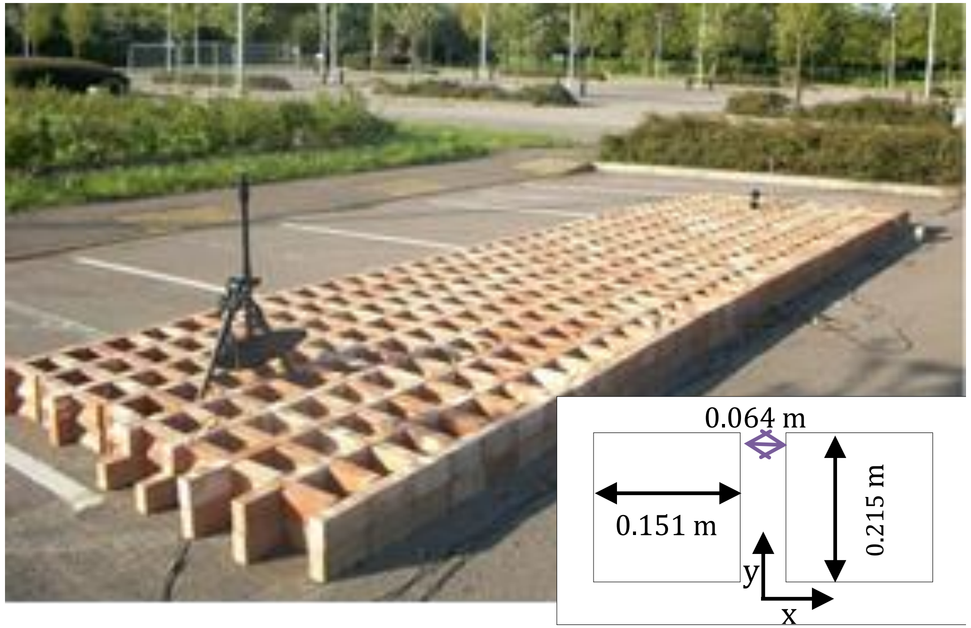

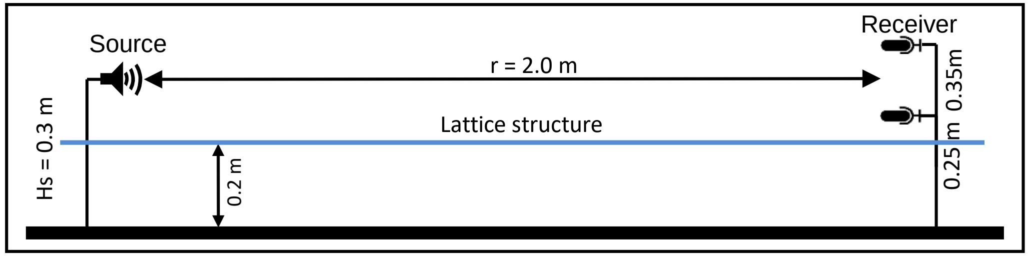

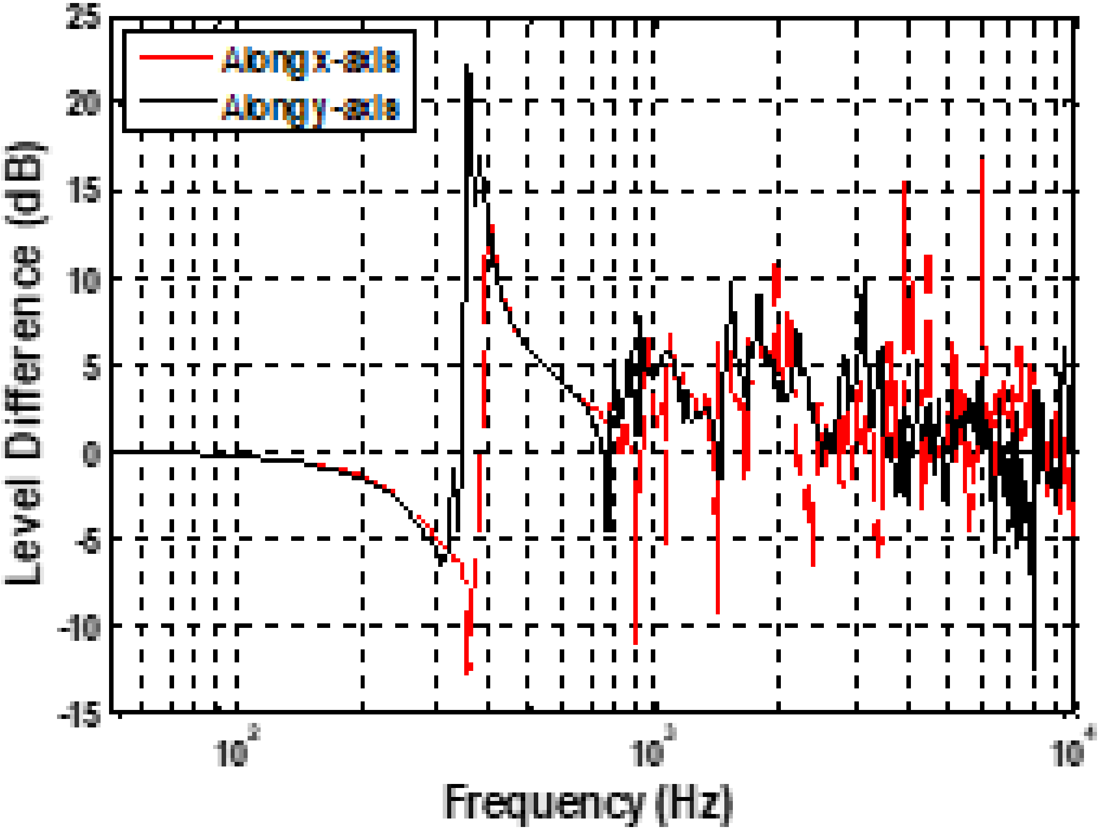

Level difference spectra measured along the 'x-axis' and 'y-axis' of the lattice corresponding to the shorter and longer sides of the cells respectively.

I. Bashir, *Acoustical exploitation of rough, mixed impedance and porous surfaces outdoors*, PhD Thesis, Engineering and Innovation, The Open University, 2014

Measurements v slit pore layer predictions with receivers over artificial roughness

source height above lattice is 0.1 m

I. Bashir, *Acoustical exploitation of rough, mixed impedance and porous surfaces outdoors*, PhD Thesis, Engineering and Innovation, The Open University, 2014

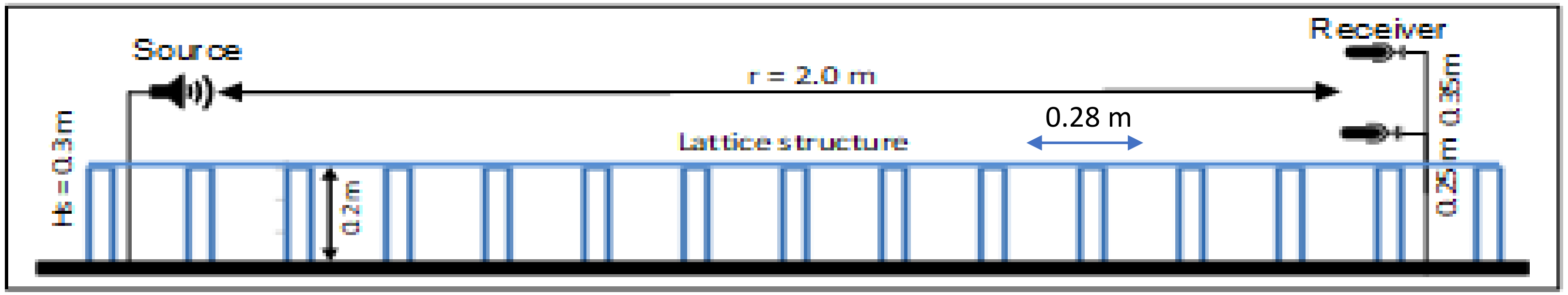

microphone heights above lattice are 0.05 m and 0.15 m

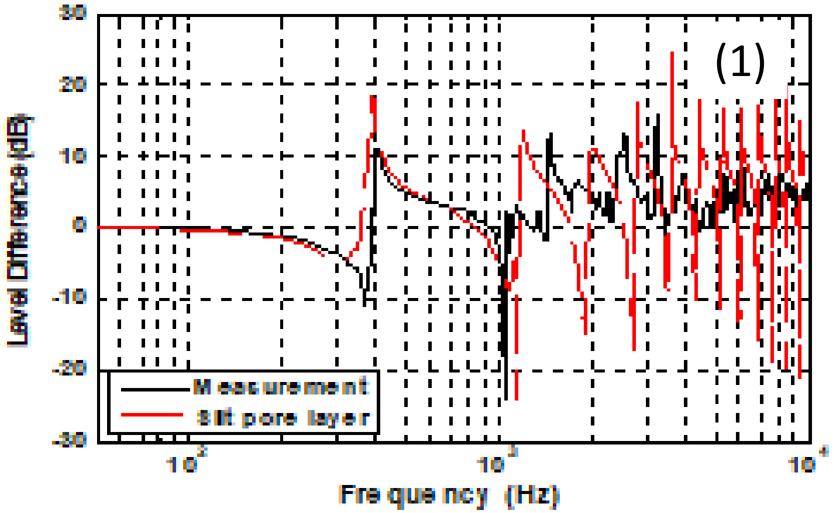

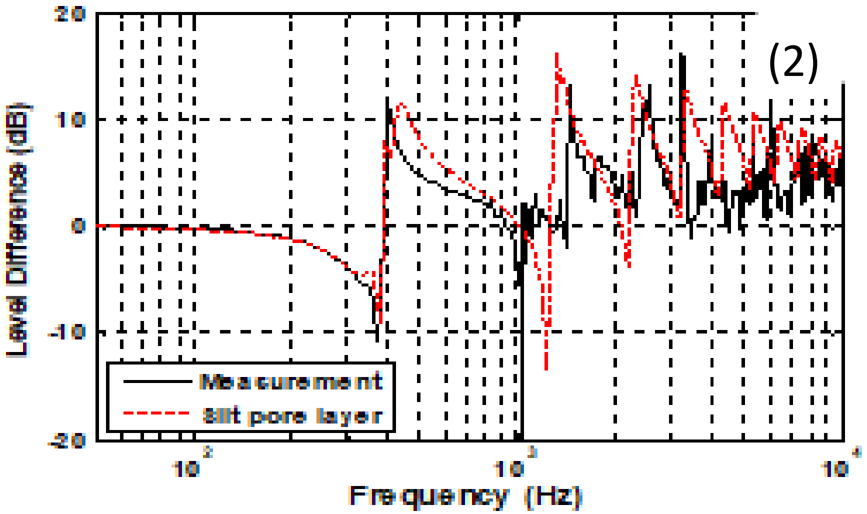

measured level difference spectra v BEM predictions with lattice modelled as raised slit pore layer impedance
(1) lattice geometry parameters (flow resistivity = 0.04 Pa s m^{-2}. porosity = 0.54 and layer depth = 0.2 m)
(2) porosity 0.54, effective flow resistivity (400 Pa s m^{-2}) and effective layer depth (0.16 m)

Measured horizontal LD v BEM 'raised impedance' predictions with receivers outside artificial roughness

I. Bashir, *Acoustical exploitation of rough, mixed impedance and porous surfaces outdoors*, PhD Thesis, Engineering and Innovation, The Open University, 2014

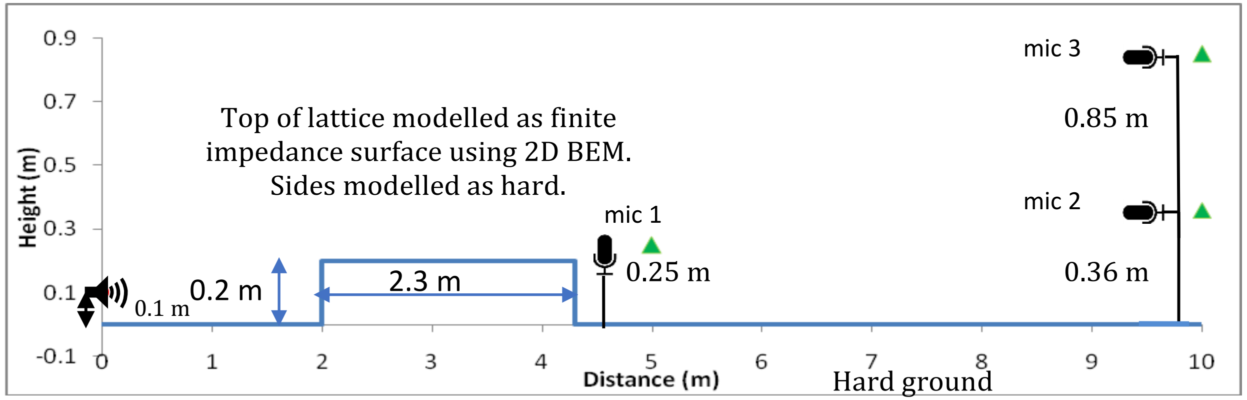

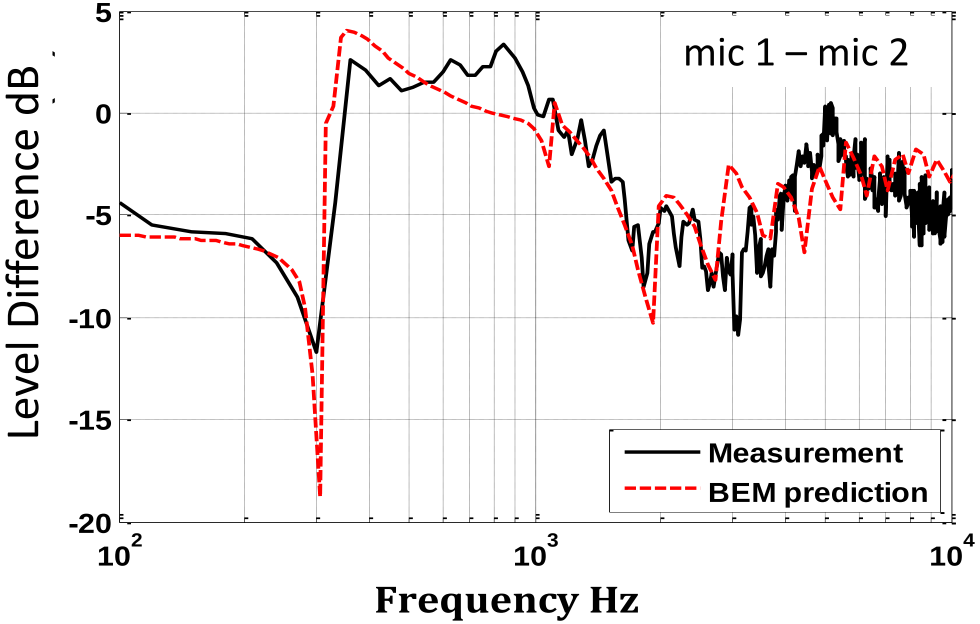

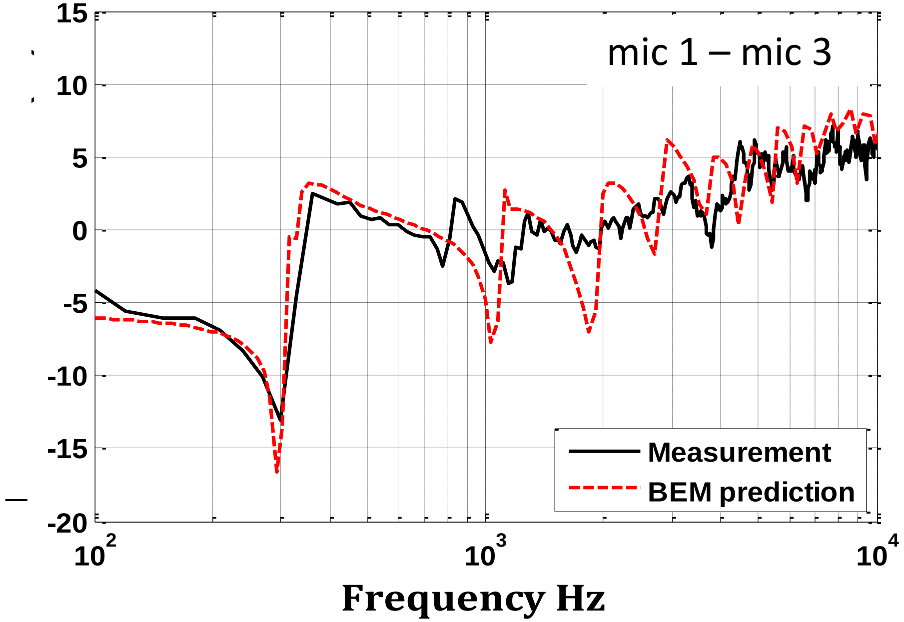

assumed impedance: slit pore layer with flow resistivity = 400 Pa s m^{-2}, porosity = 0.55 and effective layer depth = 0.16 m

Atmospheric Sound Propagation: Fundamentals – Part 2

OUTLINE

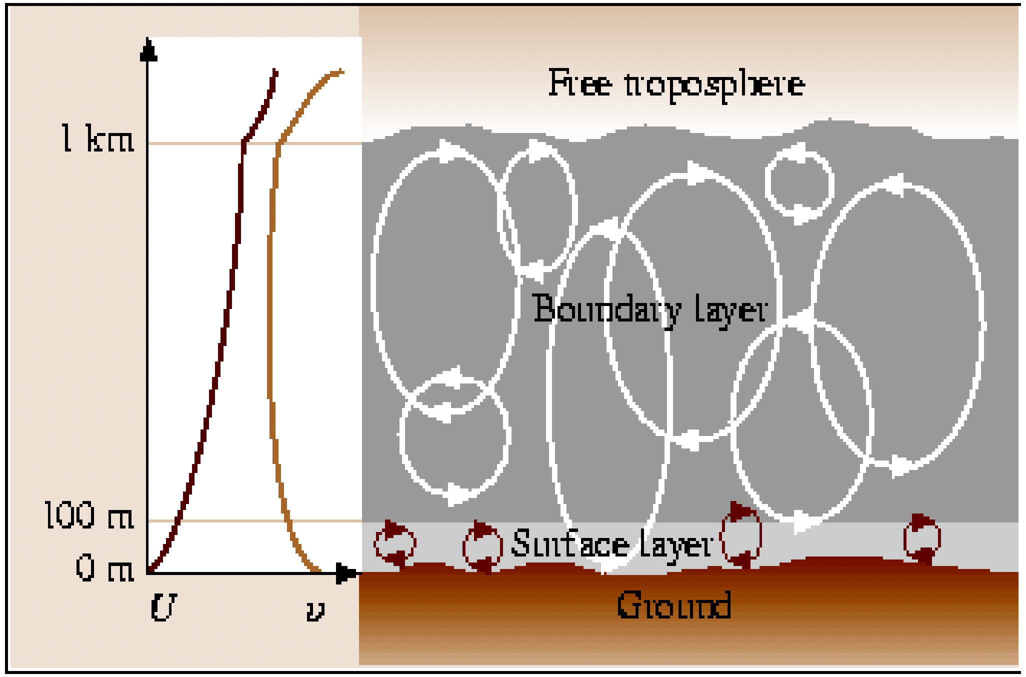

- Impedance discontinuities
  - single discontinuity
  - multiple discontinuities
  - Fresnel zone, semi-analytical methods and BEM v laboratory data
- Barriers
  - single edge diffraction
  - interaction with ground
  - finite length effects
- Refraction
  - distance to shadow zone boundary for linear gradients
- Turbulence
  - ground effect reduction - *Clifford and Lataitis and Ostashev formulations*
  - Attenuation due to turbulence
- Crops
  - ground effect without and with crops
  - attenuation due to foliage
  - scattering by stems
  - incoherence due to scattering
  - predictions v data
- Forests
  - foliage effects
  - trunk scattering and reduction of ground effect
  - predictions v data
  - sonic crystal effects

Predicting effects of impedance discontinuities

Single discontinuity

B. A. de Jong, A. Moerkerken, J. D. van der Toorn, *Propagation of sound over grassland and over an earth barrier*, Journal of Sound and Vibration, **86** 23–46 (1983)

$$\frac{P}{P_1} = 1 + \frac{R_1}{R_2} Q_G e^{ik(R_2 - R_1)} + (Q_2 - Q_1) e^{-i\pi/4} \frac{1}{\sqrt{\pi}} \frac{R_1}{S_1} X \left[F_2\left(\sqrt{k(S_1 - R_1)}\right) \pm F_2\left(\sqrt{k(S_1 - R_2)}\right) e^{ik(R_2 - R_1)} \right]$$

Y. W. Lam and M. R. Monazzam, *On the modeling of sound propagation over multi-impedance discontinuities using a semiempirical diffraction formulation*, J. Acoust. Soc. Am. 120 (2006), 686 - 698

$$\frac{P}{P_1} = 1 + \frac{R_1}{R_2} Q_G e^{ik(R_2 - R_1)} + (Q_2 - Q_1) e^{-i\pi/4} \frac{1}{\sqrt{\pi}} \frac{R_1}{S_1} X \left[\mu F_2\left(\sqrt{k(S_1 - R_1)}\right) + \gamma F_2\left(\sqrt{k(S_1 - R_2)}\right) e^{ik(R_2 - R_1)} \right]$$

$\mu = -1$, hard to soft $\qquad$ $\mu = +1$, soft to hard $\qquad$ $\gamma = 1$, $D_o < D_1$ $\qquad$ $\gamma = -1$, $D_o > D_1$

hard to soft

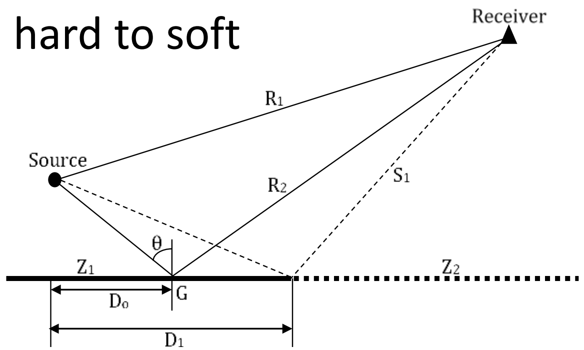

soft to hard

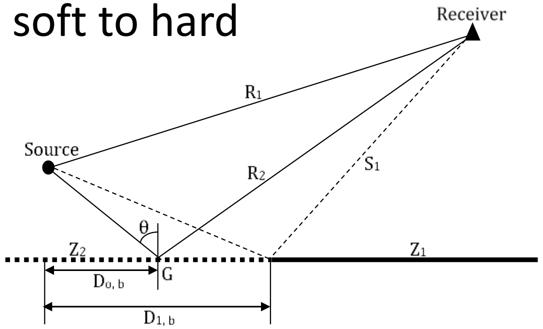

source and receiver at 0.07 m height separated by 0.7 m with the impedance discontinuity 0.6 m from the source

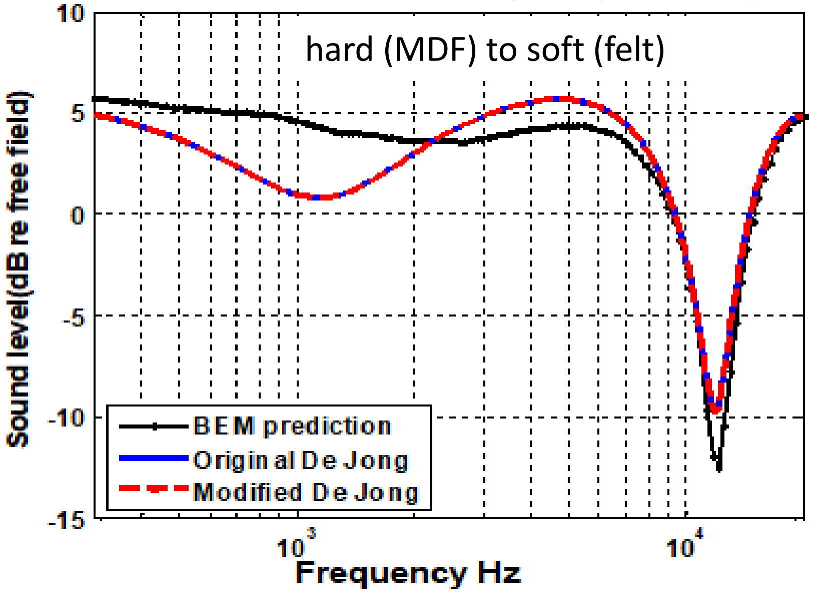

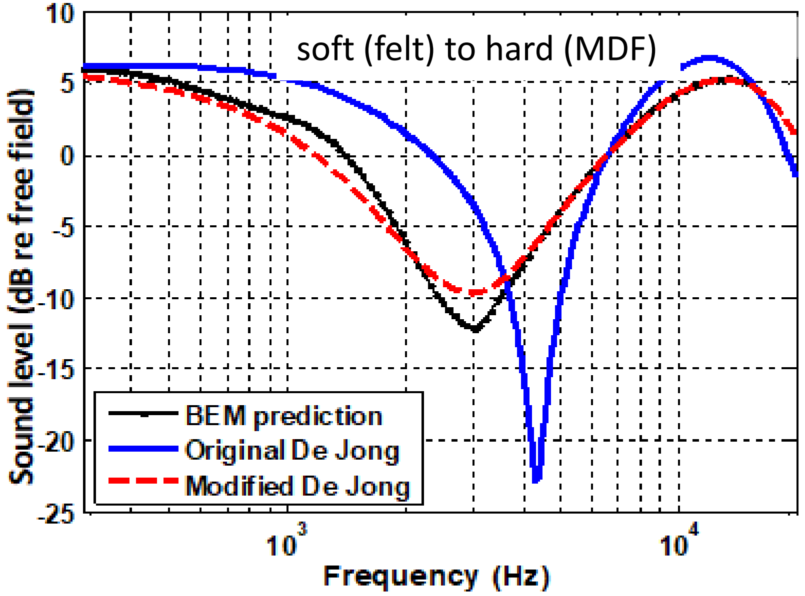

I. Bashir, *Acoustical exploitation of rough, mixed impedance and porous surfaces outdoors*, PhD Thesis, Engineering and Innovation, The Open University, 2014

Multiple discontinuities

Laboratory data

I. Bashir, *Acoustical exploitation of rough, mixed impedance and porous surfaces outdoors*, PhD Thesis, Engineering and Innovation, The Open University, 2014

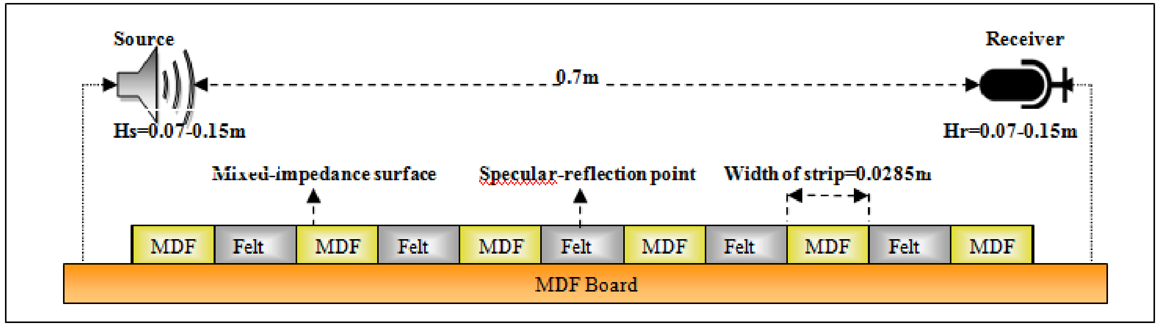

source and receiver heights = 0.05 m, separation 0.7 m

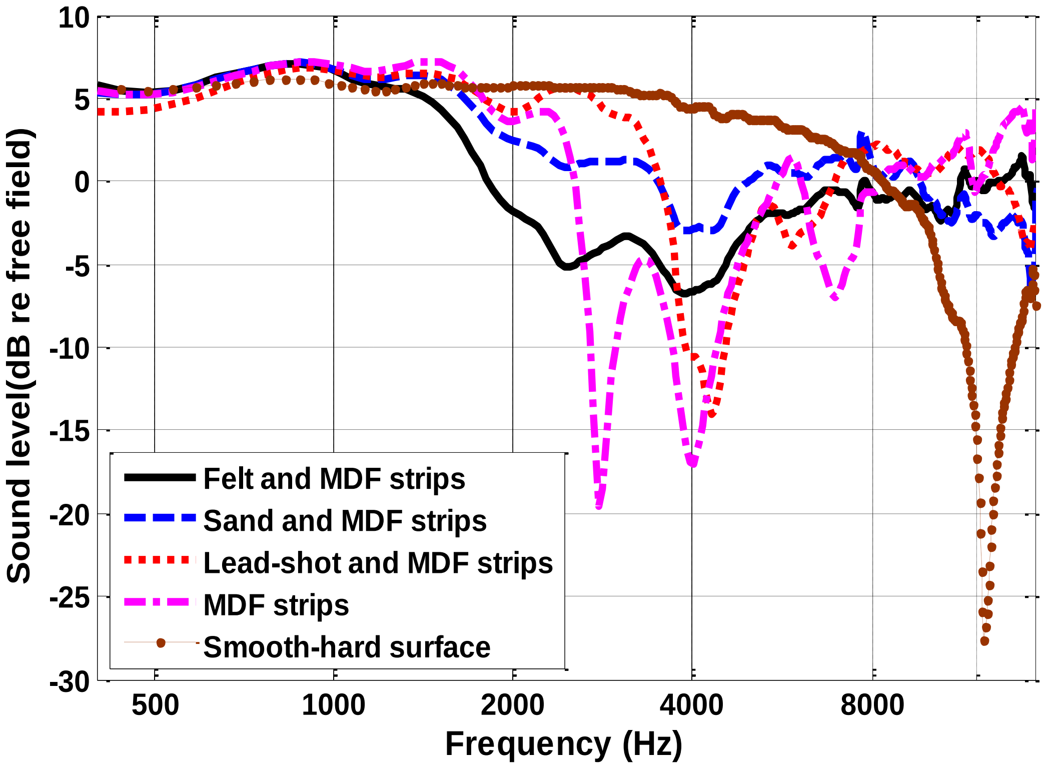

Fresnel Zone Methods

The Fresnel-zone is the elliptical area around the specular reflection point

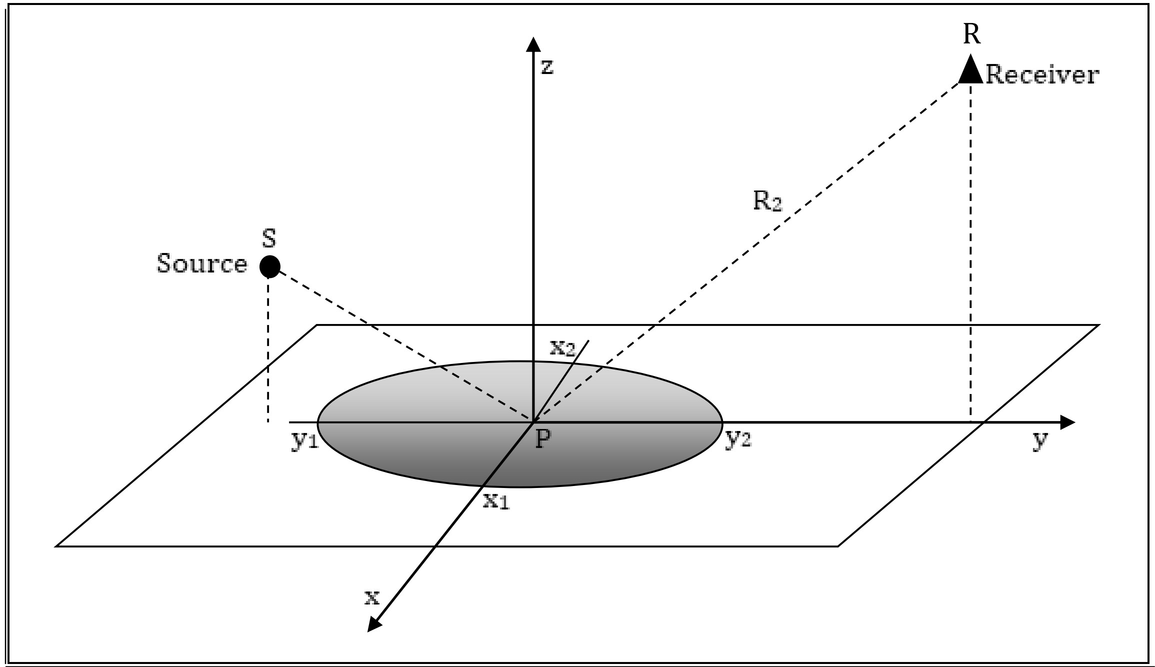

*D. C. Hothersall and J. N. B. Harriott, *Approximate models for sound propagation above multi-impedance boundaries*, J. Acoust. Soc. Am. 97 918 – 926 (1995)

μ = proportion with surface impedance Z_1
(1 - μ) = proportion with surface impedance Z_2
inside the Fresnel zone

Hothersall and Harriott*, linear interpolation of EA

$$\frac{P}{P_1} = \mu 20\log\left|1+\frac{R_1}{R_2}Q_1 e^{ik(R_2-R_1)}\right| + (1-\mu)20\log\left|1+\frac{R_1}{R_2}Q_2 e^{ik(R_2-R_1)}\right|$$

Boulanger *et al***, linear interpolation between the pressures

$$\frac{P}{P_1} = 20\log\left\{\mu\left|1+\frac{R_1}{R_2}Q_1 e^{ik(R_2-R_1)}\right| + (1-\mu)\left|1+\frac{R_1}{R_2}Q_2 e^{ik(R_2-R_1)}\right|\right\}$$

No difference between predictions of alternative Fresnel zone formulations for hard-to-soft

P. Boulanger, T. Waters-Fuller, K. Attenborough and K. M. Li, *Models and measurements of sound propagation from a point source over mixed impedance ground*, J. Acoust. Soc. Am. **102 1432 – 1442 (1997)

Short-range predictions

original and modified de Jong v BEM

source and receiver height 0.07 m
separation 0.7 m

Hard impedance (MDF) - variable porosity (5×10^5 kPa s m^{-2}, 100 /m): **Soft** impedance (thin MDF-backed felt – variable porosity (20 kPa s m^{-2}, 100 /m)

I. Bashir, *Acoustical exploitation of rough, mixed impedance and porous surfaces outdoors*, PhD Thesis, Engineering and Innovation, The Open University, 2014

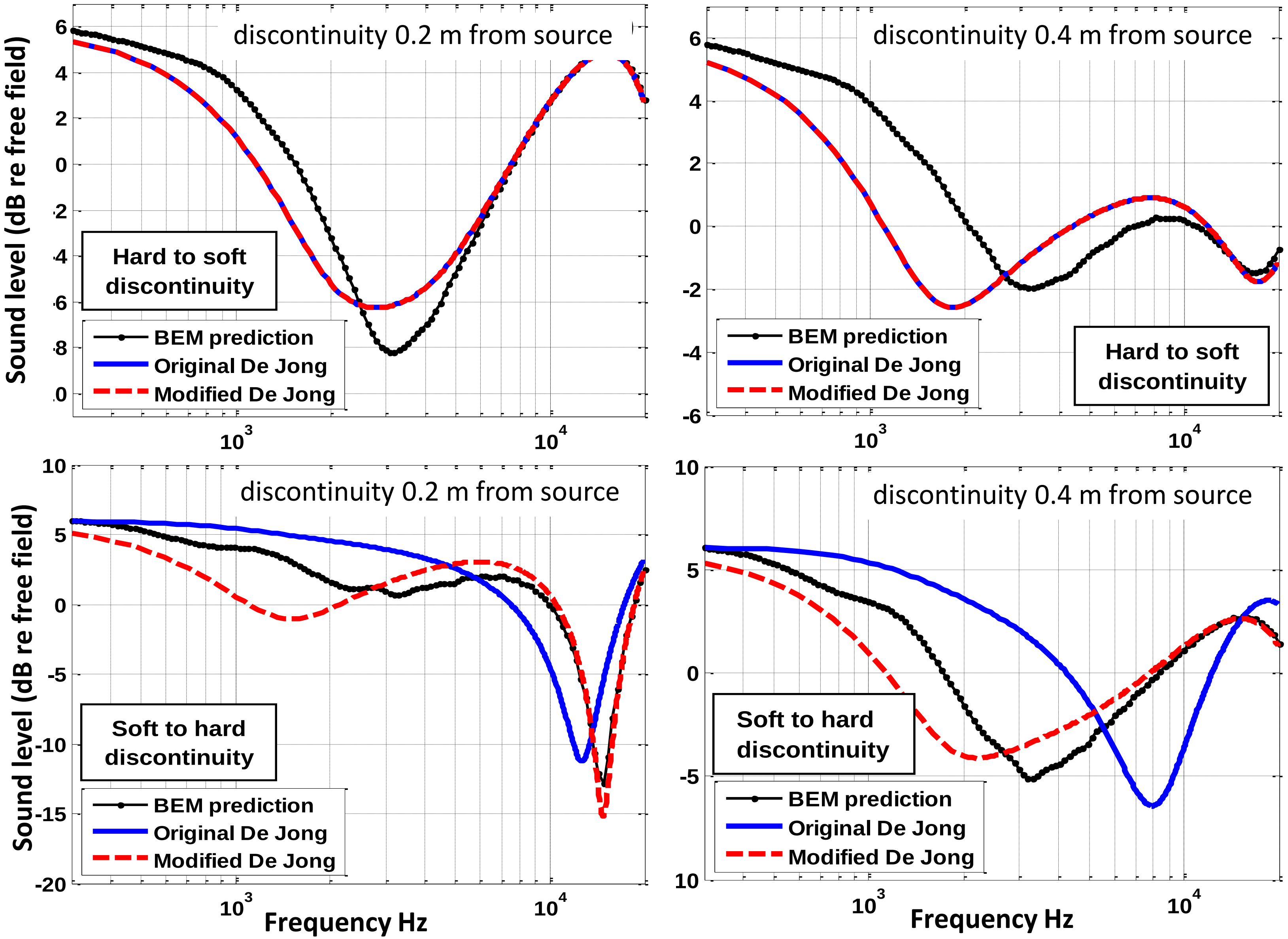

Predictions v laboratory data

multiple impedance discontinuities

modified Fresnel Zone and BEM

source and receiver height = 0.07 m; separation = 0.7 m
surface of alternating felt and MDF strips

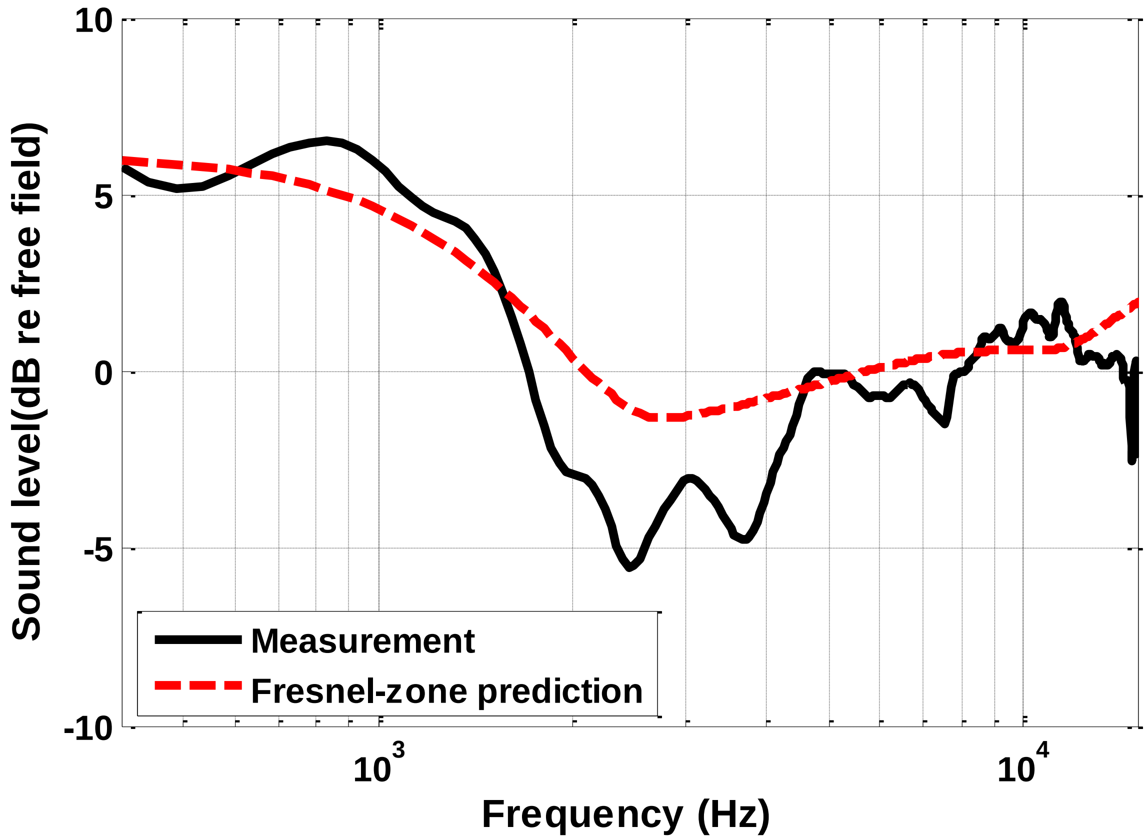

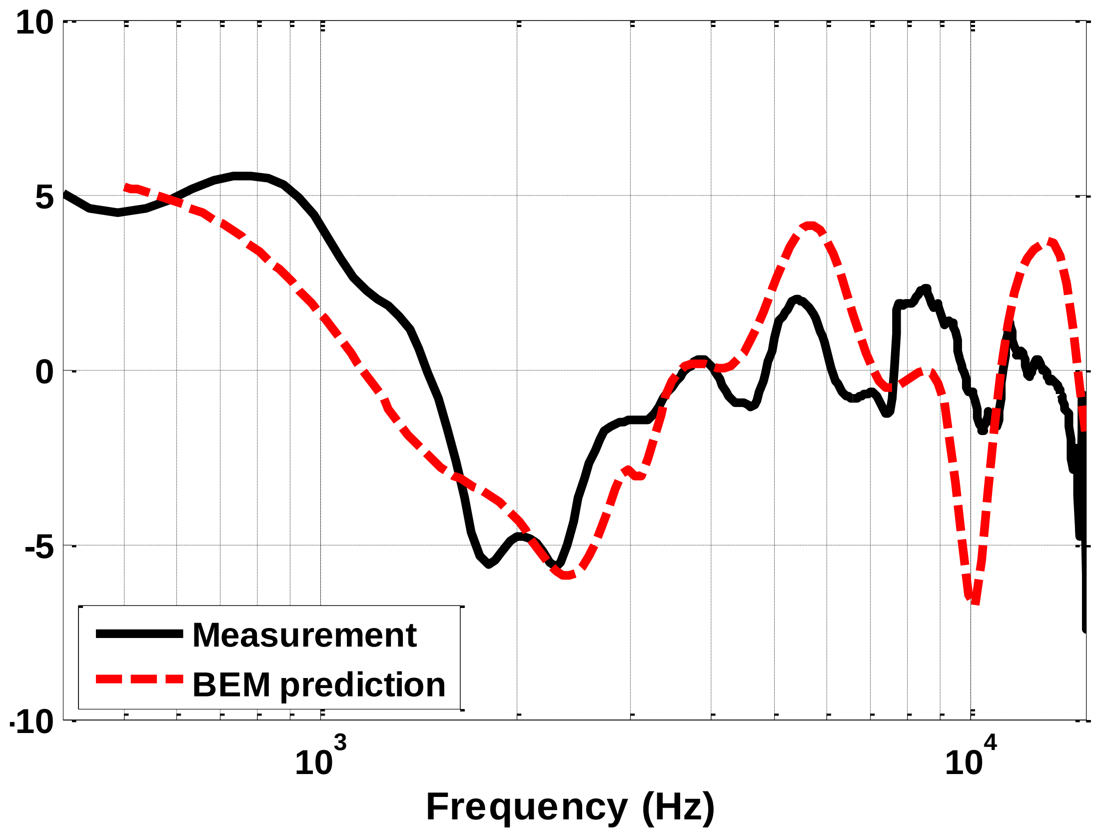

I. Bashir, *Acoustical exploitation of rough, mixed impedance and porous surfaces outdoors*, PhD Thesis, Engineering and Innovation, The Open University, 2014

Modified de Jong and Fresnel zone v BEM for a single soft finite width strip

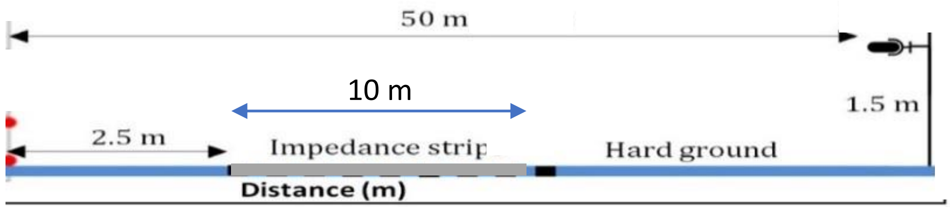

EA spectra between 0.01 m and 0.03 m high sources and a 1.5 m high receiver 50 m away predicted by modified (nMID), De Jong, Fresnel zone models

'soft' strip impedance given by the 2-parameter slit pore model with flow resistivity of 10 kPa s m^{-2} and a porosity of 0.4.

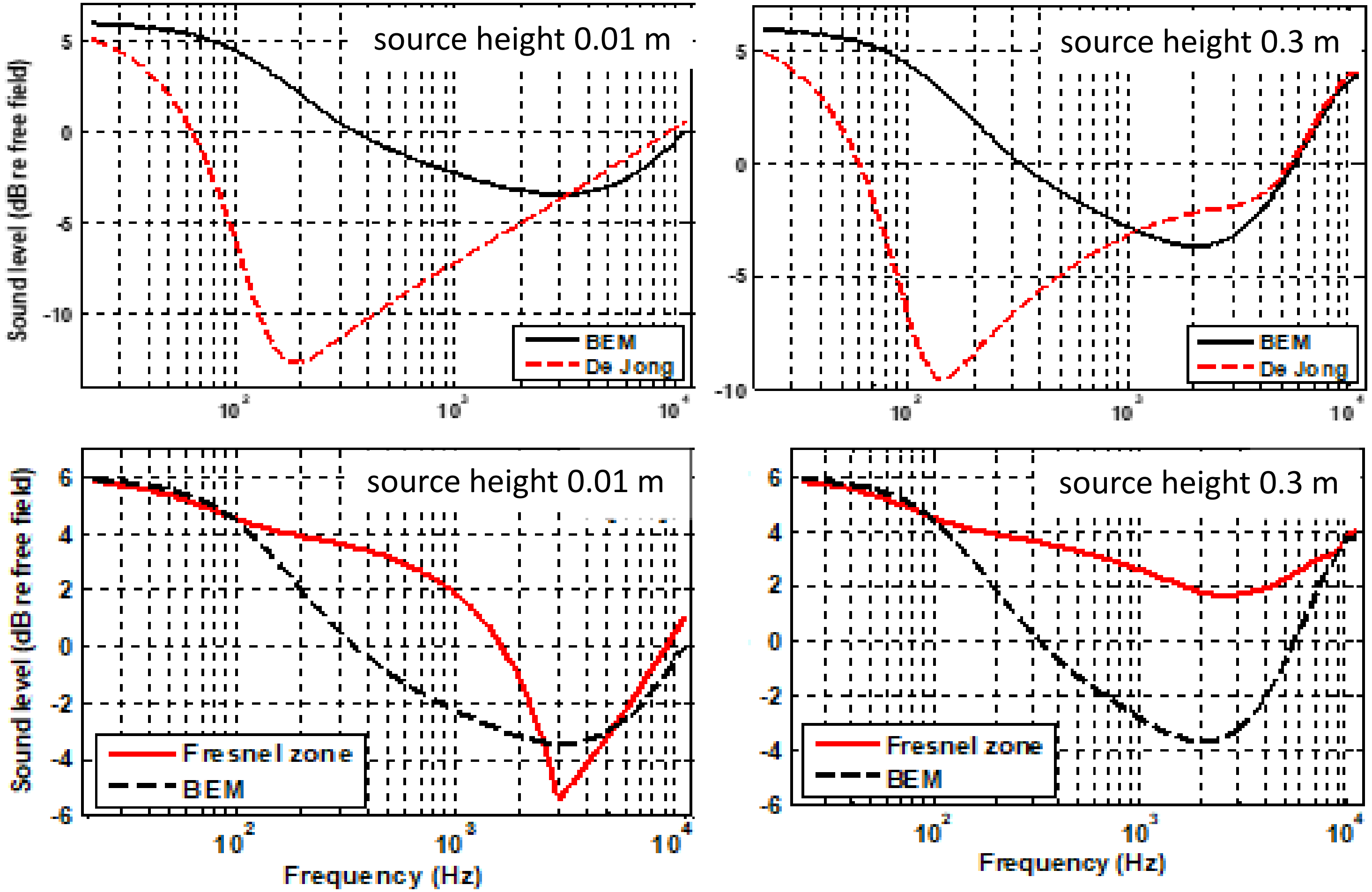

K. Attenborough, I. Bashir and S. Taherzadeh, *Exploiting ground effects for surface transport noise abatement*, Noise Mapping Journal, **3** 1- 25 (2016)

Fresnel zone v BEM predictions of insertion loss from 2-lane urban road

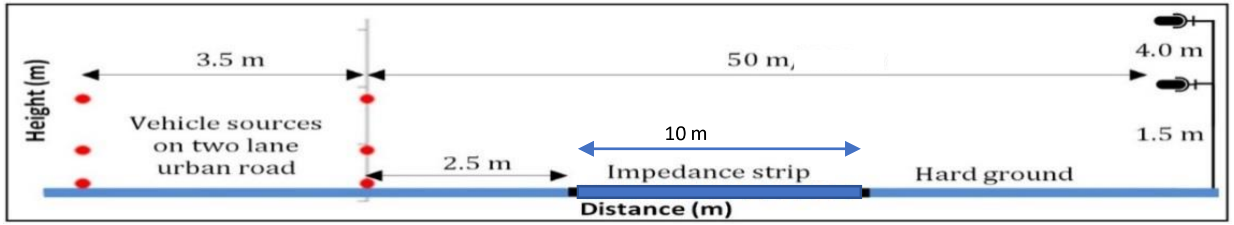

Surface description	Porosity	Flow resistivity (kPa s m^{-2})	Impedance strips length (m)	Receiver height Hr (m)	Fresnel zone predictions			BEM predictions		
					IL-Lane1 (dB)	IL-Lane2 (dB)	IL combined (dB)	IL-Lane1 (dB)	IL-Lane2 (dB)	IL combined (dB)
Multiple 1 m wide impedance strips of gravel and hard ground	0.40	10	25.0	1.5	3.5	3.1	3.3	8.0	7.1	7.5
				4.0	1.9	0.9	1.3	3.6	2.1	2.8
A continuous single 10 m wide impedance patch	0.40	10	10.0	1.5	3.0	3.1	3.2	6.8	5.9	6.3
				4.0	1.2	1.9	2.7	4.4	2.7	3.4

K. Attenborough, I. Bashir and S. Taherzadeh, *Exploiting ground effects for surface transport noise abatement*, Noise Mapping Journal, **3** 1- 25 (2016)

Diffraction by a barrier

K. Attenborough, K. M. Li and K. Horoshenkov "*Predicting Outdoor Sound*", Taylor and Francis, 2007

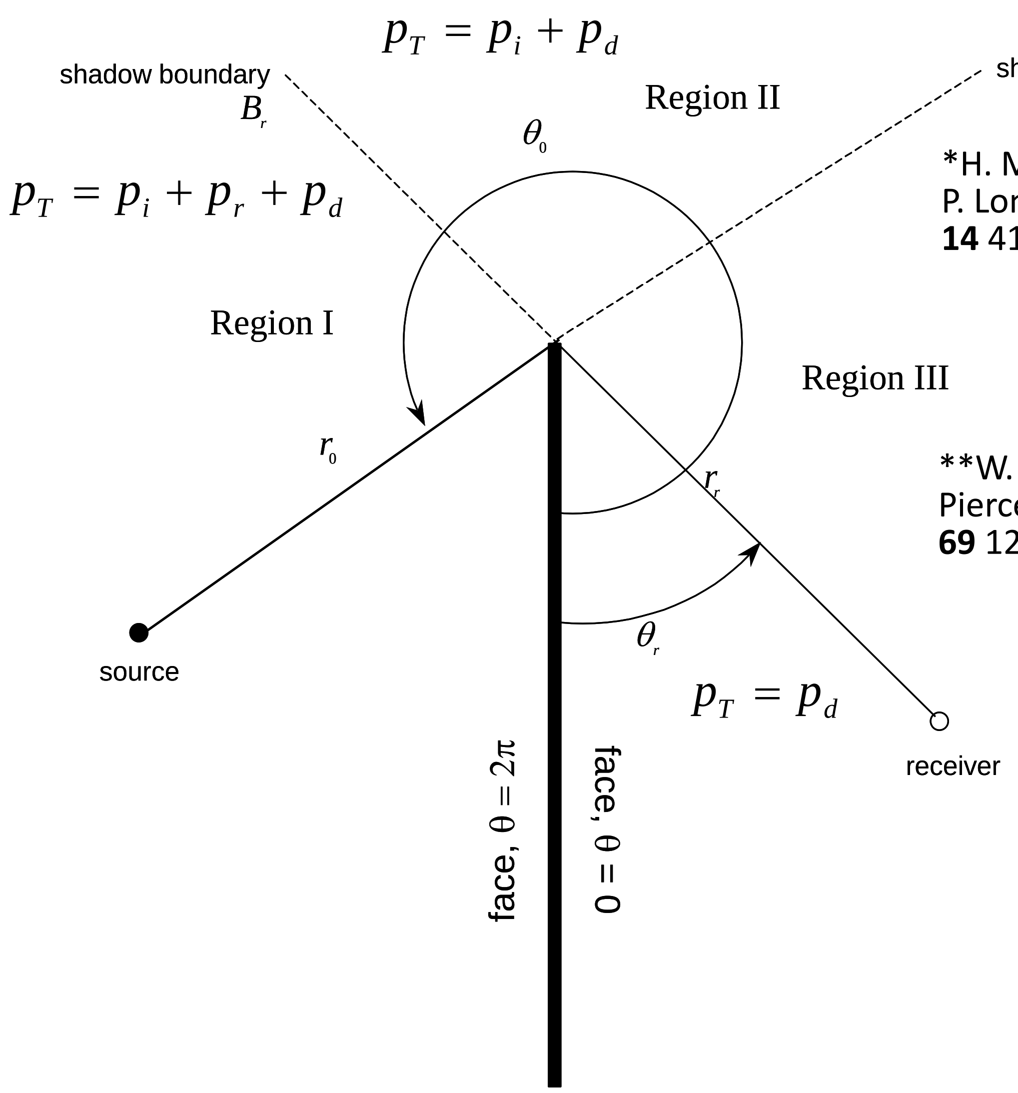

Approximate solution due to **Macdonald***

$$p_d = i\frac{e^{-i\pi/4}}{8\pi\sqrt{2\pi kR'}}\frac{e^{ikR'}}{\sqrt{r_0 r_r}}\left\{\sec\left(\frac{\theta_0-\theta_r}{2}\right)+\sec\left(\frac{\theta_0+\theta_r}{2}\right)\right\}$$

*H. M. Macdonald, P. Lond. Math. Soc. **14** 410 – 427 (1915)

Hadden and Pierce** solution

$$p_d = [(1+i)/2]\left[e^{ikR'}/4\pi R'\right][A_D(X_+)+A_D(X_-)]$$

$$X_+ = X(\theta_o+\theta_r) \qquad X_- = X(\theta-\theta_o)$$

$$X(\Theta) = -2\sqrt{2r_o r_r/\lambda R'}\cos(\Theta/2)$$

$$A_D(X) = \mathrm{sgn}(X)\left[f(|X|)-i\,g(|X|)\right]$$

$$f(x) = \left[\frac{1}{2}-S(X)\right]\cos\left(\frac{\pi X^2}{2}\right)-\left[\frac{1}{2}-C(X)\right]\sin\left(\frac{\pi X^2}{2}\right)$$

$$g(x) = \left[\frac{1}{2}-C(X)\right]\cos\left(\frac{\pi X^2}{2}\right)+\left[\frac{1}{2}-S(X)\right]\sin\left(\frac{\pi X^2}{2}\right)$$

$$C(u) = \int_0^u \cos\left(\frac{\pi t^2}{2}\right)dt \qquad S(u) = \int_0^u \sin\left(\frac{\pi t^2}{2}\right)dt$$

W. J. Hadden and A. D. Pierce, J. Acoust. Soc. Am. **69 1266 – 1276 (1981)

Thin screen insertion Loss: predictions v data

IL = total field without barrier – total field with barrier

Fresnel-Kirchoff approximation

$$IL = 10\lg 2 - \lg\left\{F_r(\infty) - F_r\left(\sqrt{2\left(a^{-1}+b^{-1}\right)/\lambda h}\right)\right\}$$

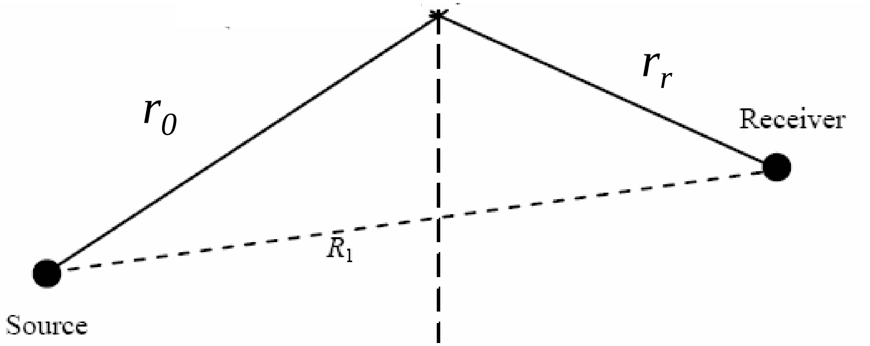

Maekawa Formula

$$Att = 10\log_{10}\left(3+20N\right)$$

$$N_1 = \frac{2\delta_1}{\lambda} \qquad \delta_1 = \left(r_0 + r_r\right) - R_1$$

Kurze and Anderson Maekawa chart fit

$$Att = 5 + 20\log_{10}\frac{\sqrt{2\pi N_1}}{\tanh\sqrt{2\pi N_1}}$$

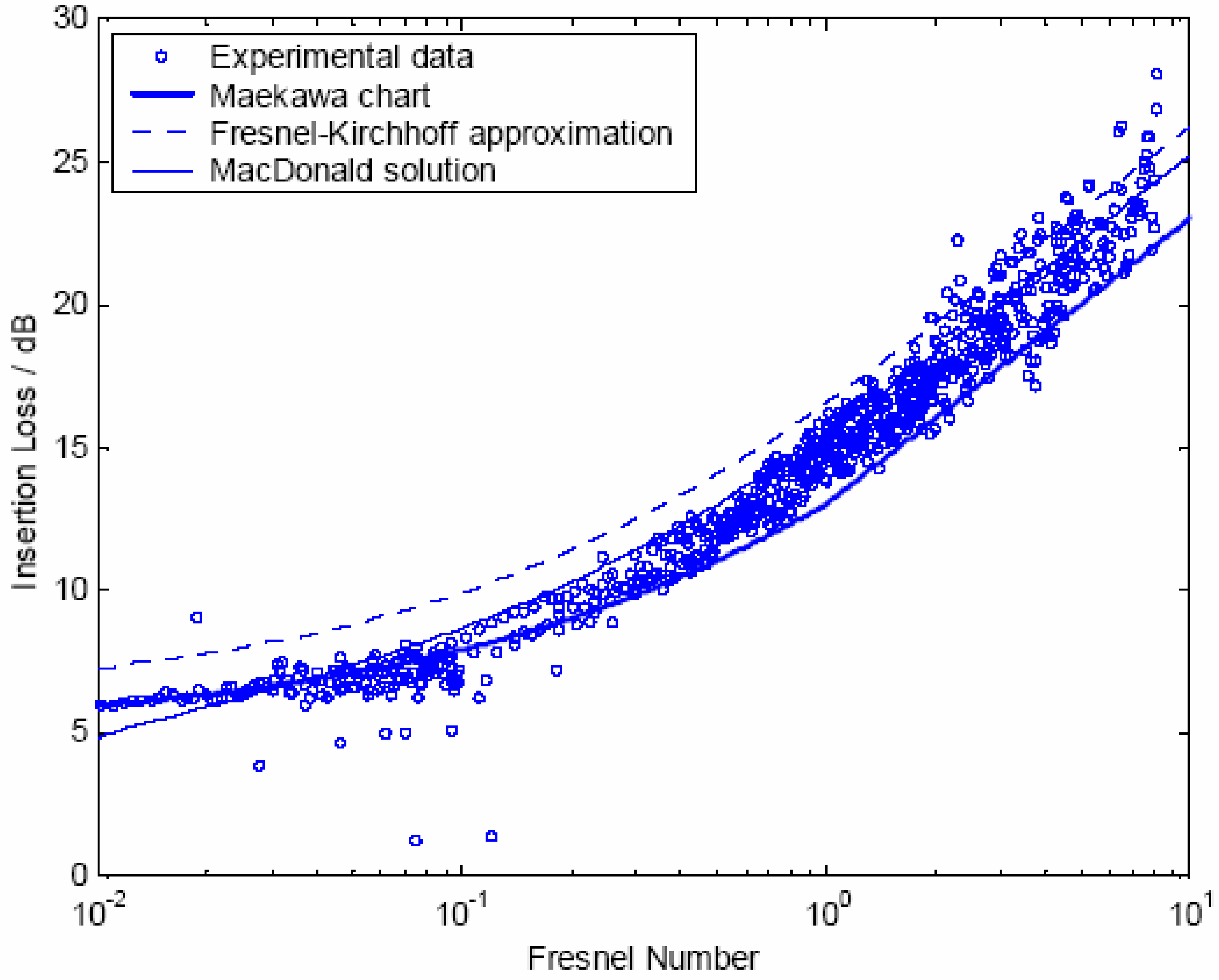

Improved by Menounou J. Acoust. Soc. Am. 110, 1828-1838, (2001)

Long thin barrier on impedance plane

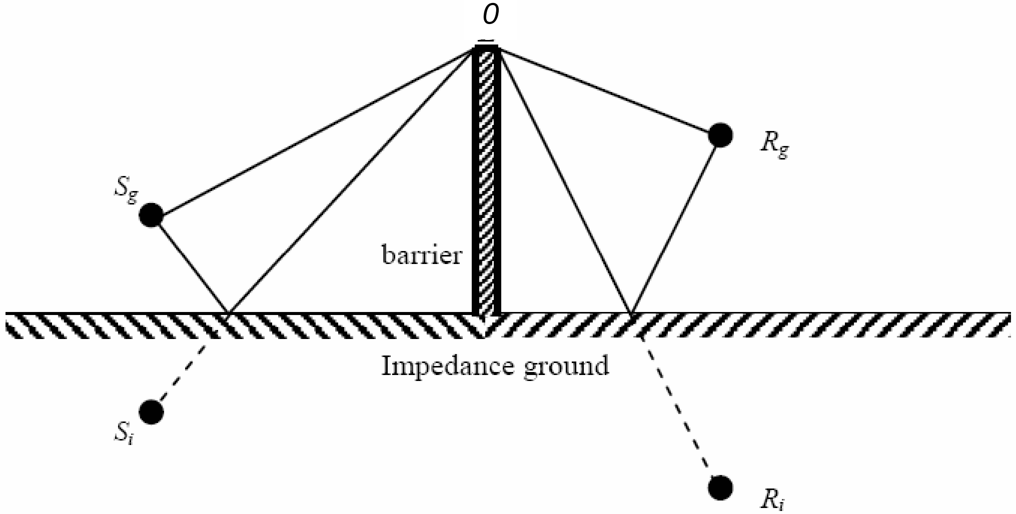

$$P_1 = P(S_g, R_g, E),$$
$$P_2 = P(S_i, R_g, E),$$
$$P_3 = P(S_g, R_i, E),$$
$$P_4 = P(S_i, R_i, E)\,.$$

$$P_T = P_1 + Q_s P_2 + Q_R P_3 + Q_s Q_R P_4$$

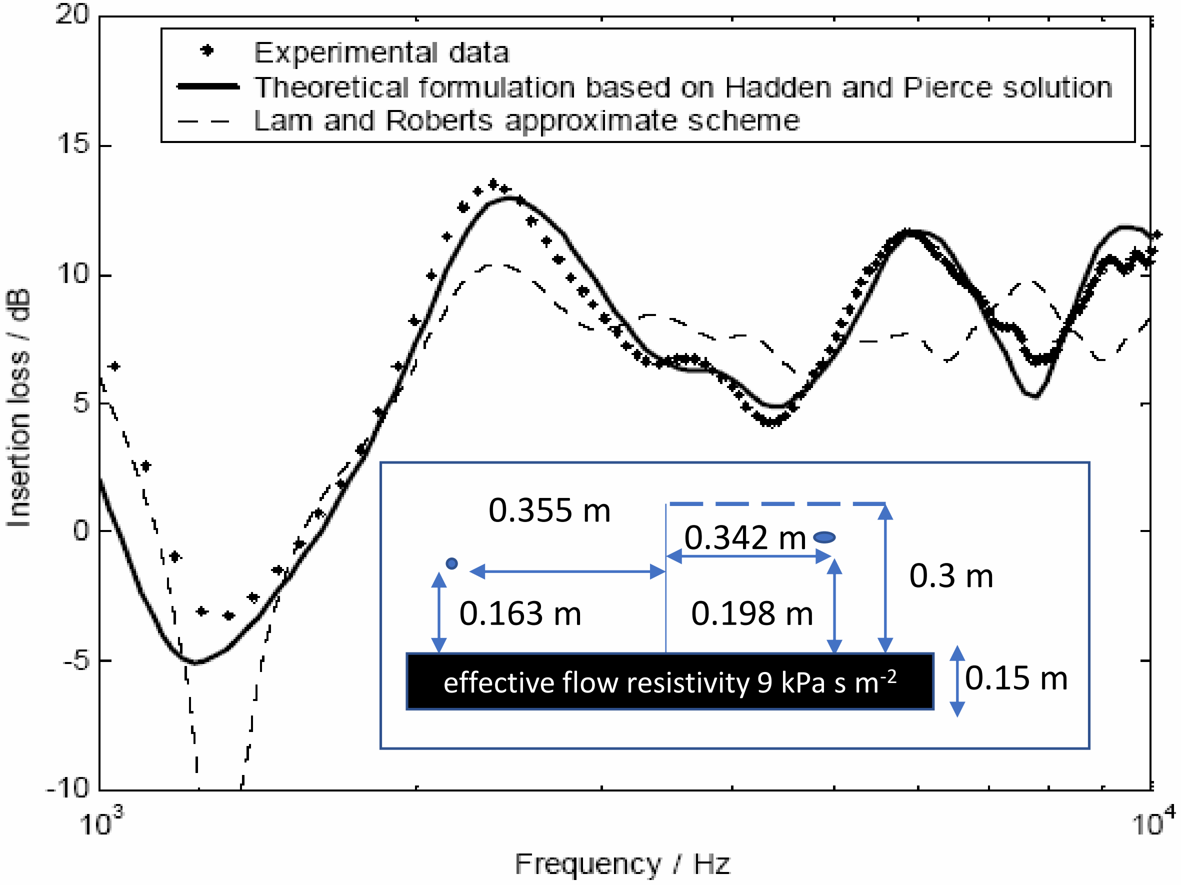

Y. W. Lam and S. C. Roberts, *A simple method for accurate prediction of finite barrier insertion loss*, J. Acoust. Soc. Am. 93, 1445-1452, (1993)

Finite barrier on impedance plane

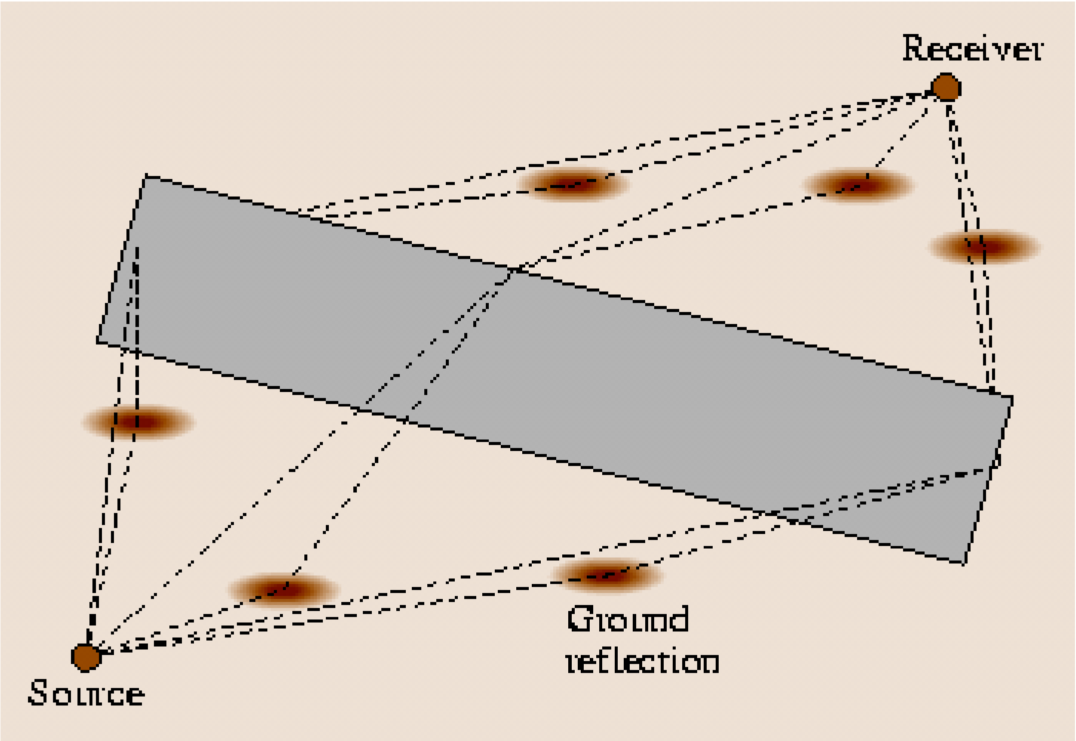

$$P_T = P_1 + Q_s P_2 + Q_R P_3 + Q_s Q_R P_4 + P_5 + Q_R P_6 + P_7 + Q_R P_8$$

Y. W. Lam and S. C. Roberts, *A simple method for accurate prediction of finite barrier insertion loss*, J. Acoust. Soc. Am. 93, 1445-1452, (1993)

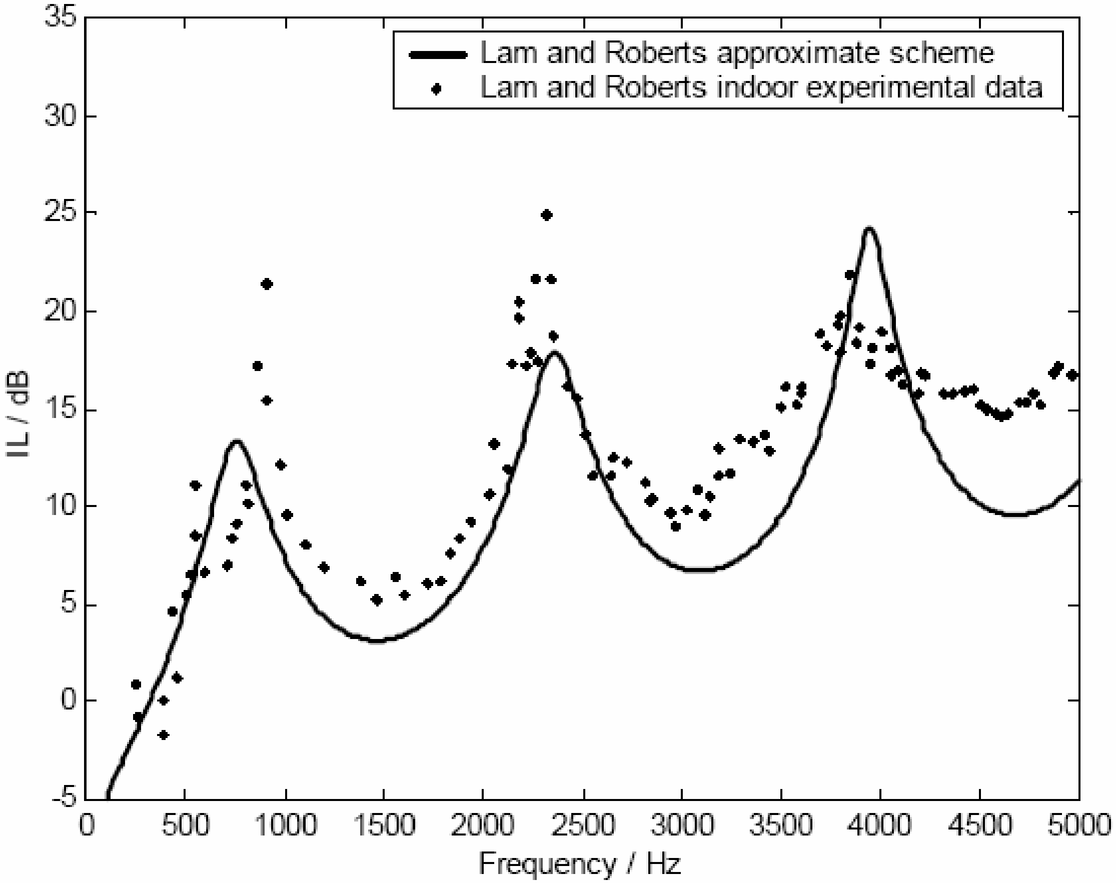

0.3 m high and 1.22 m long barrier on hard ground.
source height 0.033 m 1.009 m from the barrier.
receiver on the ground 1.491 m from the barrier.

Atmospheric Refraction

Ray-based interpretations

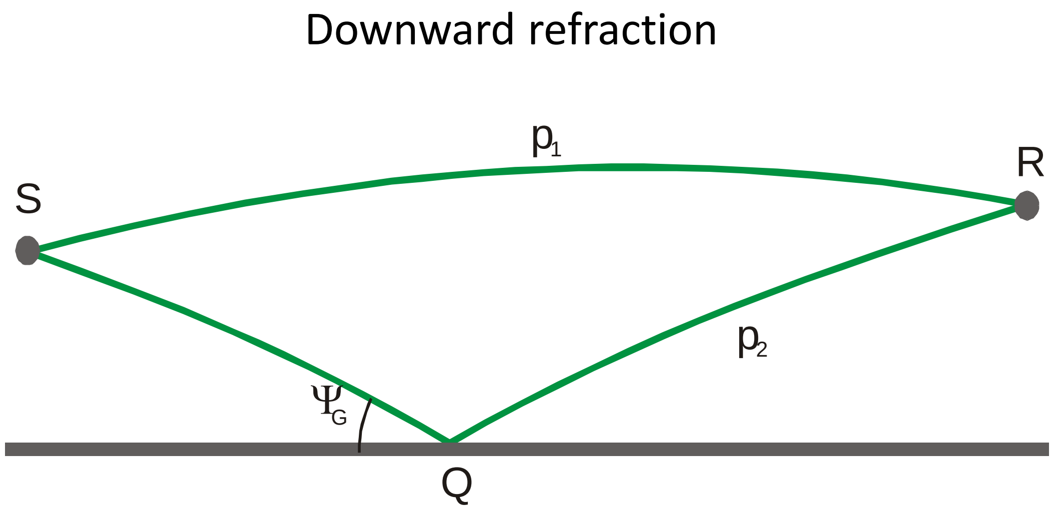

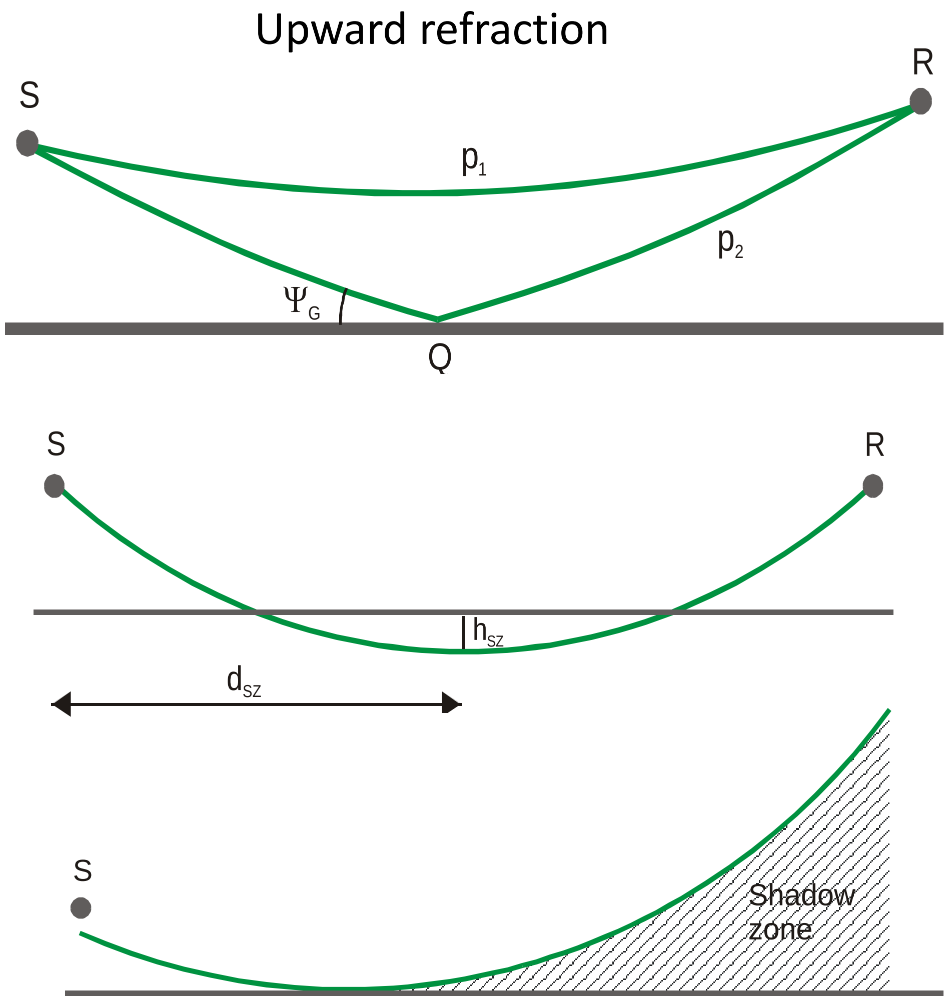

Shadow zone boundary for linear sound speed gradient

$$c(z) = c_0(1+\zeta z)$$

$$p = \{\exp(-jk_0\xi_1) + Q\exp(-jk_0\xi_2)\}/4\pi d$$

$$\xi_1 = \int_{\phi_<}^{\phi_>} \frac{d\phi}{\varsigma \sin\phi} = \varsigma^{-1}\log_e\left[\tan(\phi_>/2)/\tan(\phi_</2)\right]$$

$$\xi_2 = \int_{\theta_<}^{\theta_>} \frac{d\theta}{\varsigma \sin\theta} = \varsigma^{-1}\log_e\left[\tan(\theta_>/2)\tan^2(\theta_0/2)/\tan(\theta_</2)\right]$$

ζ is the normalised sound speed gradient ((dc/dz)/c_0) (units /m)

$\phi(z)$ and $\theta(z)$ are the polar angles of direct and reflected waves

Approximation for small sound speed gradients

$$r_c = \left[2c_0\Big/\frac{du}{dz}\cos\beta - \frac{dc}{dz}\right]^{1/2}\left(\sqrt{h_s}+\sqrt{h_r}\right)$$

β is the angle between the direction of the wind and the line between source and receiver

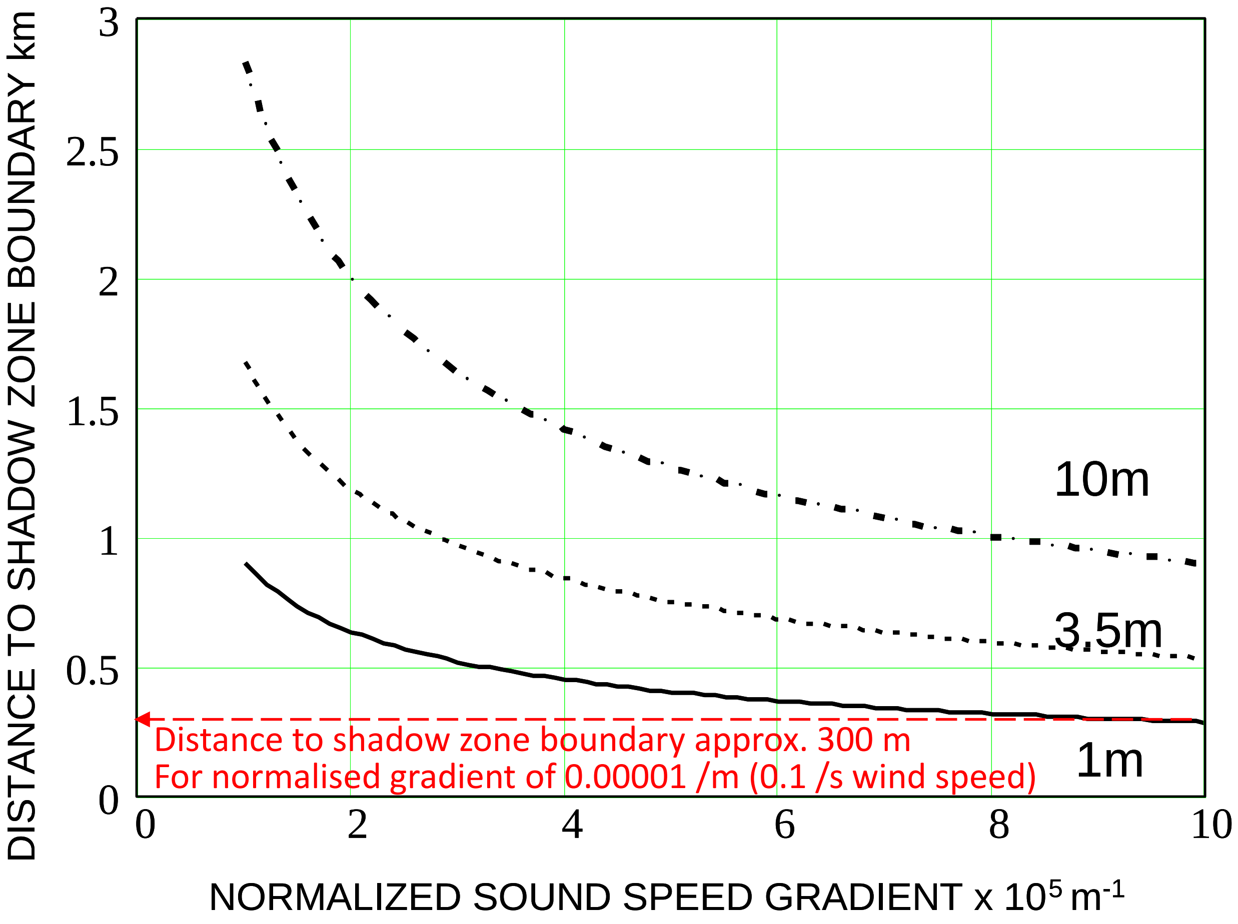

$\beta_c = \cos^{-1}\left(\frac{dc}{dz}\Big/\frac{du}{dz}\right)$ critical angle at which effect of wind counteracts that of temperature gradient and there is no shadow zone

$\langle\mu^2\rangle$ is the variance of the index of refraction

LABEX CELYA Université de Lyon

Influence of turbulence on ground effect

Clifford and Lataitis formulation (J. Acoust. Soc. Am. **73**, 1545-50 (1983))

The Open University

Mean square pressure above an impedance plane in the presence of turbulence

$$\langle p^2\rangle = \frac{1}{R_1^2} + \frac{|Q|^2}{R_2^2} + \frac{2|Q|}{R_1 R_2}\cos[k(R_2 - R_1) + \theta]T$$

where Q is the spherical wave reflection coefficient and T is the coherence factor

$$T = e^{-\sigma^2(1-\rho)} \qquad \sigma^2 = A\sqrt{\pi}\langle\mu^2\rangle k^2 R L_0$$

L_0 = outer scale of turbulence, R = range,

$\langle\mu^2\rangle$ = variance of the index of refraction

$$\langle\mu^2\rangle = \frac{\sigma_v^2\cos^2\alpha}{c_0^2} + \frac{\sigma_T^2}{4T_0^2}$$

$\sigma_{T,V}^2$ are variances of temperature and wind fluctuations

$$\rho = \frac{\sqrt{\pi}}{2}\frac{L_0}{h}\mathrm{erf}\left(\frac{h}{L_0}\right) \qquad \frac{1}{h} = \frac{1}{2}\left(\frac{1}{h_s} + \frac{1}{h_r}\right)$$

$$\mathrm{erf}(x) = \frac{2}{\sqrt{\pi}}\int_0^x e^{-t^2}\,dt$$

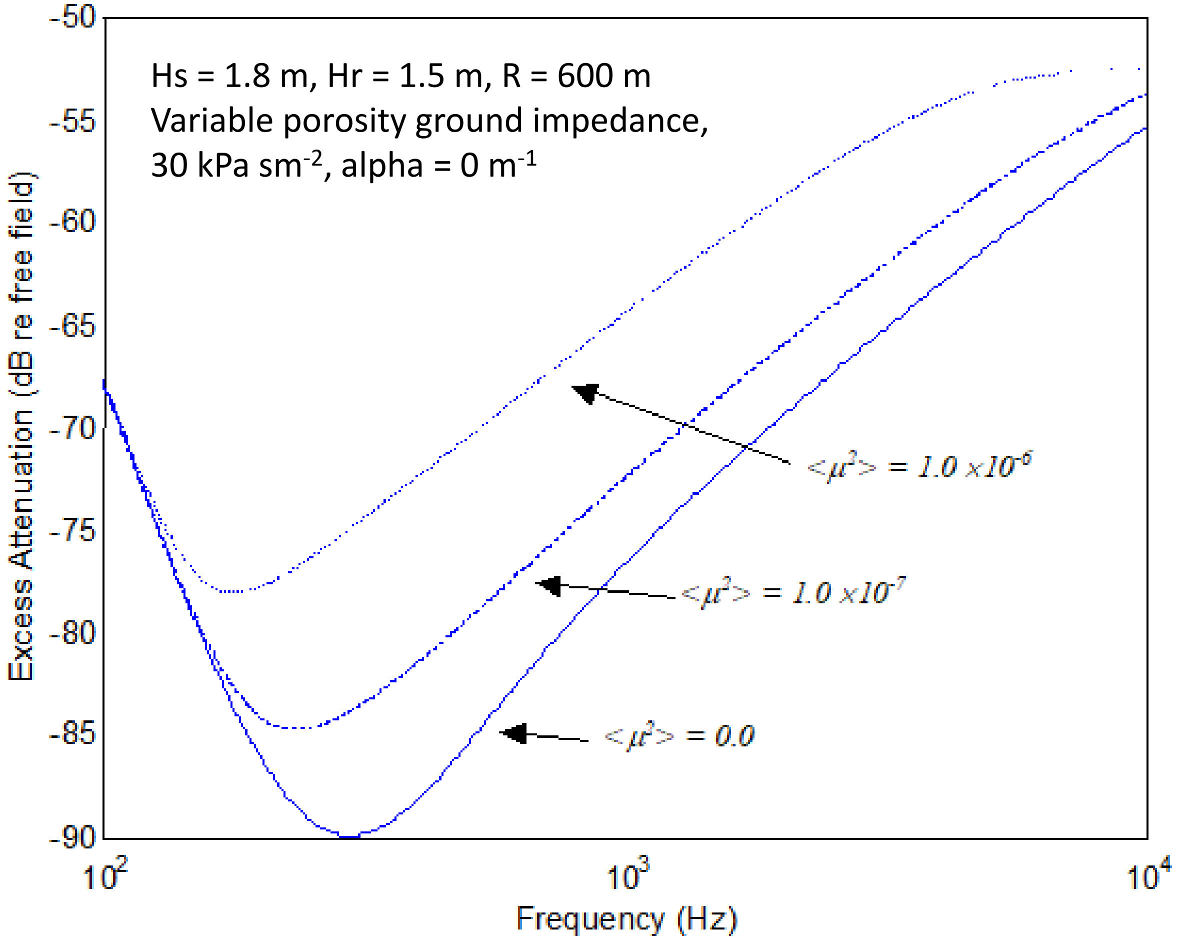

LABEX CELYA Université de Lyon

The Open University

Use of Clifford & Lataitis with Hucknall data

K. Attenborough, K. M. Li and K. Horoshenkov "*Predicting Outdoor Sound*", Taylor and Francis, 2007

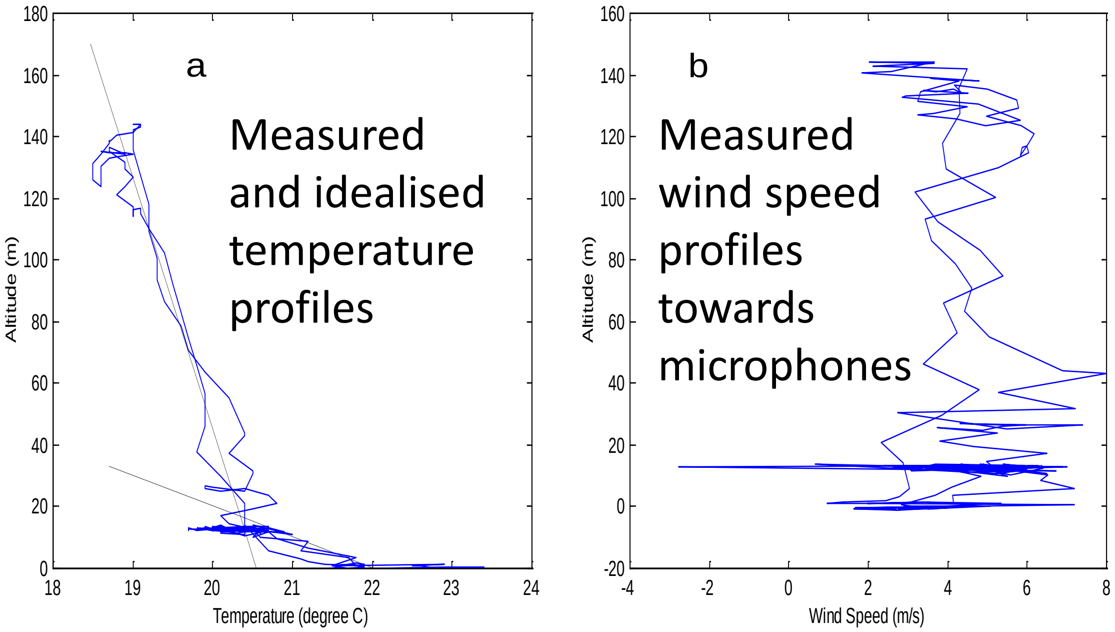

Predictions assume constant 4 m/s wind speed

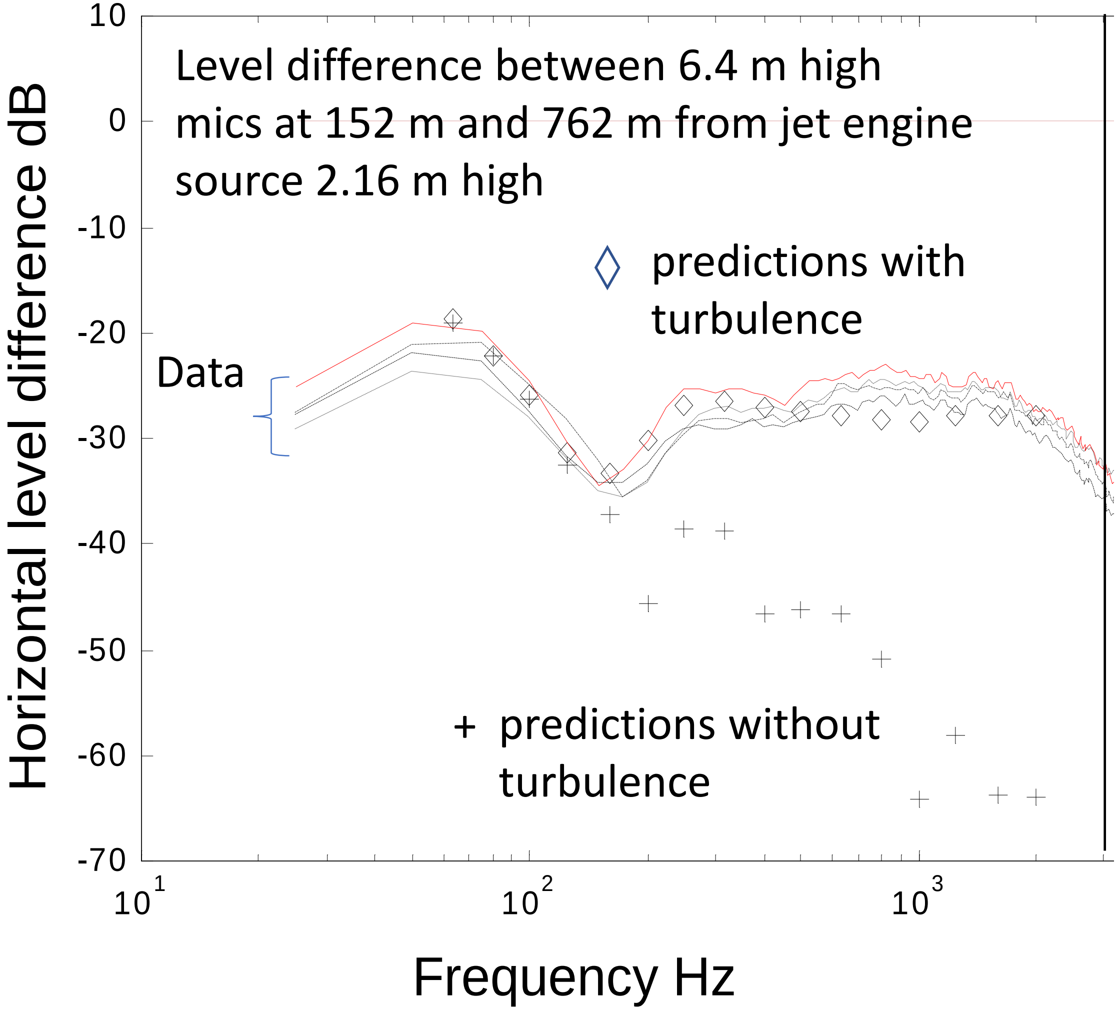

Predictions use FFP modified to include turbulence
ground impedance – variable porosity (30 kPasm^{-2}, 20 /m)
variance of index of refraction $(<\mu^2>) = 8.0 \times 10^{-6}$:
outer scale of turbulence (L_0) = 1.1 m.

But the Clifford and Lataitis formulation is valid only for thermally-driven turbulence

More accurate expression for the coherence factor with Gaussian turbulence spectrum due to Ostashev

(V. Ostashev and D. K. Wilson, *Acoustics in moving inhomogeneous media* 2nd edition)

Different length scales for thermally- (L_T) and wind-driven (L_v) turbulence

$$T_G = \exp\left\{-2A\gamma_T^G R\left[1-\frac{\sqrt{\pi}}{4D_G}\mathrm{erf}(D_G)\right]-2A\gamma_v^G R\left[1-\frac{\sqrt{\pi}}{4D_G}\mathrm{erf}(D_G)-\frac{1}{2}e^{-D_G^2}\right]\right\}$$

$$D_G = h/L_0 \quad \gamma_T^G = \sqrt{\pi}k_0{}^2\sigma_T^2 L_T/8T_0{}^2 \quad \gamma_v^G = \sqrt{\pi}k_0{}^2\sigma_v^2 L_v/8c_0{}^2$$

source and receiver heights = 0.3 m, separation 1 m

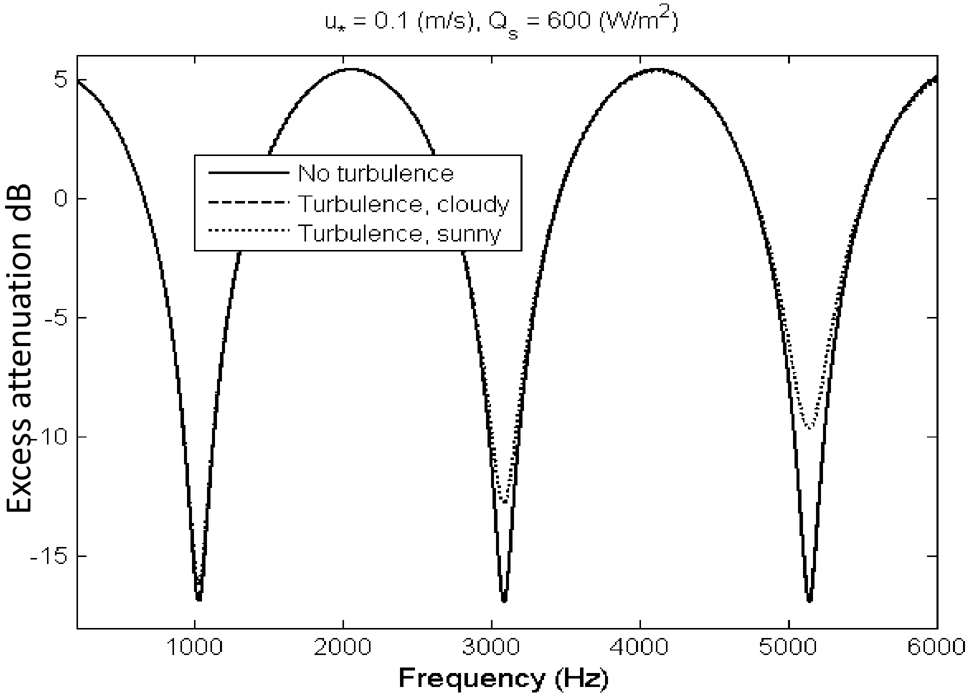

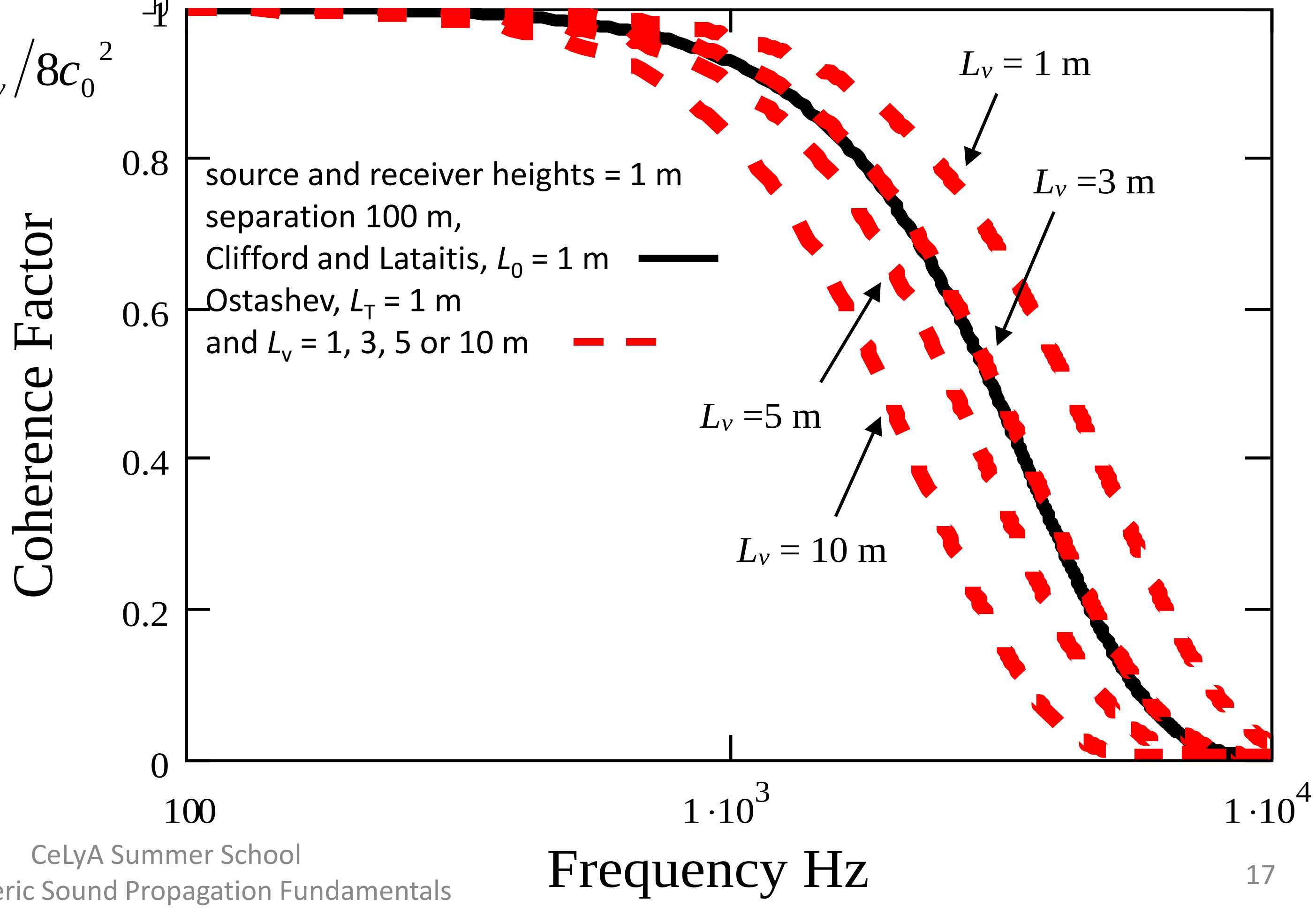

Attenuation due to turbulence

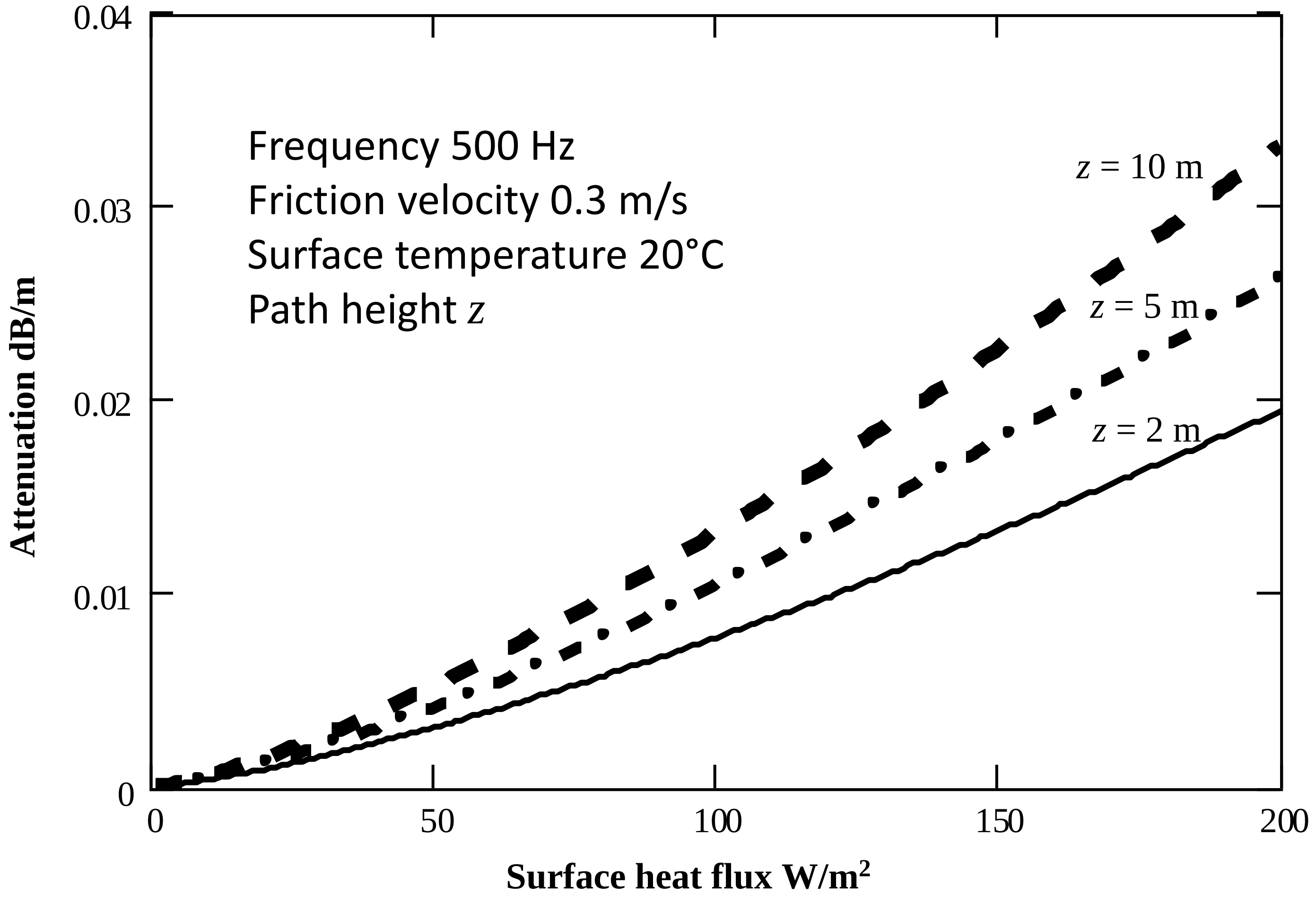

Attenuation due to turbulence is greater than that due to air absorption (⇒ 0.01 dB/m at 2 kHz)

Propagation through 0.5 m high crops
(winter wheat)

Bashir *et al*, J. Acoust. Soc. Am. **137** 154 - 164 (2015)

Source height = 0.3 m,
Upper microphone height = 0.3 m,
Lower microphone height = 0.15 m

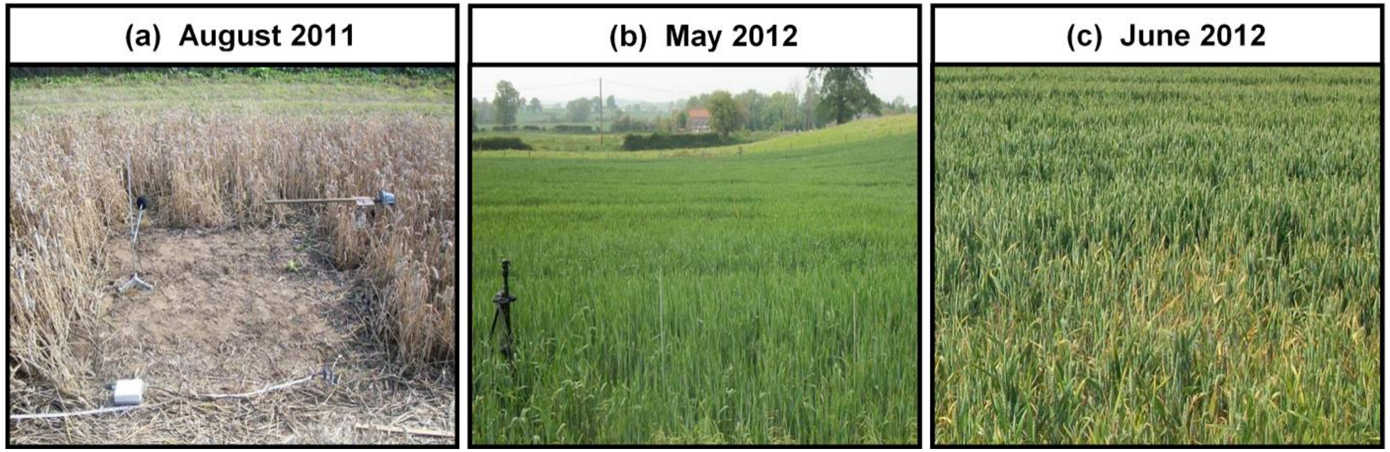

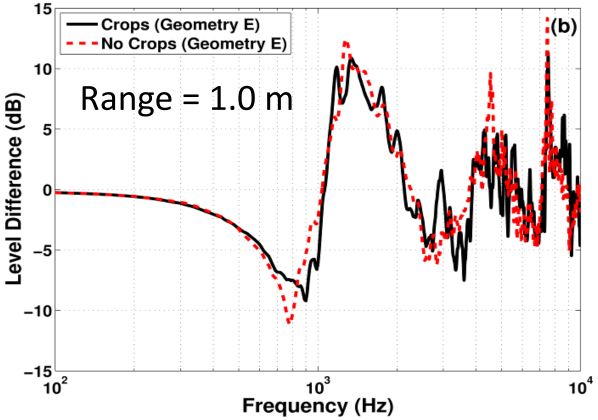

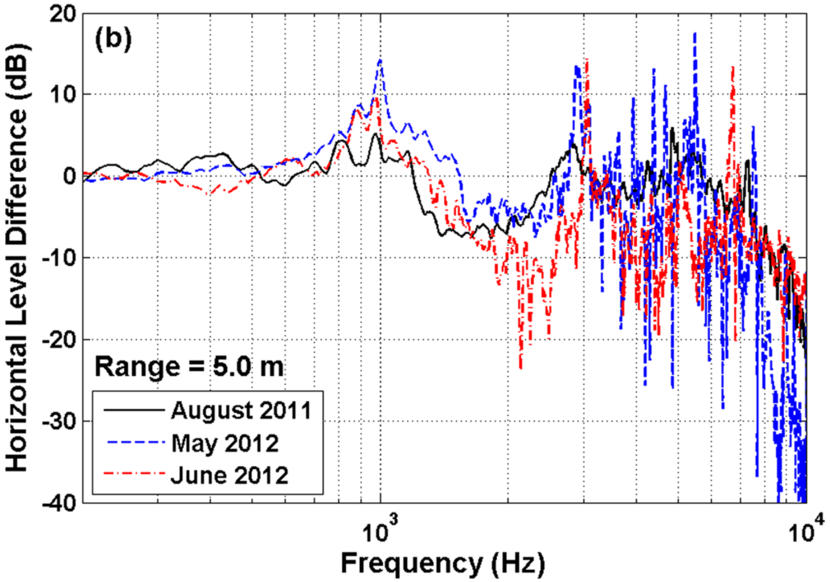

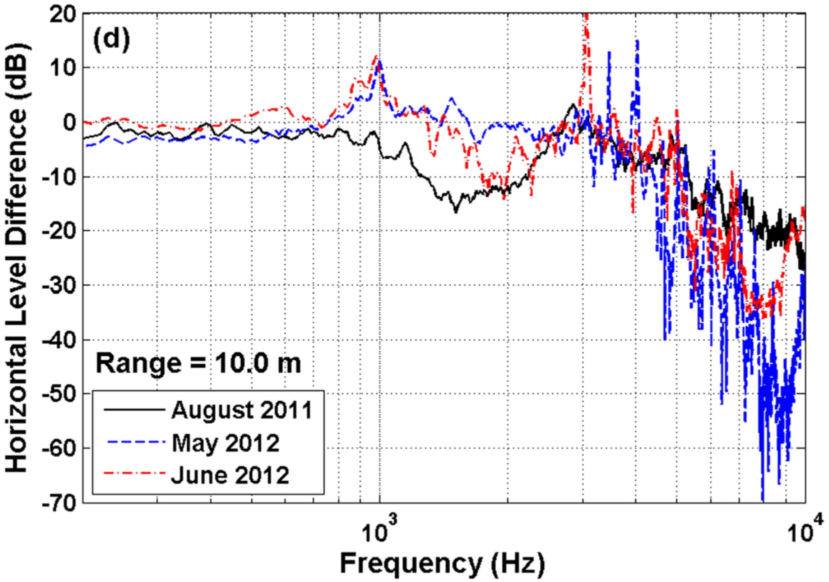

negligible effect of crops at 1 m

Empirical Formulae for Foliage Attenuation

D. E. Aylor, J. Acoust. Soc. Am., **51**(1), 411 -414 (1972)

F/m = foliage area per unit volume (similar to leaf area density index),
L m =length of propagation path,
k (wave-number) = *2πf/c*,
c = adiabatic sound speed in air,
a m = mean leaf width

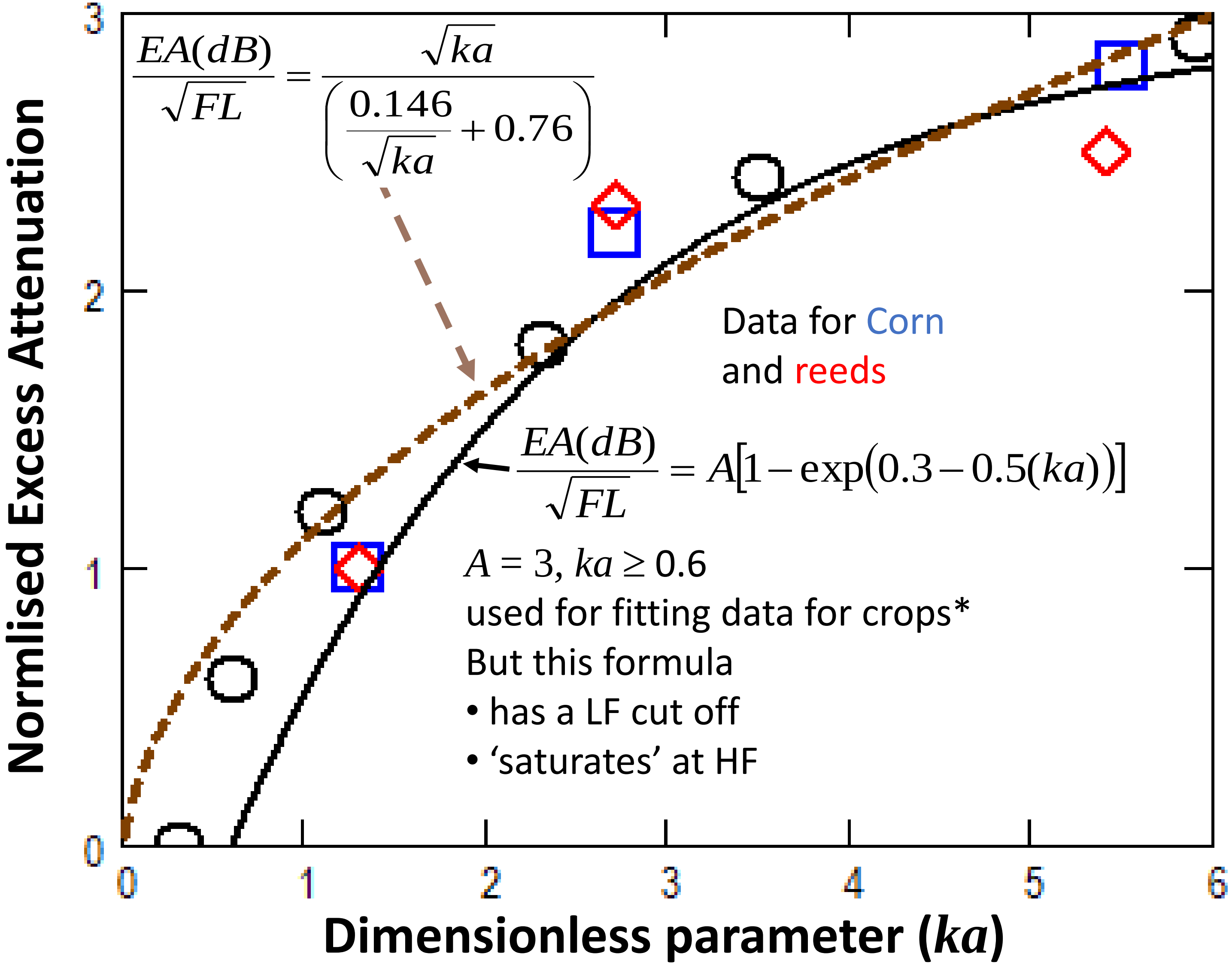

*I. Bashir *et al*
J. Acoust. Soc. Am. **137**, 154 - 164 (2015).

Comparisons of crop data with predictions

- attenuations due to ground effect, stem scattering, incoherence and foliage treated as independent
- simple predictions add ground effect and 'formula based' foliage attenuation only

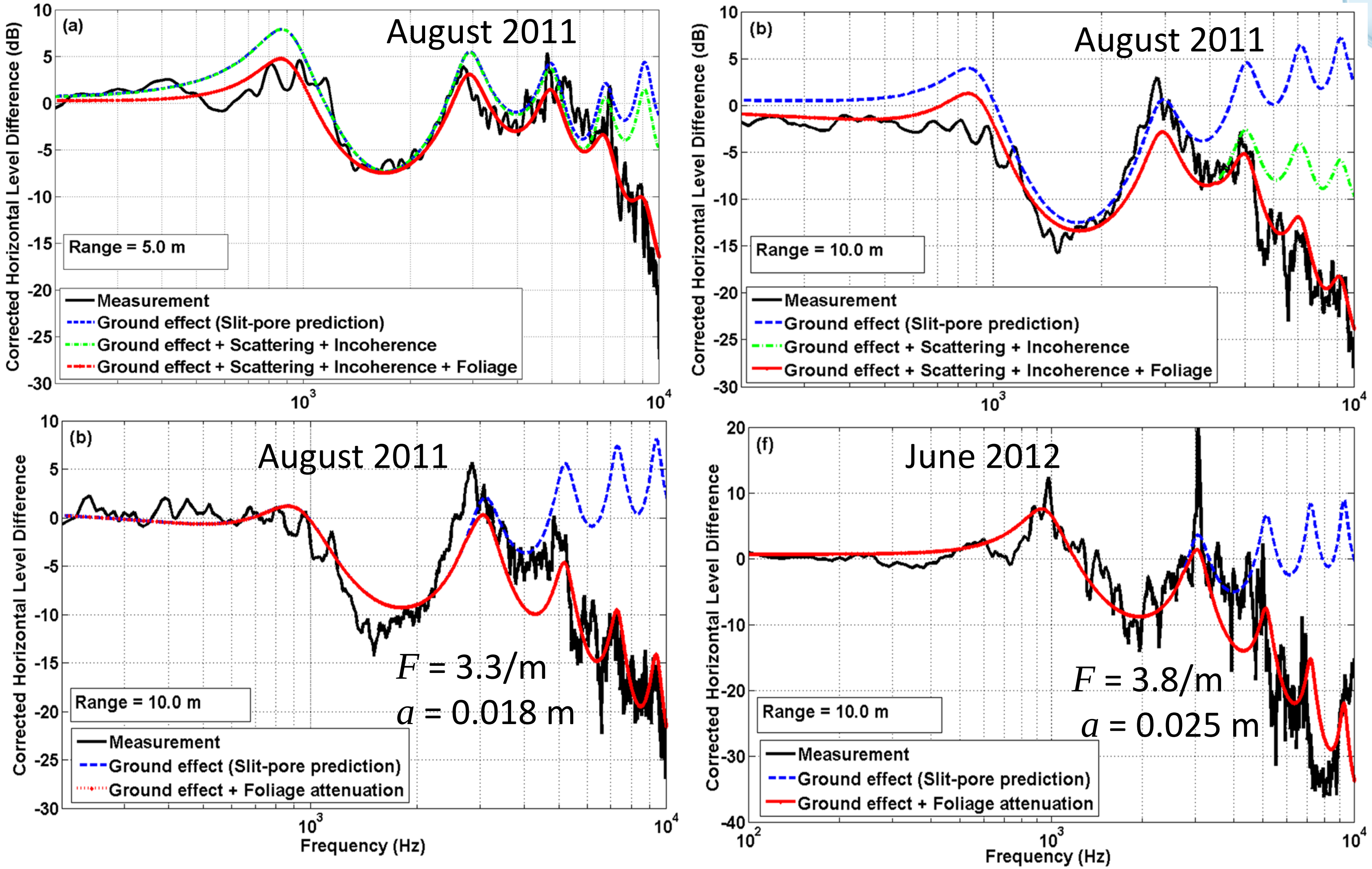

The *F* and *a* values are those that give the same mean attenuation between 1 and 2 kHz when used in the revised empirical equation for foliage attenuation as the unrealistically high values that give best fit with the 'original' version but the revised equation predicts higher attenuation above 2 kHz.

Sound Propagation through forests

Note recent developments:
Ostashev *et al Application of a 3D multiple scattering theory to forest acoustics*, 17th LRSP proceedings

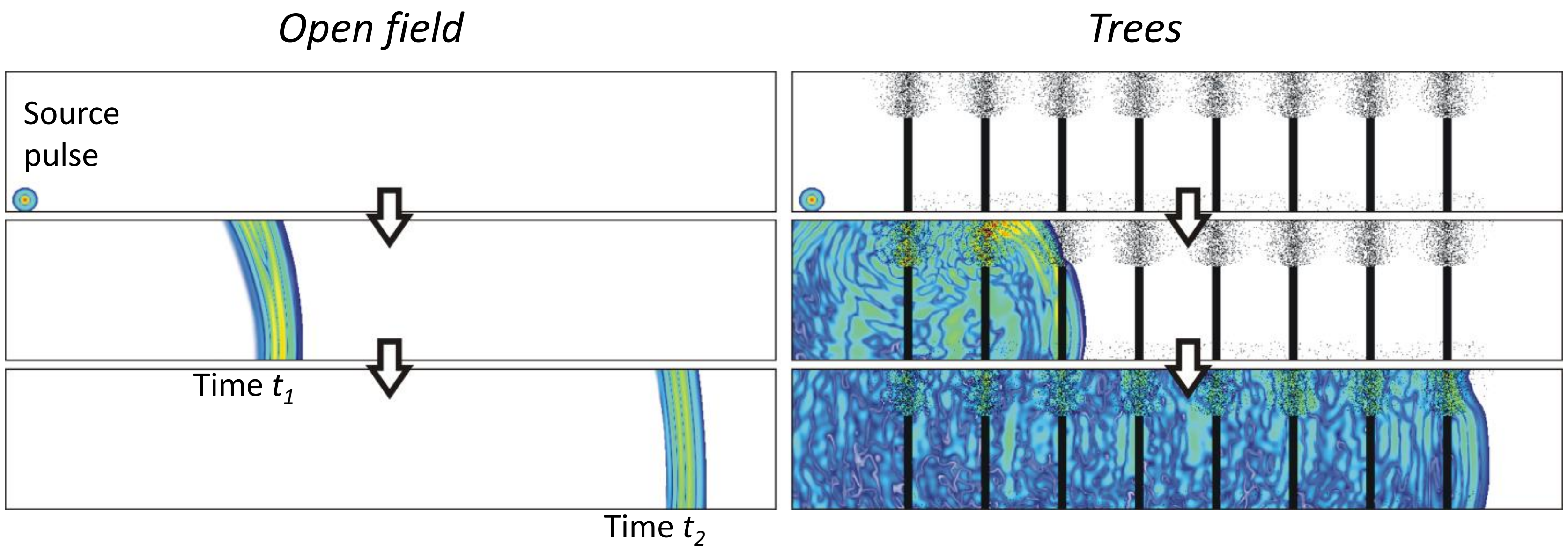

FDTD simulation from Renterghem *et al* Ch.5 of *Environmental Methods for surface transport noise reduction*, ed. Nilsson *et al*, Taylor and Francis 2015

Measured Attenuation

Corrected level difference spectra between microphones at 2 m and 72 m in a mixed *deciduous* wood

Price *et al* J. Acoust. Soc. Am., **84**(5), 1836-1844 (1988)

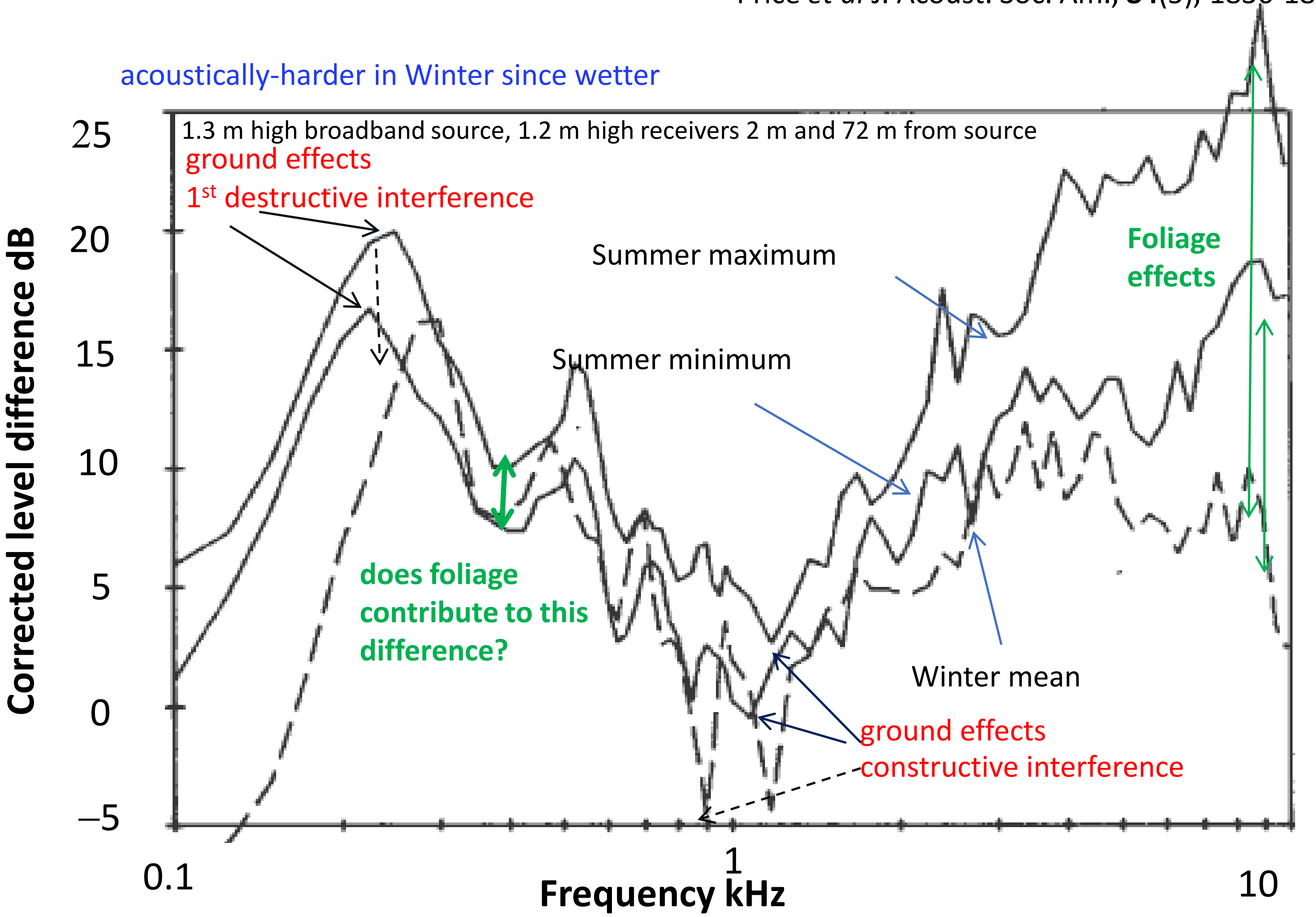

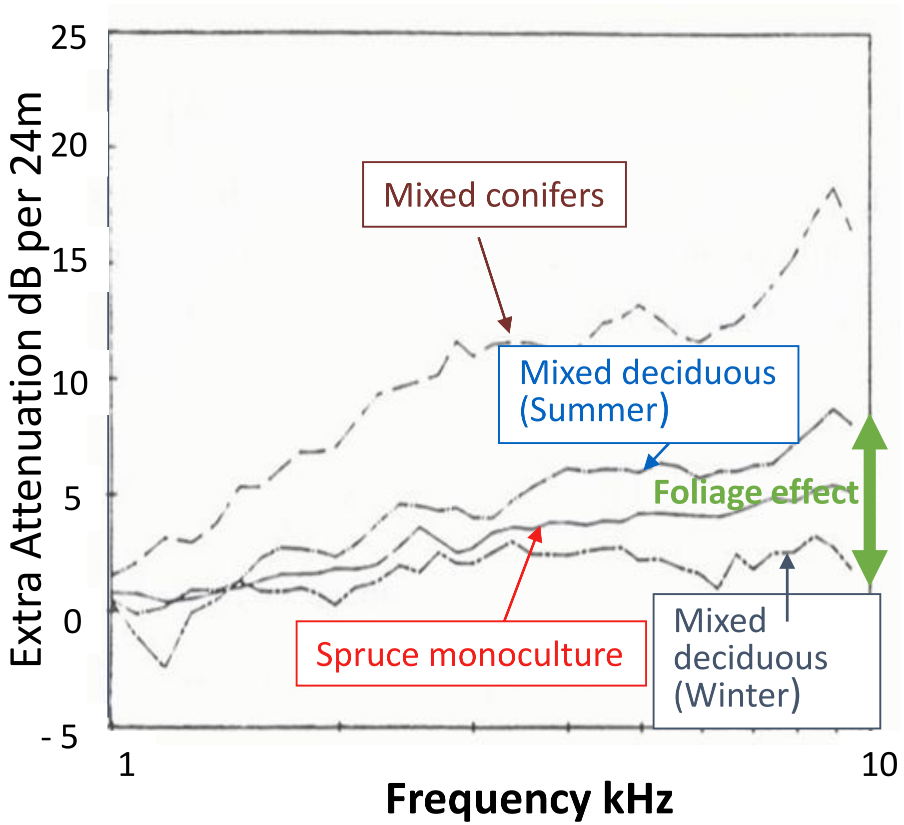

Empirical Formula for Foliage Attenuation

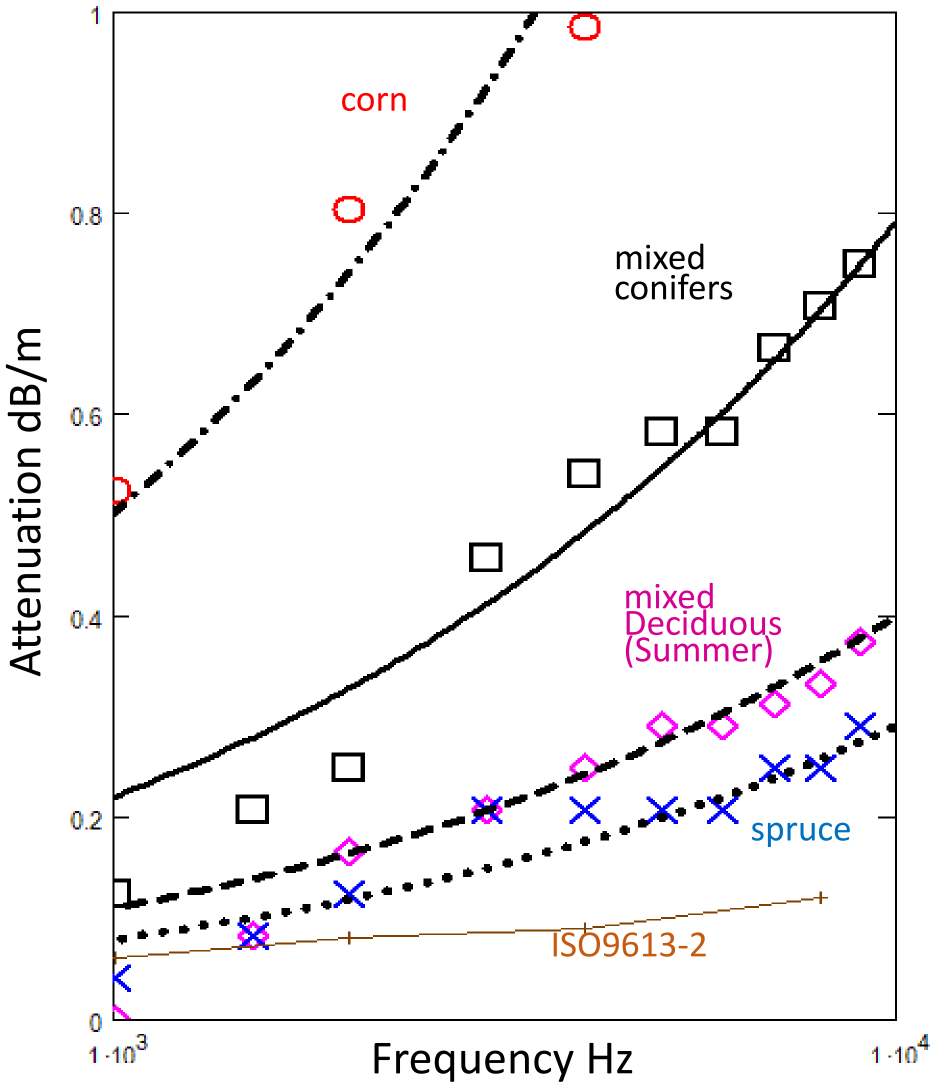

D. E. Aylor, J. Acoust. Soc. Am., **51**(1), 411 -414 (1972);
Price *et al* J. Acoust. Soc. Am., **84**(5), 1836-1844 (1988):
Bashir *et al*, J. Acoust. Soc. Am. **137** 154 - 164 (2015)

$$Attenuation\,\frac{dB}{m} = \frac{\sqrt{kaF}}{\left(\frac{0.146}{\sqrt{ka}} + 0.76\right)\sqrt{L}}$$

Leaf type	*F* /m	*a* m
corn	4.50	0.074
winter wheat	3 – 3.8	0.018 – 0.025
reeds	3.00	0.032
mixed conifers	1.20	0.045
mixed deciduous	0.40	0.035
spruce	0.25	0.03

Pine forest data at 100 m v predictions

(a) Measurements made during calm clear night
Loudspeaker source of **swept tones** –
4 spectra superimposed (thick solid lines);
Source height 1 m
Receivers at 100 m and at heights of 4.5 m, 2.5 m and 1 m.

(b) Predictions include: ground effect alone (solid lines) using a variable porosity model

$$Z = \frac{1+i}{\sqrt{\pi\gamma\rho_0}}\sqrt{\frac{R_e}{f}} + \frac{ic_0\alpha_e}{8\pi\gamma f}$$

(R_e = 7.5 kPa s m^{-2}, α_e = 25 /m)

(c) Ground effect modified by incoherence (particle bounce model; speckled area)
(d) Ground effect plus incoherence plus attenuation due to foliage calculated from reverberation time (dashed lines)

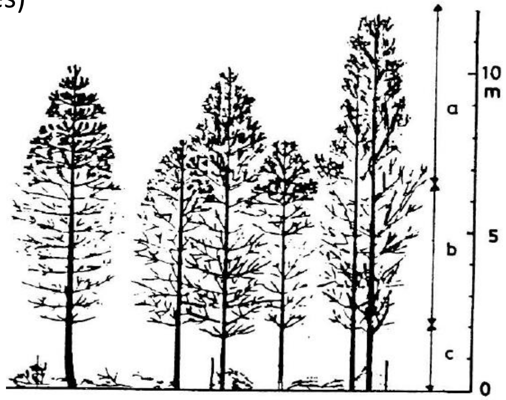

W T J Huisman, K Attenborough, *"Reverberation and attenuation in a pine forest: measurements and models"* J. Acoust. Soc. Amer. 90(5) 2664-2677 (1991).

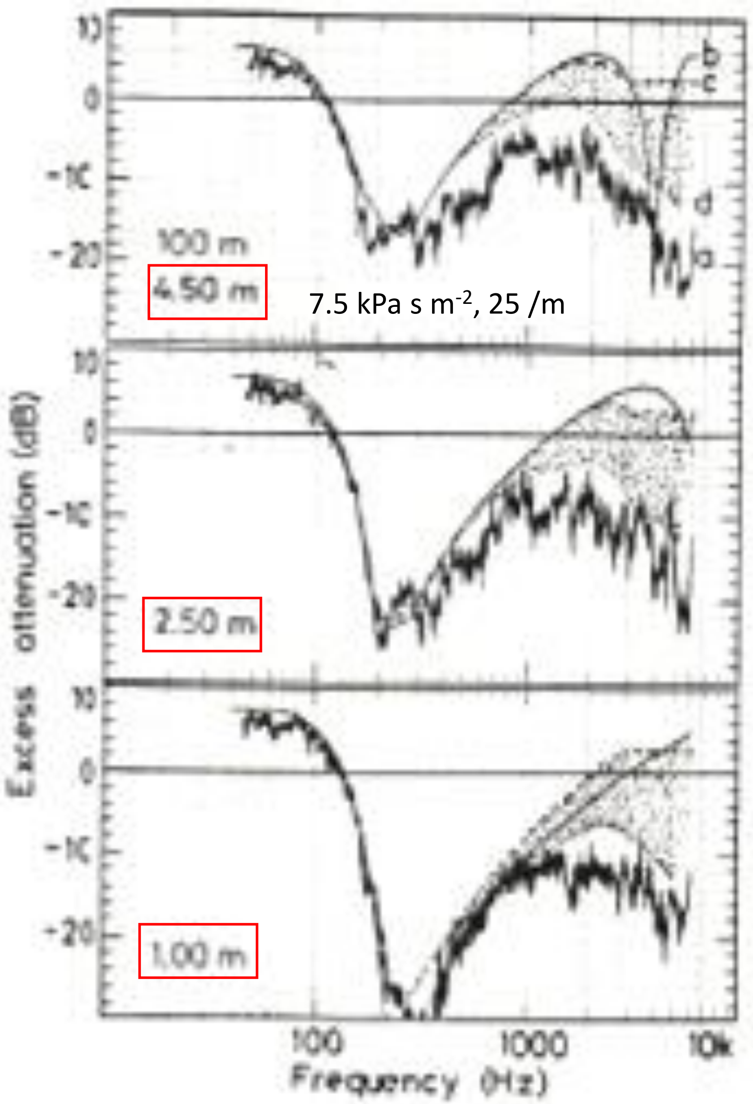

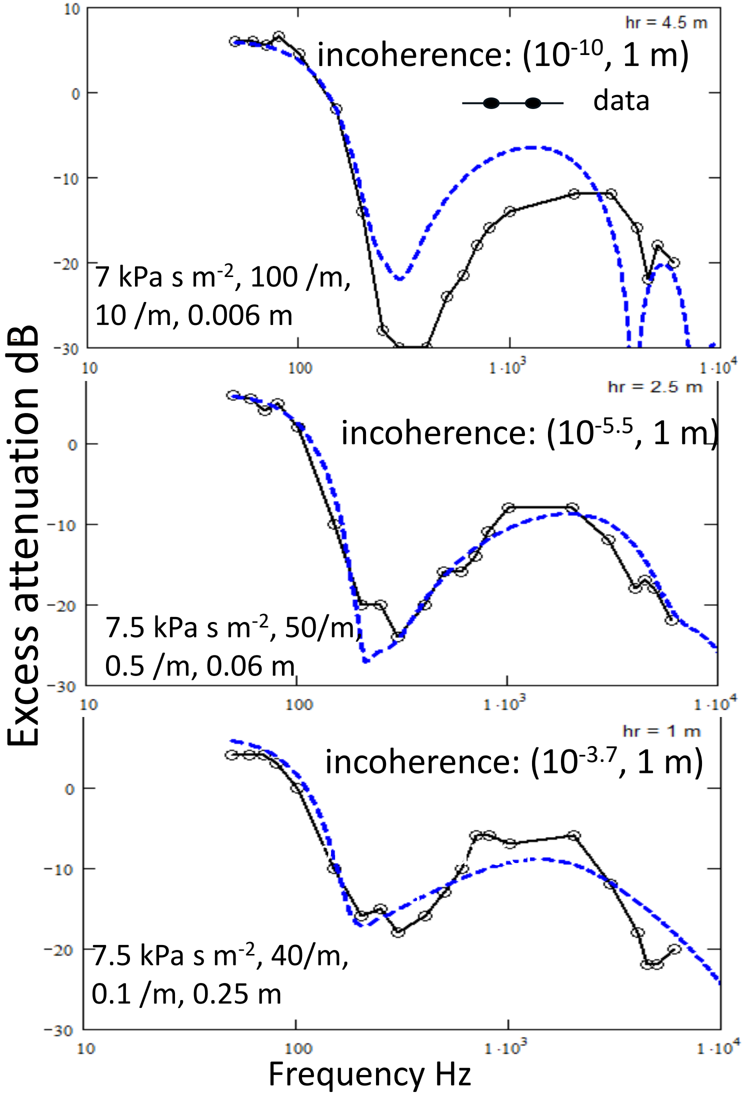

Mean tree height 11.2 m;
according to Lalic *et al* J. Appl. Met. **43** 641-645 (2004)
expected mean height of max. LAD = 0.4× mean tree height = 4.48 m

Sonic crystal effects with trees

Bragg Diffraction

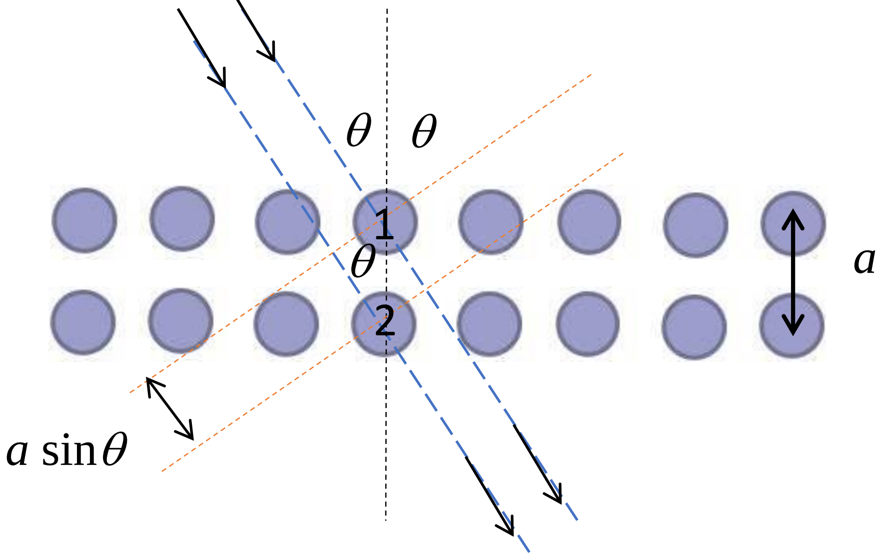

First **constructive** interference for transmitted waves occurs when $\lambda = a \sin\theta$

At normal incidence $\theta = 90°$, $\sin\theta = 1$, *so* $\lambda = a$ *or* $c/f = a$ *or* $f = c/a$

(lattice spacing = wavelength => first ***pass band***)

Destructive interferences when $(2n+1)\lambda/2 = a \sin\theta$

At normal incidence $\theta = 90°$, $\sin\theta = 1$ so first (n = 0) destructive transmission interference when $\lambda/2 = a$ (lattice spacing equals half a wavelength) *or* $c/2f = a$ *or*

$f = c/2a$ => *first **stop band or band gap***

LABEX CELYA Université de Lyon

2D theory for Multiple scattering by cylinders

The Open University

C. M. Linton and D. V. Evans, "The interaction of waves with arrays of vertical circular cylinders," *Journal of Fluid Mechanics*, 215 (1), 549, 2006.

direct and reflected — Single scattering

$$P=\sum_{n=-\infty}^{+\infty}J_n(kr_s)e^{in\theta_s}\left[H_n(kS_{s1})e^{-in\sigma_{s1}}+H_n(kS_{s2})e^{-in\sigma_{s2}}\right]+\sum_{n=-\infty}^{\infty}A_n^sZ_n^sH_n(kr_s)e^{in\theta_s}$$

Multiple scattering

$$+\sum_{j=1,\,j\neq s}^{N}\sum_{n=-\infty}^{\infty}A_n^jZ_n^j\sum_{m=-\infty}^{m=\infty}J_m(kr_s)H_{n-m}(kR_{js})e^{im\theta_s}e^{i(n-m)\alpha_{js}}$$

acoustically-soft

$$Z_n^j=\frac{q_jJ_n'(ka_j)J_n(k_ja_j)-J_n(ka_j)J_n'(k_ja_j)}{q_jH_n'(ka_j)J_n(k_ja_j)-H_n(ka_j)J_n'(k_ja_j)}\qquad q_j=z_j/\rho c$$

acoustically-hard

$$Z_n^j=\frac{J_n'(k_0a_j)}{H_n'(k_0a_j)}$$

Coefficients calculated from

$$A_m^s+\sum_{\substack{j=1\\j\neq s}}^{N}\sum_{n=-M}^{M}A_n^jZ_n^jH_{n-m}(kR_{js})e^{i(n-m)\alpha_{js}}=-H_m(kS_{p1})e^{-im\sigma_{p1}}-H_m(kS_{p2})e^{-im\sigma_{p2}}$$

Laboratory measurements with cylinder arrays on a plane

Bashir *et al* J. Acoust. Soc. Am. **123** (4) EL323-328 (2013)

Source – receiver separation 1 m; receiver height 0.1 m

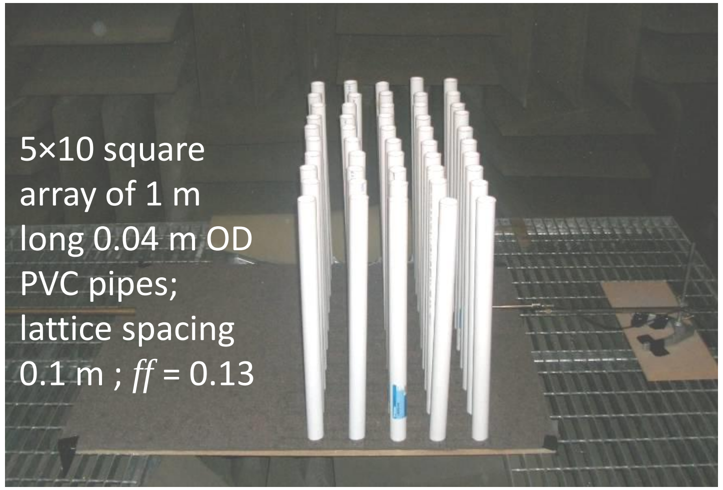

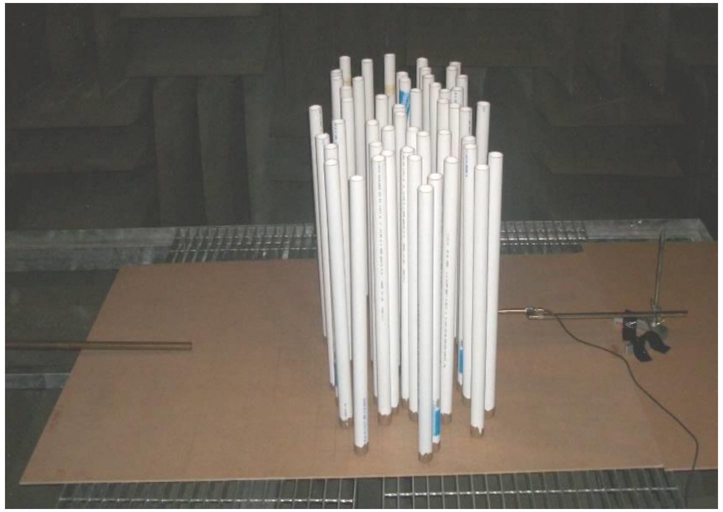

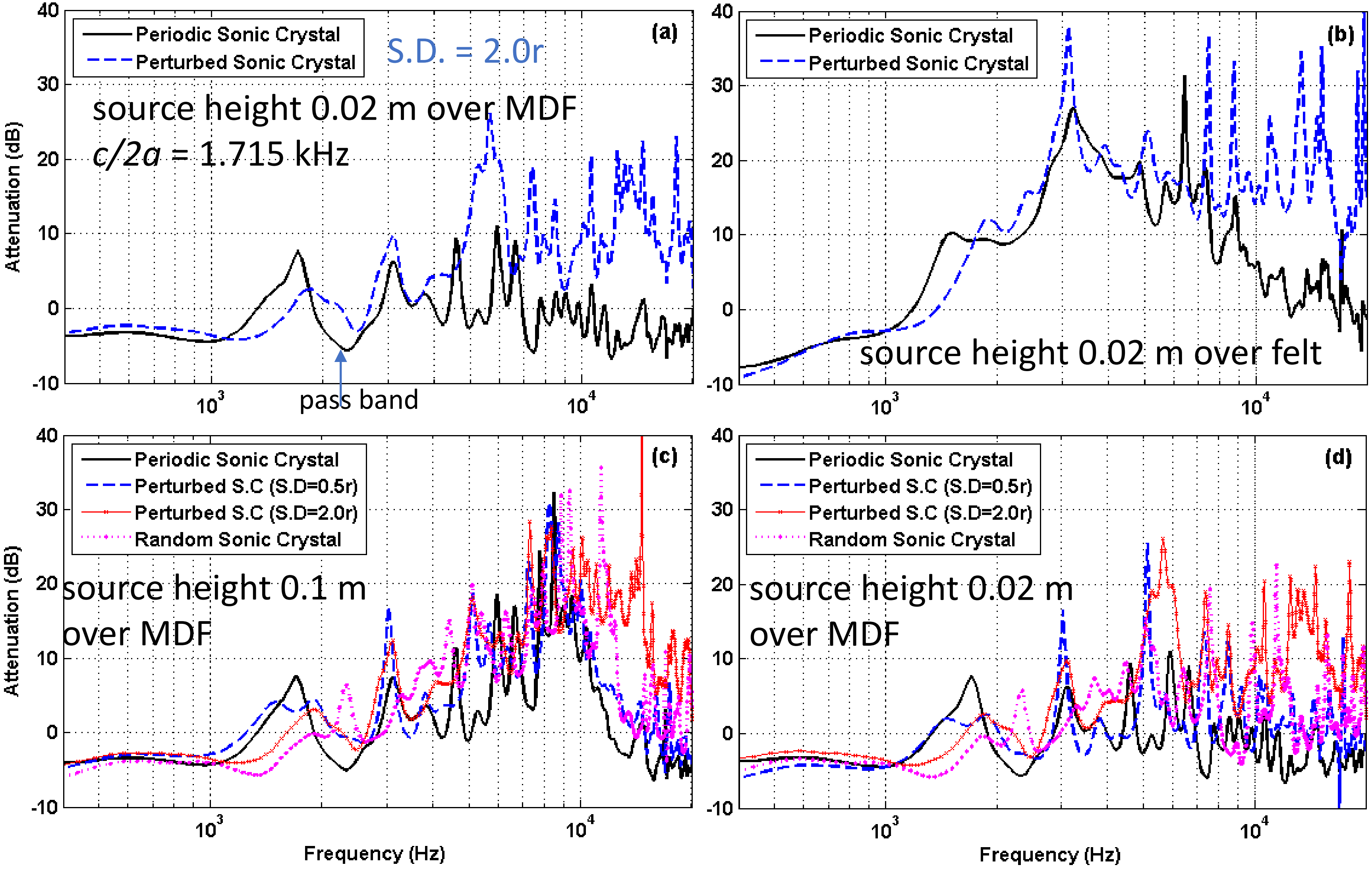

Predictions v laboratory data

Predictions obtained by adding ground effect and scattering loss

Bashir *et al* J. Acoust. Soc. Am. **123** (4) EL323-328 (2013)

Source to receiver separation 1 m; source and receiver height 0.1 m

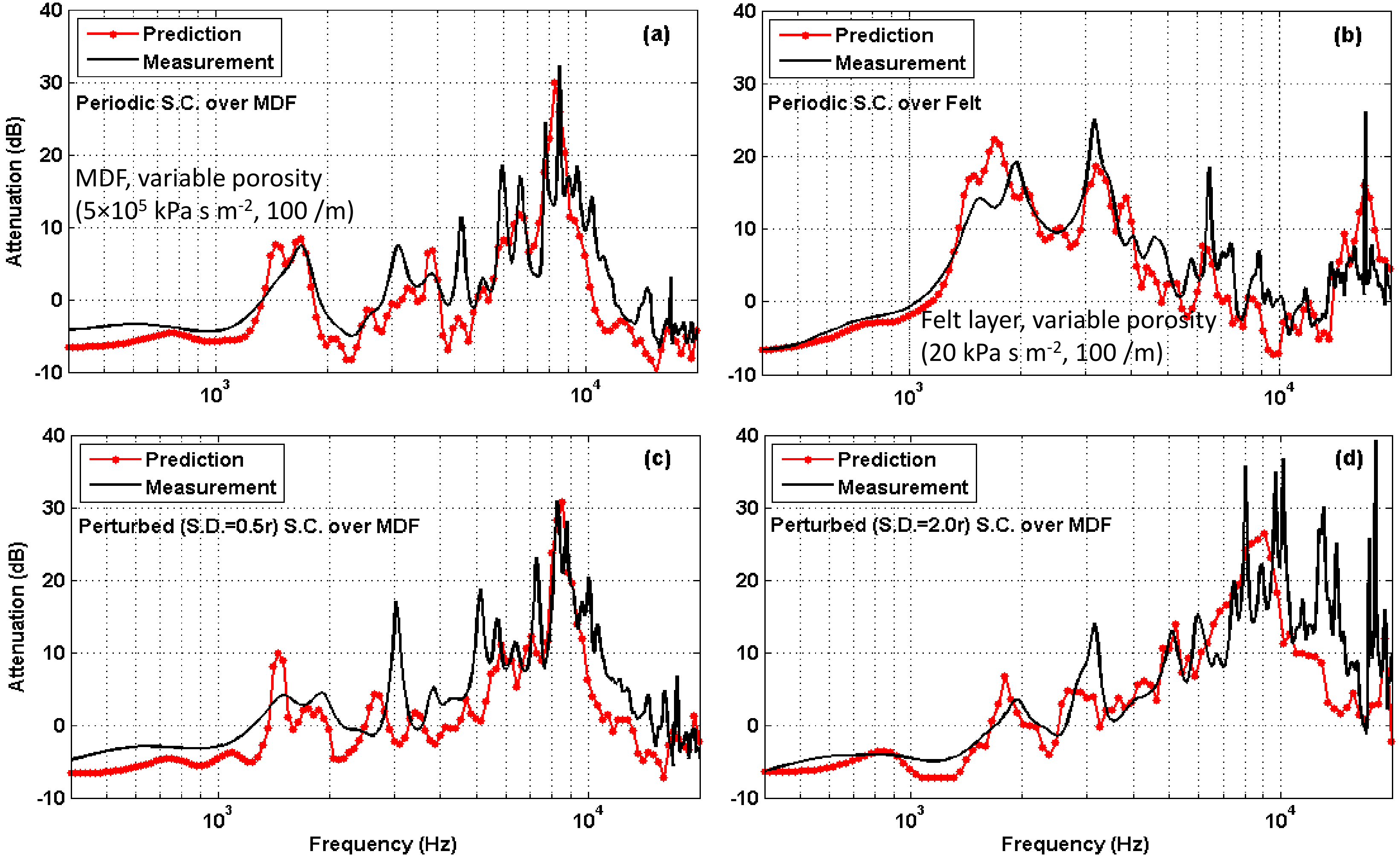

Designs for traffic noise reducing Tree Belts

Van Renterghem and Botteldooren, Proc. Euronoise, Prague 2012

But these predictions do not take meteorological effects into account

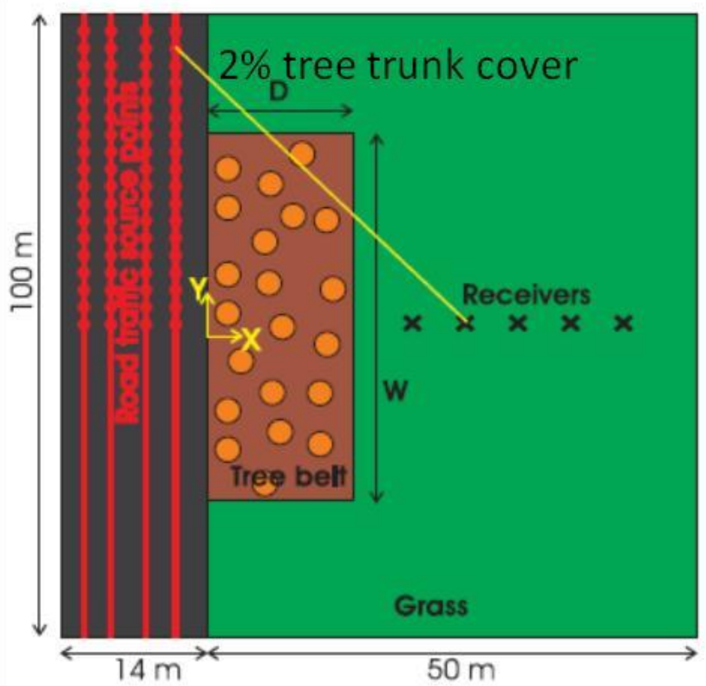

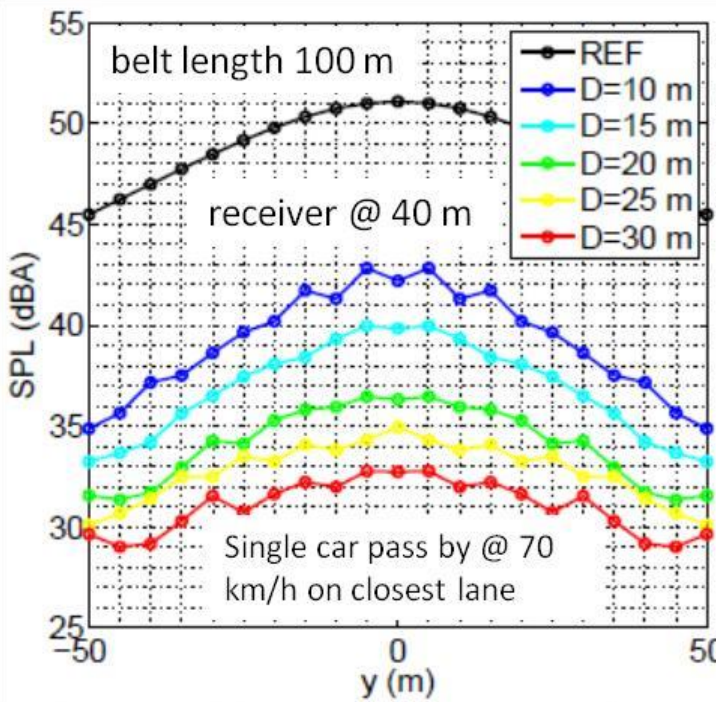

REF *assumes propagation entirely over grassland* (150 kPa s m^{-2})

Predicted insertion loss for 100 m long and 15 m wide tree belt near a 4-lane road

diameter	randomness in stem centre shifts	IL
uniform 22 cm	regular	9.6 dBA
uniform 22 cm	shifts < 25%	11.6 dBA
uniform 22 cm	shifts < 50%	11.0 dBA
uniform 22 cm	shifts < 100%	10.7 dBA
uniform 22 cm	fully random	10.5 dBA
gaussian (μ=22 cm, σ=5 cm) distributed	regular	10.7 dBA
gaussian (μ=22 cm, σ=5 cm) distributed	shifts < 25%	11.4 dBA

(Only light vehicles, 70 km/h; receiver at 40 m)

Approximately 3 dB of overall attenuation is due to 'forest floor' ground effect (phenomenological model 10 kPa s m^{-2}, porosity 0.6, tortuosity=1/porosity)

Meteorological effects on sound in forests

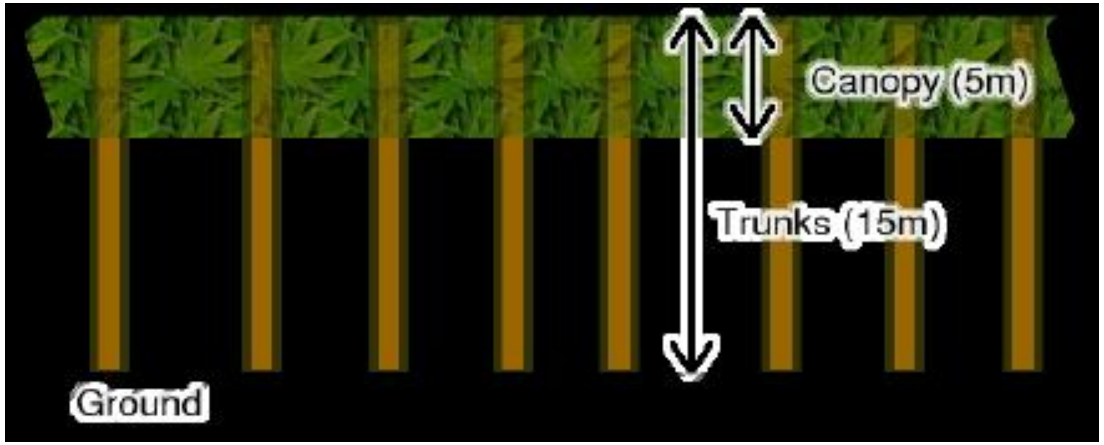

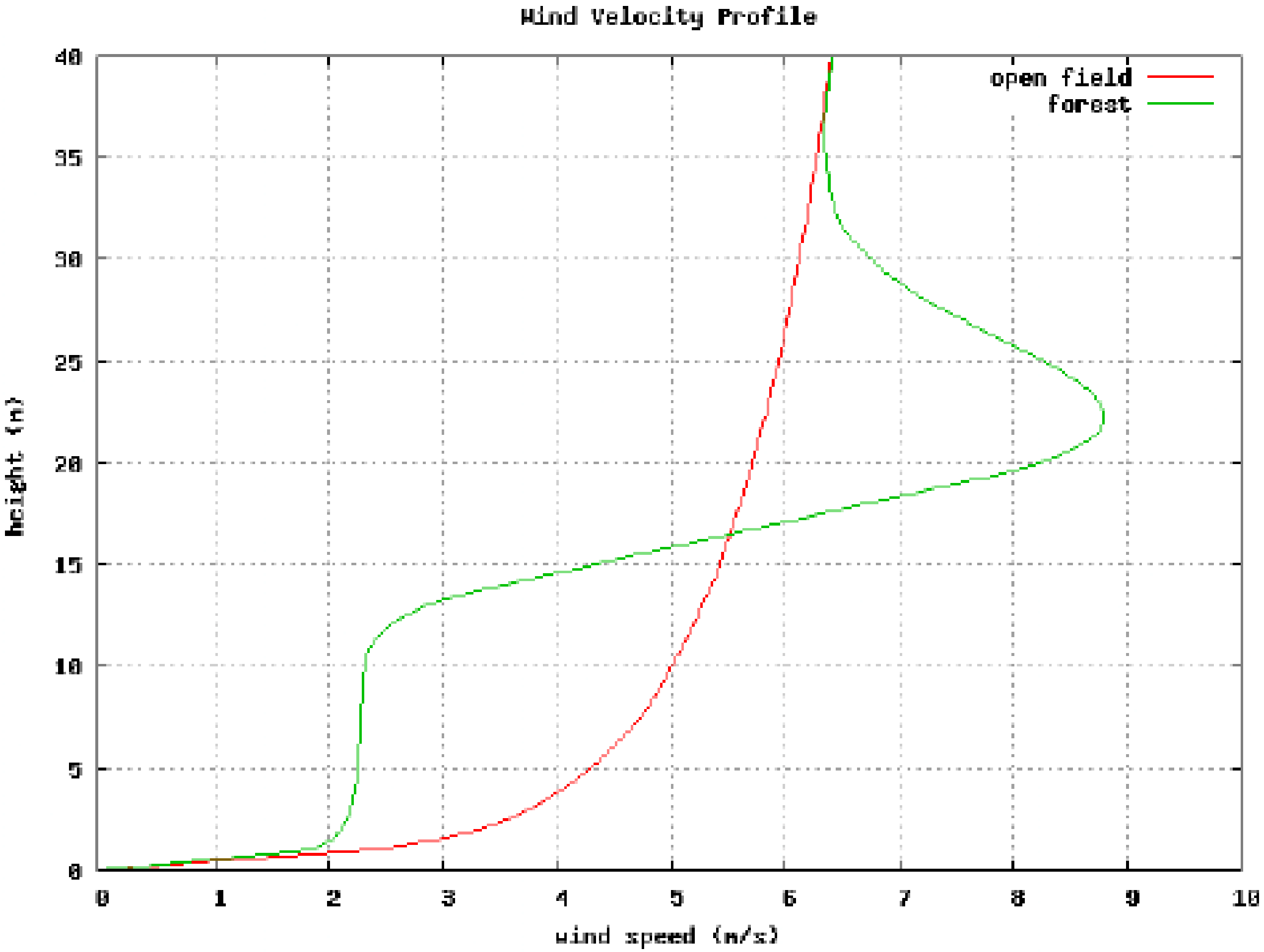

From Michelle E. Swearingen and Michael J. White, Proc. 11th LRSPS Vermont June 2004

Downwind energy is trapped by Canopy

Simulations using GFPE Michelle E. Swearingen and Michael J. White, Proc. 11th LRSPS Vermont June 2004

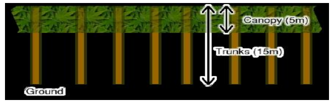

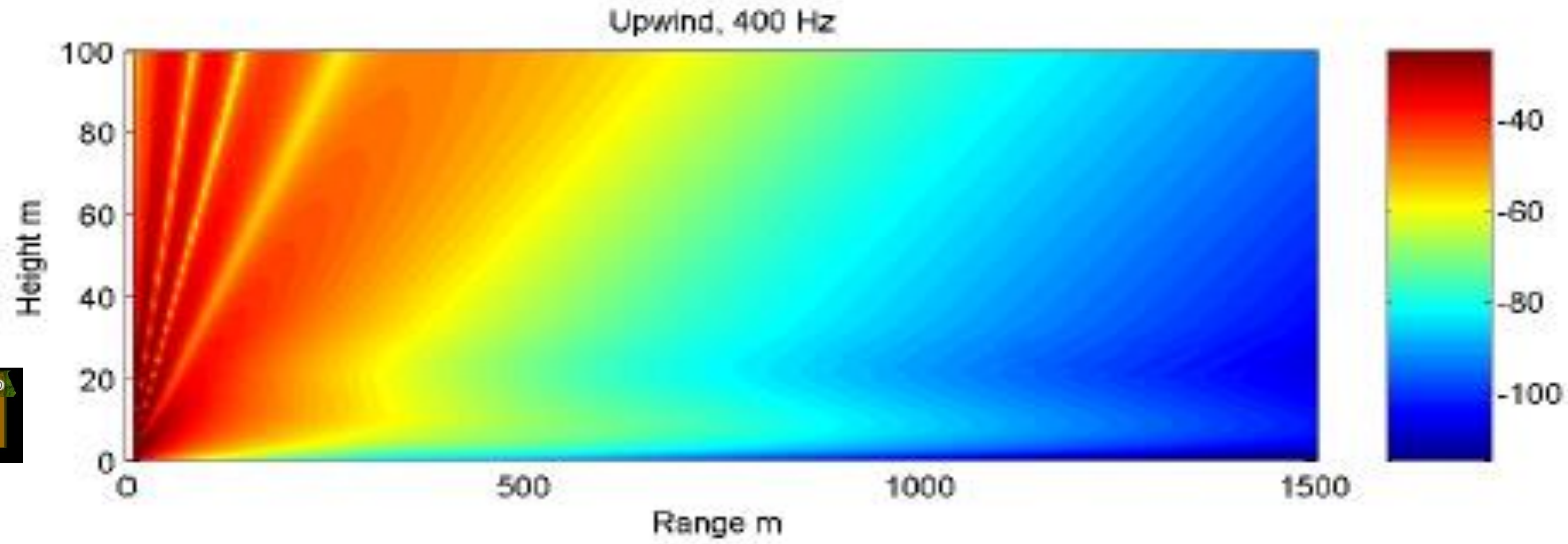

See also Swearingen and White J. Acoust. Soc. Am. **122** 113 – 119 (2007)

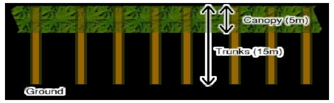

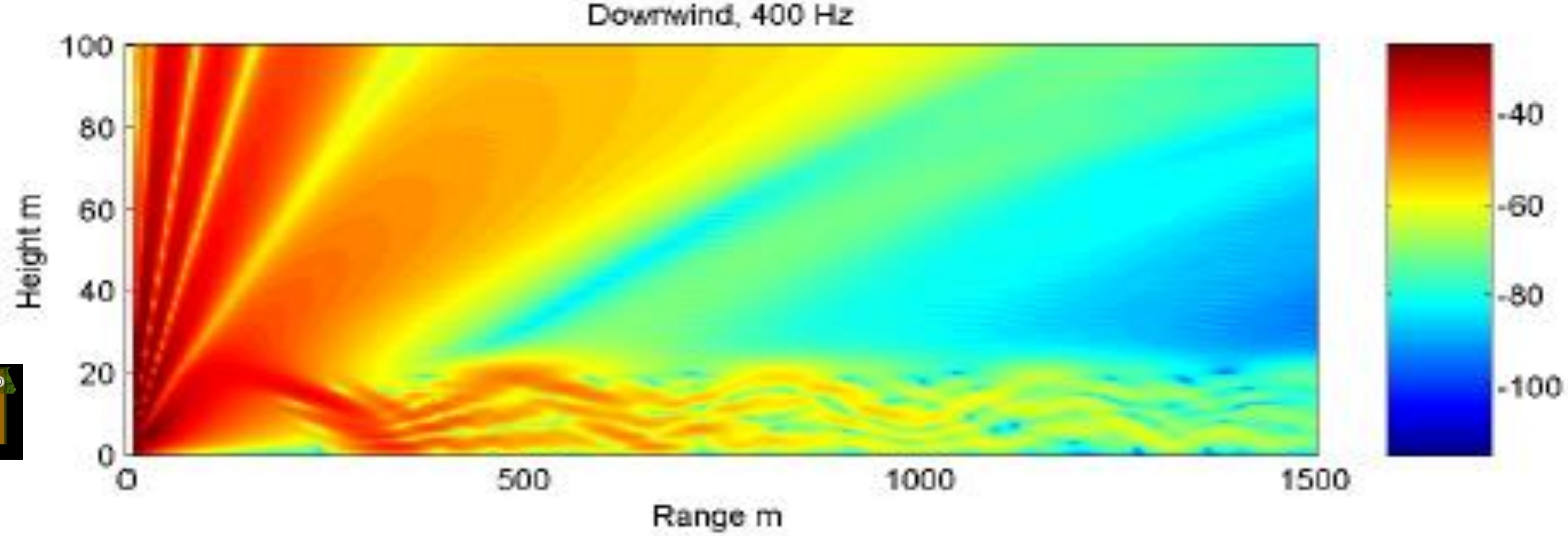

Trees with Noise Barriers

Van Renterghem T., Botteldooren D., Acta Acustica, **88** 869-878 2002

Experiment in Belgium (Aalst)

Barrier height
4m
Trees approx.
8m high

Peak flow 9000
vehicles/hr

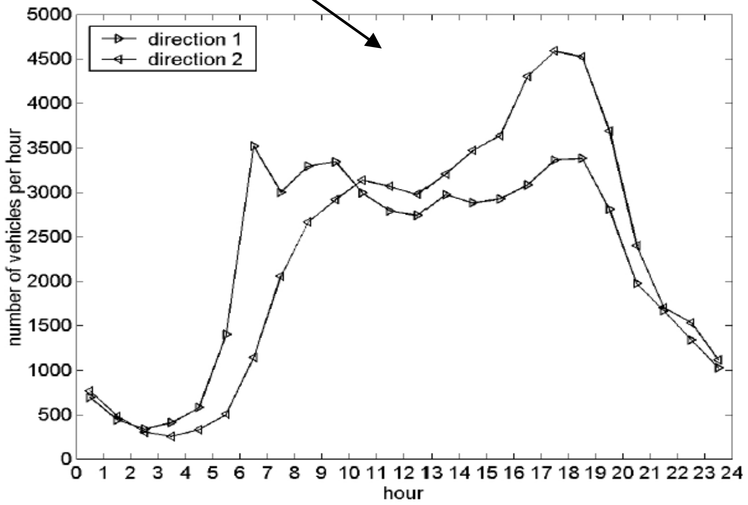

Effects of a Row of Trees on performance of a Noise Barrier in Wind

Van Renterghem T., Botteldooren D., Acta Acustica, **88** 869-878 2002

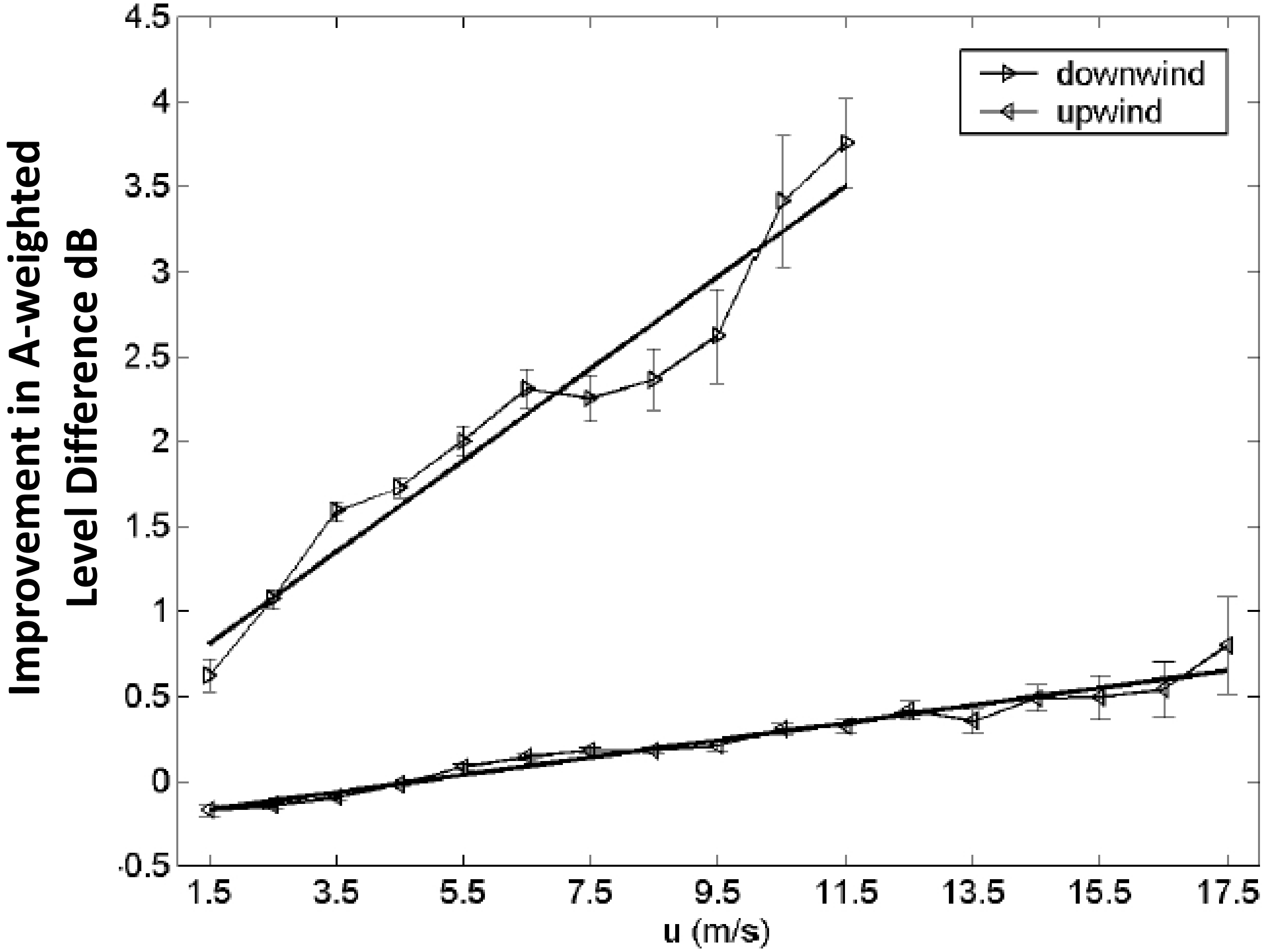

Wind Speed m/s

Trees included ashes (*Fraxini*) rowan trees (*Sorbus aucuparia L.*) oaks (*Querci*) and small bushes.

Porosity of canopy
13 % to 15 %.

MEASURED EFFECTS OF TREE CLEARNG ON ESHER COMMON

8 December 2003; slight inversion

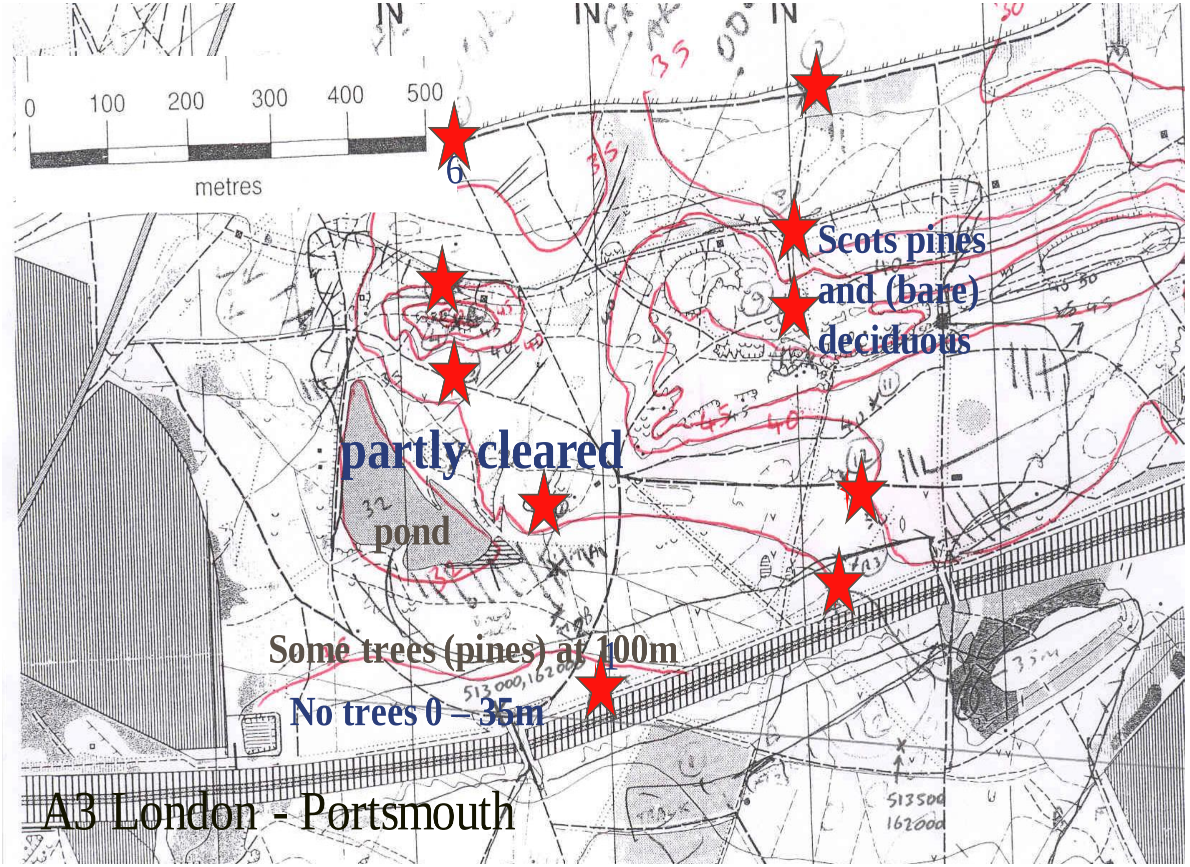

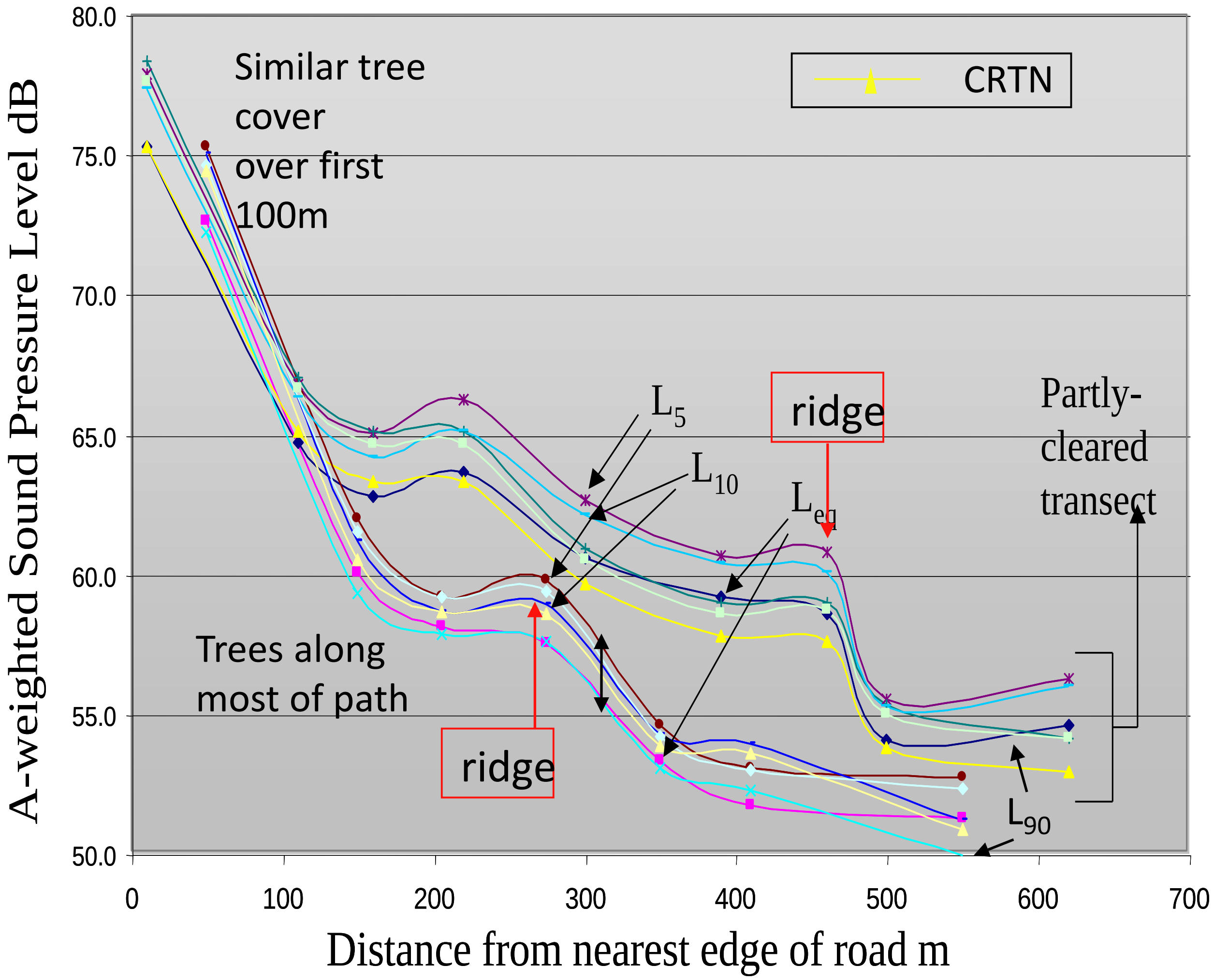

Prediction Schemes

$$L_p = L_w - 20\lg r - 11 + DI - L_{Atten}$$

$$L_p = L_W - 20\log r - 11 + D - A_{air} - A_{ground} - A_{refraction} - A_{barrier} - \ldots$$

Source-specific

Calculation of Road Traffic Noise (CRTN) Calculation of Railway Noise (CRN)

Road noise prediction *2 -Noise propagation computation method including meteorological effects (NMPB 2008)* SETRA (2009)

Annex to Commission Directive 2015/996 in Official Journal of the European Union L168 (2015)

Source-independent

ISO, Acoustics—Attenuation of Sound During Propagation Outdoors—Part 2: A General Method of Calculation (**ISO 9613-2**). (ISO, Geneva, Switzerland, 1996)

R. Nota, R. Barelds, D. Van Maercke, Harmonoise WP 3 Engineering method for road traffic and railway noise after validation and fine tuning, Deliverable of WP3 of the HARMONOISE project. Document ID HAR32TR-040922-DGMR20, 2005